ALMA MATER STUDIORUM - UNIVERSITÀ DI BOLOGNA

CAMPUS DI CESENA

DIPARTIMENTO DI

INGEGNERIA DELL'ENERGIA ELETTRICA E DELL'INFORMAZIONE

"GUGLIELMO MARCONI"

CORSO DI LAUREA MAGISTRALE IN INGEGNERIA BIOMEDICA

TITOLO DELLA TESI

KNEE MONITOR: MOTION AND PHYSICAL ACTIVITY MONITORING IN DAILY
LIFE USING A NOVEL DUAL SENSOR WEARABLE

Tesi in

BIOINGEGNERIA DELLA RIABILITAZIONE

Relatore   Presentata da

Ch.mo Prof. Lorenzo Chiari   Daniele Testa

                                                                         Matr. 0000852598

Anno Accademico 2019/2020

INDEX

INTRODUCTION

1.1 Risks and Assessment of knee health in clinic

It is well known in the scientific literature that a good level of movement has a positive impact on our overall health. Physical activity (PA) can be used as a parameter for the diagnosis, treatment or evaluation of the results of correct health care. Moreover, in orthopaedics, physical activity is a fundamental parameter in the analysis as the movement apparatus is directly affected [1]. A very important concept in human motion analysis is that of functional mobility. Functional mobility means the ability to walk safely in a free-living environment. This translates into the ability to walk, run, climb, even when handling support devices such as walkers, crutches and sticks [2] [3] [4]. Unfortunately, a large number of illnesses and/or accidents can compromise an individual's level of mobility and especially the gait function. In general, gait pathologies can be classified into four major categories: rehabilitation-related gait patterns, neurological gait disorders, psychiatric gait abnormalities, and gait degradation due to ageing. Of all these injuries, the musculoskeletal ones and chronic conditions are prevalent [5] [6] [7].

Figure 1.1 Osteoarthritis most often occurs in the hands (at the ends of the fingers and thumbs), neck, lower back, knees, and hips.

In this thesis elaboration, we will concentrate our discussion on a fundamental joint for human locomotion, the knee. The most frequent problems affecting this joint are:

- Osteoarthritis (OA), is a type of joint disease caused by a progressive deterioration of joint cartilage and underlying bone. The most affected body areas are hands (at the ends of the fingers and thumbs), neck, lower back, knees, and hips as shown in Figure 1.1. Often occurs in subjects between 40 and 50 years of age. Bolik et al. [8] reported that the OA disables approximately 10% of persons over the age of 60 years. For end stage knee OA, total knee replacement (TKR) has developed into a successful treatment option and it is one of the most performed elective surgical procedures nowadays. However the high impact on quality life of the disease is well documented [9] [10];

- Knee injuries, like anterior cruciate ligament (ACL) and/or meniscus rupture [11] [12];

All these types of injury can have different levels of severity based on several factors like subject's age, his/her clinical history, weight, etc. but all of them introduce, in the patient's life, a certain grade of disability for a period of time. Vargas-Valencia et al. [4] reported that about 15% of the world's population live with some disability condition, of which 2%–4% suffer significant functional problems [13]. In this scenario, clinicians and physiotherapists' aim is to reduce the number of patients, or at least to improve their living conditions, through neuromuscular rehabilitation. An efficient rehabilitation program, in fact, can improve subjects' mobility, especially after lower limbs surgery. In the first 2-3 weeks after the intervention, the patient has to regain the gait function and to restore the range of motion (RoM) of the articulation (i.e. differences between maximum knee angle and the minimum knee angle) at pre-surgery levels, in order to avoid mobility problems in the future [14]. Clinicians can determine the patient's level of autonomy and the optimal care he should receive based on assessments of functional activities, such as walking. [15].]. Therefore, it is essential to improve diagnosis, treatments and measure patient evolution, to understand and systematically characterize movement disorders [4]. For the diagnosis and management of knee health (e.g., following an acute knee injury during rehabilitation), it is now a standard procedure to use is a combination of physical exams and medical imaging, where imaging provides information limited for rehabilitation planning (e.g. duration of therapeutic interventions), the management of which is usually based on repeated physical examinations focused on subjective measures of pain, RoM, edema, and rattle during the execution of examination maneuvers (for example front drawer test, pivot test, etc.) [16]. More in general, in clinical practice there are some subjective tools like patient reported outcome measures (PROMs), clinician-administered scales (CAS), and also by performance tests such as the Timed Up-and-Go (TUG) [17], or the 6-Minute Walk test (6MWT) [18]. These tests have positive predictive values below 20% [19]. during the rehabilitation period, the medical team and the patient rely mainly on subjective analysis, on the symptoms reported by the patient and on the levels of functional activity of daily life, to best calibrate the treatment regimen to be adopted. These variations are unique and exclusive for each clinical case analysed. This necessitates the creation/adoption of a more sensitive and objective method to monitor the rehabilitation process after joint injuries [16] and, most in general, for knee monitoring. In response to this need to objectively judge patients' performance the motion analysis is extensively used for the quantitative and qualitative assessment of motor function in basic research as well as clinical and sport applications. The estimation of joint angular displacements is a fundamental part of human motion analysis and involves the detection of joint position and spatial orientation [20]. As reported by Vargas et al. in [4] :"The

relevance of these parameters is observed in many clinical scenarios such as gait training after surgery and rehabilitation in patients with stroke, Parkinson's disease and cerebral palsy [21] [22] [23]".

1.2 Gait analysis

The health status of a subject's musculoskeletal apparatus can be evaluated by extracting from the gait some parameters that allow certifying the level of mobility and/or which a certain pathology affects the mobility of the subject. The gait is one of the most natural action for the human being but, at same time, one of the most complex one to analyze under the clinical/engineeristic aspects. During the gait many muscles, in different areas of the body and with specific aims, are involved: some muscles avoid the pure movement (for example the muscles of leg), meanwhile others promote the balance and the rhythmicity of the gait (for example the oscillatory movement of the arms). Since is not possible to quantify the contribute of the single muscle or body segment to the general gait, for the clinical and engineeristic analysis of the gait, the necessary information is extracted by global data (speed, moments, accelerations, displacements, etc). This data can be global or belonging to a specific body segment (i.e. a joint, upper limbs, lower limbs, etc). Each of these parameters, known as "gait measures", describe a particular aspect of subject's gait. There are a lot of gait measures and they do not necessarily all need to be used when doing gait analysis, it depends by on each case. In the article [7] a table with the most general parameters available in gait analyses in literature are reported.

Table 1. *Quantifiable gait measures for clinical use* [7]

Quantifiable Gait Measures	Gait Disorders
Gait speed	Slow walking
Step length	Parkinson gait, small steps, gait with little steps
Step frequency (cadence)	Slow walking, gait efficiency
Stride-stride variability	Abnormal rhythm of gait

Step width	Cerebellar gait (ataxic gait), wide base, extremely narrow base
Step height, in the sense of vertical displacement of the center of mass	Peripheral neuropathic gait, foot drop, high stepping gait
Transverse plane signal amplitude	Hemiplegic gait, diplegic gait, circumduction, scissor gait
Knee joint angle	Crouch gait, drop foot, equine gait, stiff knee
Ankle joint angle	Equine gait, crouch gait
Number of steps during turning	Difficulty with turning
Hip flexion	Myopathic gait, waddling gait, excessive hip sway, drop of pelvis
Heel-strike amplitude, ground reaction forces	Sensory gait, stomping, stamping
Motion signal distribution	Tremor
Stance time	Antalgic gait, hesitation
Swing time	Difficulty in clearing off at toe off, difficulty in swinging
Double support time	Steadiness
Bilateral sensor comparison	Gait asymmetry
Gait stability measure	Wobbly gait, unstable gait
Gait complexity measure	Choreiform gait, hyperkinetic gait, jerky gait
Gait regularity measure	Reduced gait variability
Moment	Weakness during toe off
Muscle force from EMG	Muscle weakness, abnormal muscle activity

1.3 State of art

Other parameters very used in the gait analysis are the maximal knee flection, the maximal knee extension and tibial acceleration. In the field of motion analysis the gold standard is represented by the three-dimensional (3D) optical motion capture systems, such as the VICON (Oxford Metrics Limited, Oxford, United Kingdom) shown in figure 1.2 [24].
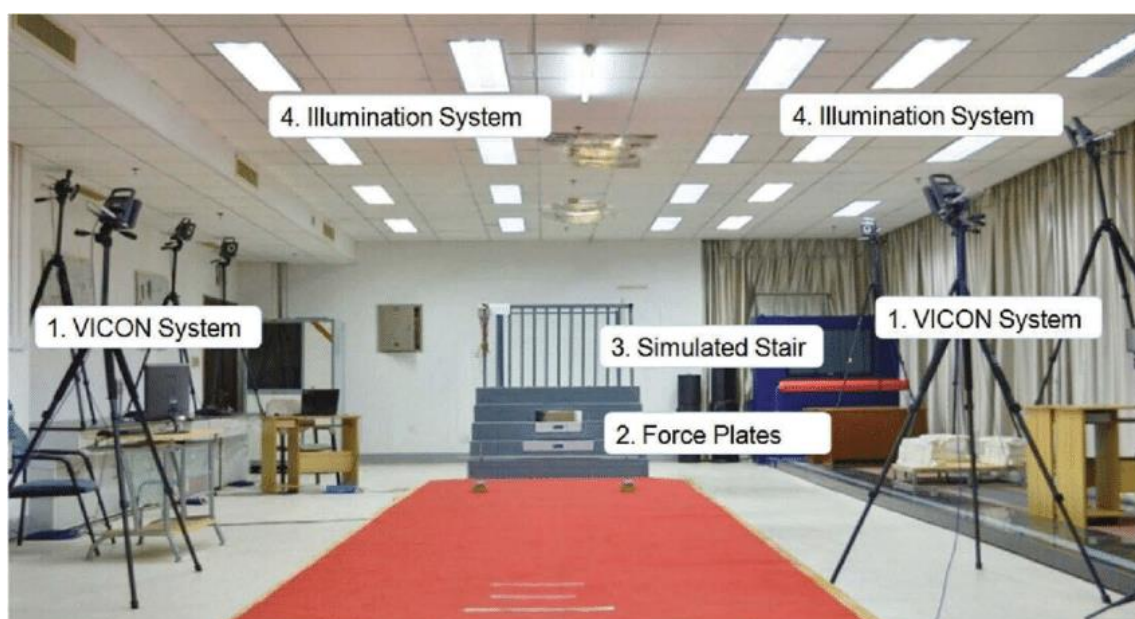
Figure 1.2 *A typical set-up for gait analyses with optical motion capture system* [25]

With infrared cameras capturing body motion defined by the reflective markers, these systems track spatial information and human motion, and provide high-precision data at a sampling rate of 100–200 Hz. Although such systems can deliver highly accurate human movement analysis, they are relatively expensive and require expert operation [26]. It means that only some specialized centers and clinics have adopted this standard gait analysis tool. Usually, these systems are used in combination with force plates (like in Figure 1.2) and electromyography (EMG) systems, that are two other quantitative gait analysis tools commonly used in those specialized centers. Force plates measure ground reaction forces (GRFs) during walking, and when synchronized with kinematic information recorded by optical motion capture systems, can provide kinetic information based on inverse dynamics.

Figure 1.3 *Surface electrodes for EMG*   ***Figure 1.4*** *Force plates*

EMG systems measures the electrical activity (i.e., whether the muscle is at rest or firing at a certain time) of a contracting muscle via either surface electrodes or fine wire electrodes. The surface electrodes are attached to the skin, though such a setup is subject to noise from the near by muscles. The more accurate and precise measurement approach is to insert fine wire electrodes into the muscle using a hypodermic needle, but it is highly invasive and can even be painful.

Either approach can only give information about whether and when the muscle is firing, but not quantitative information such as muscle forces or the amplitude of the muscle activity. However, with mathematical modelling, muscle forces can also be extracted from EMG signals [27]. EMG measurements can be critical to clinical gait assessment. Gage et al. [28] used EMG data to guide surgery for children with cerebral palsy, during which a muscle tendon may be transferred to a different location in order to correct the action of the muscle. For such surgery, EMG must be used in advance, so muscular contraction is corrected accordingly. EMG can also be used with neuroconduction studies to test peripheral neuropathy. During such tests, the EMG electrodes release an electric shock in order to stimulate the nerves of the subject, and the speed of the signals of the nerve response (i.e., nerve conduction speed) is measured. A significant delay and weakness in the response signals indicates peripheral neuropathy [29].

1.4 Inertial Measurements Unit

It is essential to replace the current gait analysis systems that provide kinematic information and EMGs, with easier to use, more economical, and portable platforms. For more than twenty years, scientific research in this field has moved towards the development and validation of a new class of wearable devices. The result was a new technology, well-known as *Micro Electro Mechanical Systems (MEMS),* that in its most general form can be defined as miniaturized mechanical and electro-mechanical elements (i.e., devices and structures) that are made using the techniques of microfabrication [30]. MEMS sensors are usually low-cost, small in size, and can be manufactured into a wrist watch size [31], which is suitable for the data collection of wearable devices. This technology was used to build, on the same integrated circuits a multi-axial combination of accelerometers, gyroscopes and eventually magnetometers that are widely available and used for orthopaedic outcome assessment [32]. This new class of wearable sensors are the Inertial Measurements Units (IMU), commonly referred to as IMUs or inertial sensors. In contrast to camera-based laboratory systems for measuring joint angles, wearable sensors present advantages of lower cost, higher flexibility, portability and adaptability [14], [33]. These sensors are which can be attached to different body segments to estimate joint kinematics.

Using the inertial/magnetic measurement technique, several advantages can be achieved. The two main advantages are:

1. Missing of intrinsic latency (all delays are attributed to data transmission), making it the measurement technique suitable for real-time measurements

2. In contrast with electromagnetic, acoustic and optical devices, that require a source of emissions to be able to trace objects, IMUs can be used on the object/subject without any kind of self-emission source [34] [35] .

Considering their usability in indoor and outdoor environments, in addition to a reduced dressing time, these sensors represent a technology, becoming an alternative to high-cost optical systems [4] [36] [37] [38] [39] [40] .
Among the quantifiable gait measures above mentioned in Table I, one of the most important is the knee joint angle. The RoM of this joint is a functional parameter related to the outcome along the rehabilitation path and the level of mobility of both a patient undergoing surgery and a healthy subject. In fact, restricted RoM of the lower limb joints hinders the performance of activities of daily living (ADL) [41] such as walking, standing up, and climbing stairs. [42], [43], [44] Patients may also have difficulty with activities such as dressing, using the toilet, bathing, picking up objects, crouching, tying shoelaces, and clipping toenails. [42], [43], [45],

[46]. Other important parameters, linked to RoM, are max knee extension and max knee flexion. In literature, there are many different approaches to calculating this parameter that differ to use accelerometers, gyros and magnetometers individually or combined. We have provided some interesting examples below that could, shortly, be used in clinical evaluations:

1. The "DynaPort Knee Test" (DPKT) produces mobility parameters during predetermined activities using accelerometers (e.g. walking, sit-stand), which are correlated with knee function, and evaluates execution quality based on an ordinal scale [47].

2. Eric Allseits et al. [48] have developed a novel gyroscope only (GO) algorithm which calculates knee angle from integration of a gyroscope derived knee angular velocity (KAV) signal. As explained in [49], the main characteristics of this algorithm is "To eliminate drift in the integral of angular velocity, a zero-angle update (ZAU) derived from a characteristic point in the knee angular velocity is applied to every stride. This point is identified using gait phase knowledge provided by a previously published noise-zero crossing (NZC) gait phase algorithm".

3. The system KINEMATICWEAR – developed by M. Schulze et al. [50] in close collaboration of computer scientists and physicians performing knee arthroplasty - consists of two sensor nodes with combined tri-axial accelerometer, gyroscope and magnetometer to be worn under normal trousers.

In many applications described in the literature, 3 or more sensors are used that are not necessarily IMU but are often miniature accelerometers or gyroscopes made using MEMS technology. Even when the IMUs are used, however, the information is extracted from one of the devices and the data of the other two are used for corrections or for obtaining outline information. Using only the accelerometer or gyroscope has the advantage of easily understanding the output data, but also the following disadvantages: the accelerometers data are sensitive to placement variability and can contain significant amounts of Gaussian noise and gait cycle-dependent noise from vibratory modes, while with gyroscopes data are affected by drift problem and by gimbal lock problem. The gimbal lock problem can be described as the loss of information by one plane of gyroscope. This happens when, during movement, two rotating axes align towards the same direction and the gyroscope lose one degree of freedom. Magnetometers are often used to derive the orientation respect to the Earth's magnetic field and therefore allow to establish the position in a global three-dimensional reference system if there is not the presence of electromagnetic source that can alter the measurements. This topic has

evolved into a wide and solid field of research, but clinical applications involving the use of IMUs are still largely unexplored in the literature, despite many research groups have spent resources and efforts to introduce, over the years, a lot of different approaches and algorithms based on the use of IMUs. Although there are a few commercial offerings such as GaitUp (Renens, Switzerland), Dynaport (Den Haag, Netherlands), Xsens (Enschede, Netherlands), Delsys (Natick, MA) and Shimmer (Dublin, Ireland) also offer proprietary software algorithms for motion analysis or activity monitoring the most published studies in orthopedic have used self-developed algorithms.

1.5 IMUs' problems

Recently, a systematic review [51] was done to compare the performance of 17 algorithms present in scientific literature based on influence of sensor position, analysed variable and computational approach in gait timing estimation. The authors' conclusions at the end of this review was that no proposed algorithm can be, generally, preferred over the others.

The lack of supremacy by an algorithm, type of sensor or approach has two reasons:

1. Only a few manufacturing companies produce sensitive units for data collection (for example Bosch, Invensene, STM). This means that few manufacturers supply almost all manufacturers of hardware devices for IMUs. The consequence of this market condition is the low variability between features of a lot of different devices, like for example basic sensor resolutions, ranges and accuracies. Generally, they differentiate themselves in:

   - design (shape, size, weight influencing patient compliance, skin movement artefact
   - functionality (for example control switches and LED, battery life, charging, configuration options, data output format)
   - connectivity (cable, wireless)
   - data pre-processing which can produce derived parameters or use sensor fusion in combination with e.g. Kalman filters to increase accuracy [52].

2. No standardized guidelines both for placing sensors on body segments and defining joint coordinate systems (JCS) are defined. Also, there are some studies that questioned the accuracy of these systems [53] [54] [55] [56] [57]. The conclusions were that the

calibration stages of the individual sensors (i.e., accelerometer, gyroscope, and magnetometer), biases, sensibilities and different noise types, in addition to sensor fusion algorithm issues, influence significantly the accuracy of the orientation estimation.

Against this background, a fundamental problem of the IMU-based gait analysis is to how define an appropriate measurement protocol and to draw up a common protocol for the placing of the sensors on the body segments [58]. Different research teams have presented in the literature different methods to determine the sensor frame's orientation, after they have been applied to the human body [29-31] [59]. However, those approaches suffer from some limitations linked to which sensor is mostly used. For example, with algorithms based only on data from accelerometers and gyroscopes [27] [29] [60] [61] the difficulty is to measure 3D angles directly and, to solve this problem, a second global reference axis is necessary. This second global reference system is usually along with the gravity vector. Another important problem within systems that involve only accelerometers and gyroscopes is the heading drift. The approaches presented in literature to overcome this issue and to correctly define the axis of joint motion are:

- the performing of predefined movements by the subject [27]
- use supplementary devices such as cameras [41], anatomical landmark pointers [28] or exoskeleton harnesses [29]
- performing complex movements while keeping some specific postures [29, 30, 39]
- maintaining the same orientation or joint angle between two postures [11, 41]

However, these approaches are not optimal because they need additional tools, experienced personnel and they increase the experiment duration, without considering that may not be applicable to subjects with motor disabilities. Some solutions to easily align the sensors to the body segments are proposed [62] [63] but none are incorporated into a standardized clinical procedure.

A possible solution to the problems of alignment and positioning into a 3D space seems to be the use of quaternions in the analysis of movement.

1.6 Quaternion

The quaternion is a mathematical entity discovered by William Rowan Hamilton in 1843. Recently it has become widely used in fields like 3D graphics, virtual reality, robotics, theorical physic and human motion because they particularly indicated for the calculate or the simulation of movements.

A more complete discussion, with all mathematical definitions and proprieties about this topic, is reported in the Appendices.

The quaternion is a complex number and it can describe the orientation and the rotation of a body in 3D space. Every rotation, in 3D space, can be defined as a combination of an axis and a rotation angle. The quaternion is a simpler way to represent it than rotation matrix but is less intuitive for the user.

In the article [64] , Lee JK and Jung WK presented a new quaternion-based local frame alignment method has been proposed, where the equations of angular velocity transformation are used to determine the frame alignment orientation in the form of quaternion. Although the IMU sensor was not attached to the body above a plastic ruler of the right triangle, the alignment was almost perfect (an error less than 3° degrees), showing that with the use of this mathematical tool it is possible to overcome the alignment problem

1.7 Our project

Almost all the articles and papers in the literature aim to make parameter calculation methods more precise, trying to obtain the same results as the state-of-the-art tools but with wearable and less expensive technologies. All validation tests are performed in well-controlled environments that do not mimic the real conditions of daily human activities well, without considering the well-known fact that supervised patients in a laboratory environment strive to walk particularly well, thus presenting themselves with artificial gait patterns. To assess the real status of knee health, it would be necessary to matching motion laboratory measurements with continuous knee monitoring in real life. To our knowledge, several projects, in the scientific literature and the commercial field, has been developed to monitor the knee function outside the environment of motion laboratory, such for example [49] [64] [65] [65]. Although all these projects have achieved promising results (like a high correlation with motion capture system) and have interesting aspects (sensor placement, extraction of gait features,

applications to daily life), they use commercial sensors (some projects are commercial solutions covered by copyright) and algorithms based on gyroscope and accelerometer, incurring in the above-mentioned problems.

In order to overcome all the limitations linked to the acquisitions in a well-controlled environmental, cover the clinical needs of biomechanical monitoring of knee motions in daily life and to provide simple solution for knee monitoring in real life conditions, a team research of the Luxembourg Institute of Health (LIH) is carrying on a project to develop, validate and apply a knee monitoring solution based on such wearable sensors. The candidate was involved in the initial phase of this project and, in this master thesis work, the selected methodologies and the results obtained will be describe.

It is the aim of this phase of the project to:

1)   make a low-cost (few tens of euros), self-assembled IMU/Arduino system operational to be used as a developmental dual-IMU activity monitoring platform (by e.g. software for connection, communication, configuration, etc.).

2)   Write, adapt and develop further a pre-existing algorithm to calculate knee angles, primarily flexion angles based on the quaternion outputs.

3)   Test and take steps towards validating the output of the sensor/algorithm set-up against a gold standard (3-D motion capture) for several activities relevant for patients with knee pathologies and outcomes.

References

[1] v. L. S. S. R. H. I. G. B. Lipperts M., «Clinical validation of a body-fixed 3D accelerometer and algorithm for activity monitoring in orthopaedic patients,» *Journal of Orthopaedic transltion,* vol. 29, pp. 11-19, 2017.

[2] B. . Belgen, M. Beninato, P. Sullivan e K. Narielwalla, « The association of balance capacity and falls self-efficacy with history of falling in community-dwelling people with chronic stroke.,» *Arch. Phys. Med. Rehabil.,* vol. 87, n. 1, p. 554–561, 2006.

[3] N. Chrysagis, E. Skordilis, G. Tsiganos e D. Koutsouki, «Validity evidence of the Lateral Step Up (LSU) test for adolescents with spastic cerebral palsy.,» *Disabil. Rehabil,* vol. 35, n. 2, p. 875–880, 2013.

[4] E. A. R. E. B.-F. T. F. A. Vargas-Valencia LS, «An IMU-to-Body Alignment Method Applied to Human Gait Analysis.,» *Sensors,* vol. 12, p. 16, 2016.

[5] A. K. Woolf AD, «Understanding the burden of musculoskeletal conditions.,» *BMJ,* vol. 322, n. 3, p. 1079–1080, 2001.

[6] P. B. Woolf AD, «Burden of major musculoskeletal conditions,» *Bull World Health Organ,* vol. 81, n. 4, p. 646–656, 2003.

[7] J. L. B. L. G.-Z. Y. Shanshan Chen, «Toward Pervasive Gait Analysis with Wearable Sensors: A Systematic Review,» *IEEE JOURNAL OF BIOMEDICAL AND HEALTH INFORMATICS,* vol. 20, n. 5, p. 1521, 2016.

[8] S. Bolink e L. M. H. I. G. B. van Laarhoven SN, «Inertial sensor motion analysis of gait, sit-stand transfers and step-up transfers: differentiating knee patients from healthy controls.,» *Physiological Measurement,* vol. 33, n. 11, pp. 1947-58, 2012.

[9] S. M. v. d. A.-S. I. Z. W. a. G. J. W. Wagenmakers R, « Predictive value of the Western Ontario and McMaster universities osteoarthritis Index for the amount of physical activity after total hip arthroplasty,» *Phys. Ther.,* vol. 88, n. 6., pp. 211-218, 2008.

[10] S. M. L. a. D. M. R. Stevens-Lapsley J E, «Comparison of self-reported knee injury and osteoarthritis outcome score to performance measures in patients after total knee arthroplasty,» *PM R,* vol. 3, n. 7, pp. 541-549, 2011.

[11] G. D. M. [. a. C. E. Q. Timothy E. Hewett, «Mechanisms, Prediction, and Prevention of ACL Injuries: Cut Risk with Three Sharpened and Validated Tools.,» *J Orthop Res.,* vol. 34(11), n. 8, pp. 1843-1855, 2016.

[12] W. F. B. A. W. R. R. S. Fox AJ, «The human meniscus: a review of anatomy, function, injury, and advances in treatment.,» *Clin Anat.,* vol. 28(2), n. 9, pp. 269-287, 20154.

[13] W. H. O. &. W. B. W. R. o. Disability.. [Online]. Available: http://www.who. int/disabilities/world_report/2011/report/en). .

[14] G. Carter, «Rehabilitation Management in Neuromuscular Disease,» *J. Neuro. Rehab.,* vol. 11, n. 2, pp. 69-80, 1997.

[15] K. Hashimoto, K. Higuchi, Y. Nakayama e M. Abo, «Ability for basic movement as an early predictor of functioning related to activities of daily living in stroke patients,» *Neurorehabil. Neural Repair,* vol. 21, n. 12, pp. 353-357, 2007.

[16] W. D. T. C. H. S. P. M. M.-S. M. K. G. S. M. Inan OT, «Wearable knee health system employing novel physiological biomarkers.,» *Journal of applied physiology,* vol. 124, n. 3, pp. 537-547, 2018.

[17] d. e. o. A. A. K. r. greene Br, «Frailty status can be accurately assessed using inertial sensors and the TUG test,» *Age Ageing,* vol. 43, n. 13, pp. 406-411, 2014.

[18] h. r. h. m. t. C. r. e. B. K. dobson f, «Measurement properties of performance-based measures to assess physical function in hip and knee osteoarthritis: a systematic review,» *Osteoarthritis Cartilage ,* vol. 20, n. 14, pp. 1548-1562, 2012.

[19] O. P. K. K. Jackson JL, «Evaluation of acute knee pain in primary care.,» *Ann Intern Med,* vol. 139, n. 13, pp. 575-588, 2003.

[20] A. Muro-de-la-Herran, B. García-Zapirain e A. Méndez-Zorrilla, «Gait analysis methods: An overview of wearable and non-wearable systems, highlighting clinical applications.,» *Sensors,* vol. 14, n. 14, pp. 3362-3394, 2014.

[21] F. Casamassima, A. Ferrari, B. Milosevic, P. Ginis, E. Farella e L. Rocchi, «A wearable system for gait training in subjects with Parkinson's disease,» *Sensors,* vol. 14, n. 15, pp. 6229-6246, 2014.

[22] N. Byl, W. Zhang, S. Coo e M. Tomizuka, «Clinical impact of gait training enhanced with visual kinematic biofeedback: Patients with Parkinson's disease and patients stable post stroke,» *Neuropsychologia,* vol. 79, n. 16, pp. 332-343, 2015.

[23] J. Van den Noort, A. Ferrari, A. Cutti, J. Becher e J. Harlaar, «Gait analysis in children with cerebral palsy via inertial and magnetic sensors.,» *Med. Biol. Eng. Comput.,* vol. 51, n. 17, pp. 377-386, 2013.

[24] D. H. Sutherland, «The evolution of clinical gait analysis part III— Kinetics and energy assessment,,» *Gait Posture,* vol. 21, n. 18, pp. 447-461, 2005.

[25] J. Z. W. S. Z. C. H. G. D. M. Qipeng Song, «Long-term Tai Chi exercise increases body stability of the elderly during stair ascent under high and low illumination,» *Sports Biomechanics,* vol. 17, n. 3, pp. 1-12, 2017.

[26] S.R.Simon, «Quantification of human motion: Gait analysis-benefits and limitations to its application to clinical problems,» *J. Biomech,* vol. 37, n. 19, pp. 1869-1880, 2004.

[27] J. P. R. R. H. S. K. a. J. R. W. J. R. Gage, «Rectus femoris transfer to improve knee function of children with cerebral palsy,,» *Develop. Med. Child Neurol.,* vol. 29, n. 20, pp. 159-166, 1987.

[28] A. a. H. A.Moghtaderi, «ValidationofMichigan neuropathy screening instrument for diabetic peripheral neuropathy,» *Clin. Neurol. Neurosurg.,* vol. 108, n. 21, pp. 477-481, 2006.

[29] R. L. W. a. S. Mulroy, «The energy expenditure of normal and pathologic gait,» *Gait Posture,* vol. 9, n. 22, pp. 207-231, 1999.

[30] BUSINESS WIRE, «BUSINESS WIRE,» BUSINESS WIRE, 26 August 2016. [Online]. Available: https://www.businesswire.com/news/home/20160826005021/en/Global-Micro-Electro-Mechanical-Systems-Market-grow-CAGR-Close-12.

[31] X. Yun e E. Bachmann, «Design, Implementation, and Experimental Results of a Quaternion-Based Kalman Filter for Human Body Motion Tracking,» *IEEE Trans. Robot,* vol. 22, n. 23, pp. 1216-1227, 2006.

[32] I. Pasciuto, G. Ligorio, E. Bergamini, G. Vannozzi, A. Sabatini e A. Cappozzo, «How angular velocity features and different gyroscope noise types interact and determine orientation estimation accuracy.,» *Sensors,* vol. 15, n. 24, p. 23983–24001, 2015.

[33] W. Tao, T. Liu, R. Zheng e H. Feng, «Gait analysis using wearable sensors,» *Sensors,* vol. 12, n. 25, pp. 2255-2283, 2012.

[34] X. W. Zhang X, «A Fuzzy Tuned and Second Estimator of the Optimal Quaternion Complementary Filter for Human Motion Measurement with Inertial and Magnetic Sensors.,» *Sensors,* vol. 18, n. 10, p. 3517, 2018.

[35] H. Fourati, N. Manamanni, L. Afilal e Y. Handrich, « Complementary Observer for Body Segments Motion Capturing by Inertial and Magnetic Sensors.,» *IEEE/ASME Trans. Mechatron.,* vol. 19, pp. 149-157, 2014.

[36] H. Luinge, P. Veltink e C. Baten, «Ambulatory measurement of arm orientation,» *J. Biomech.,* vol. 40, pp. 78-85, 2007.

[37] P. Picerno, A. Cereatti e A. Cappozzo, «Joint kinematics estimate using wearable inertial and magnetic sensing modules,» *Gait Posture,* vol. 28, pp. 588-595, 2008.

[38] J. Favre, R. Aissaoui, B. Jolles, J. De Guise e K. Aminian, «Functional calibration procedure for 3D knee joint angle description using inertial sensors.,» *J. Biomech.,* vol. 42, pp. 2330-2335, 2009.

[39] A. Cutti, A. Ferrari, P. Garofalo, M. Raggi, A. Cappello e A. Ferrari, «"Outwalk": A protocol for clinical gait analysis based on inertial and magnetic sensors.,» *Med. Biol. Eng. Comput.,* vol. 48, n. 30, p. 17–25., 2010.

[40] E. Palermo, S. Rossi, F. Marini, F. Patanè e P. Cappa, « Experimental evaluation of accuracy and repeatability of a novel body-to-sensor calibration procedure for inertial sensor-based gait analysis.,» *Meas. J. Int. Meas. Confed.,* vol. 52, pp. 145-155, 2014.

[41] R. E., «Preventive aspects of mobility and functional disability.,» *Scand J Rheumatol Suppl.,* vol. 82, n. 46, pp. 25-32, 1989.

[42] G.-M. J. G. P. M. R. O. A. Alarcon T., «Activities of daily living after hip fracture: profile and rate of recovery during 2 years of follow up.,» *Osteoporos Int.,* vol. 22, p. 1609–1613., 2011.

[43] B. I. N. R. Dechartres A., «Evolution of disability in adults with hip arthroplasty: a national longitudinal study.,» *Arthritis Rheum.,* vol. 57, p. 364–371, 2007.

[44] F. A. S. A. H. W. McGrory B.J., «Correlation of measured range of hip motion following total hip arthroplasty and responses to a questionnaire.,» *J Arthroplasty.,* vol. 11, p. 565–571, 1996.

[45] H. M. D. G. Curry L.C., «Functional status in older women following hip fracture,» *J Adv Nurs,* vol. 42, p. 347–354, 2003.

[46] B. H. S. S. M. S. W. U. Hemmerich A., «Hip, knee, and ankle kinematics of high range of motion activities of daily living.,» *J Orthop Res,* vol. 24, n. 4, p. 770–781, 2006.

[47] O. G. M. R. M. A. V. d. S. R. C. V. L. J. H. V. D. B. P. R. J. B. P. I. J. M. W. N. Van den Dikkenberg, «Measuring functional abilities of patients with knee problems: rationale and construction of the DynaPort knee test,» *Knee Surg Sports Traumatol Arthrosc,* vol. 10, n. 4, pp. 204-212, 2002.

[48] K. J. K. ,. C. B. R. G. I. G. a. V. A. Eric Allseits, «A Novel Method for Estimating Knee Angle Using Two Leg-Mounted Gyroscopes for Continuous Monitoring with Mobile Health Devices,» *Sensors,* vol. 18, p. 2759, 2018.

[49] E. Allseits, J. Lucˇarevic´, R. Gailey, V. Agrawal, I. Gaunaurd e C. Bennett, « The Development and Concurrent Validity of a Real-time Algorithm for Temporal Gait Analysis using Inertial Measurement Units.,» *J. Biomech.,* vol. 55, pp. 27-33, 2017.

[50] T. C. M. G. K. W. T. L. F. S. R. B. H. W. a. M. M. M. Schulze, «Development and clinical validation of an unobtrusive ambulatory knee function monitoring system with inertial 9DoF sensors,» *34th Annual International IEEE EMBS Conference,* 2012.

[51] e. a. G.Pacini Panebianco, «Analysis of the performance of 17 algorithms from asystematic review: Influence of sensor position, analysed variable and computational approach in gait timing estimation from IMU measurements,» *Gait & Posture,* vol. 66, pp. 76-82, 2018.

[52] B. S. Grimm B, «Evaluating physical function and activity in the elderly patient using wearable motion sensors.,» *EFORT,* vol. 1, n. 5, pp. 112-120, 2017.

[53] P. Picerno, A. Cereatti e A. Cappozzo, «A spot check for assessing static orientation consistency of inertial and magnetic sensing units,» *Gait Posture,* vol. 33, pp. 373-378, 2011.

[54] E. Bergamini, G. Ligorio, A. Summa, G. Vannozzi e A. S. A. Cappozzo, «Estimating orientation using magnetic and inertial sensors and different sensor fusion approaches: Accuracy assessment in manual and locomotion tasks,» *Sensors,* vol. 14, n. 34, pp. 18625-18649, 2014.

[55] I. Pasciuto, G. Ligorio, E. Bergamini, G. Vannozzi, A. Sabatini e A. Cappozzo, «How angular velocity features and different gyroscope noise types interact and determine orientation estimation accuracy.,» *Sensors,* vol. 15, p. 23983–24001. , 2015.

[56] K. Lebel, P. Boissy, M. Hamel e C. Duval, «Inertial measures of motion for clinical biomechanics: Comparative assessment of accuracy under controlled conditions—Effect of velocity.,» *PLoS ONE,* vol. 8, p. e79945, 2013.

[57] A. Brennan, J. Zhang, K. Deluzio e Q. Li, «Quantification of inertial sensor-based 3D joint angle measurement accuracy using an instrumented gimbal,» *Gait Posture,* vol. 34, n. 37, pp. 320-323, 2011.

[58] T. Seel, J. Raisch e T. Schauer, « IMU-Based joint angle measurement for gait analysis,» *Sensors,* vol. 14, p. 6891–6909, 2014.

[59] K. O'Donovan, R. Kamnik, D. O'Keeffe e G. Lyons, « An inertial and magnetic sensor based technique for joint angle measurement.,» *J. Biomech,* vol. 40, pp. 2604-2611, 2007.

[60] J. Kavanagh, S. Morrison, D. James e R. Barrett, « Reliability of segmental accelerations measured using a new wireless gait analysis system,» *J. Biomech.,* vol. 39, p. 2863–2872., 2006.

[61] S. Tadano, R. Takeda e H. Miyagawa, «Three dimensional gait analysis using wearable acceleration and gyro sensors based on quaternion calculations.,» *Sensors,* vol. 13, pp. 9321-9343, 2013.

[62] A. E. E. R. B.-F. a. A. F. LauraSusana Vargas-Valencia, «An IMU-to-Body Alignment Method Applied to Human Gait Analysis,» *Sensors,* vol. 16, n. 44, p. 2090, 2016.

[63] M.-A. B. T. S. a. T. S. Philipp Muller, «Alignment-Free, Self-Calibrating Elbow Angles Measurement using Inertial Sensors,» *IEEE Journal of Biomedical and Health Informatics,* vol. 21, n. 45, pp. 312-319, 2017.

[64] J. W. Lee JK, «Quaternion-Based Local Frame Alignment between an Inertial Measurement Unit and a Motion Capture System,» *Sensor,* vol. 18, n. 11, p. 4003, 2018.

[65] S. B. V. L. M. L. I. H. B. G. a. R. S. L Verlaan, «Accelerometer-based Physical Activity Monitoring in Patients with Knee Osteoarthritis: Objective and Ambulatory Assessment of Actual Physical Activity During Daily Life Circumstances,» *The Open Biomedical Engineering Journal,* vol. 9, pp. 157-163, 2015.

[66] Claris Healthcare Inc, «Claris Reflex,» Claris Healthcare Inc, [Online]. Available: https://clarisreflex.com/.

[67] «TracPatch – Wearable Device for Post-op Total Joint Patients,» TracPatch, [Online]. Available: https://www.tracpatch.com/.

2. METHODS

From the fusion and adaptation of two previous solutions for the calculation of the knee angle, the project described in this thesis work was created. One solution consists of two sensors, built with Arduino components, and a Computer App, all developed by Professor Lukasz Lapaj (Department of General Orthopaedics, Musculoskeletal Oncology and Trauma Surgery, Poznan University of Medical Sciences, Poland). The other one consists of two commercial sensors and an algorithm, based on the use of quaternions, developed by professor Matthijs Lipperts (AHORSE, Department of Orthopaedics, Zuyderland Medical Centre, The Netherlands). Since we want to create a new, low expensive, user friendly and simple solution, we take, from these two solutions, the most interesting aspects.
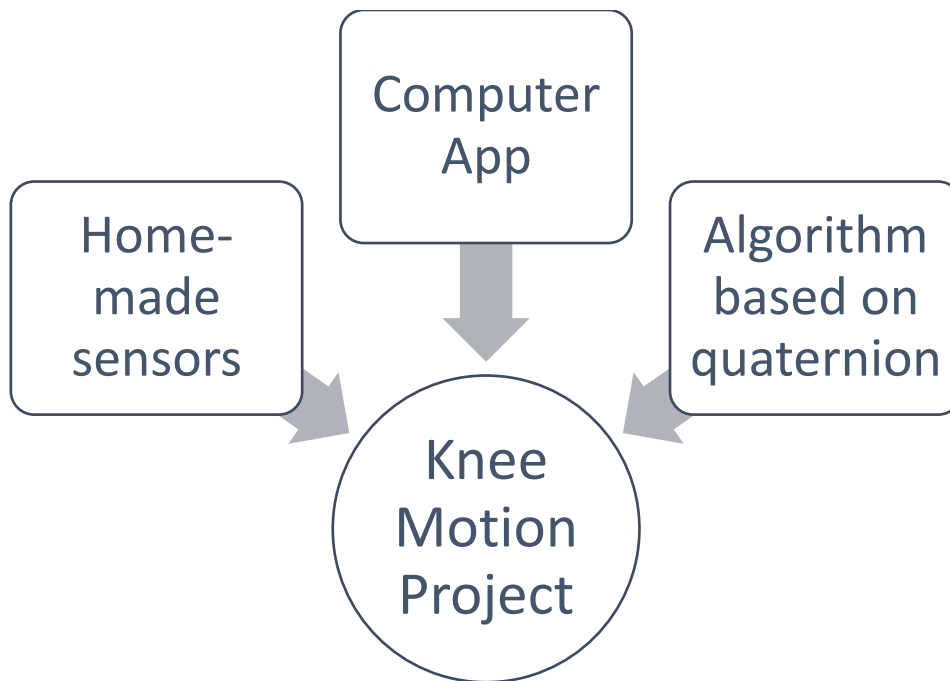
In the first and second sections of this chapter, we make a detailed explanation of all the elements that compose our project. Then we explain what we did in development phase of our solution.

2.1 Home-made sensors

Each one of these sensors is made by:

1) 1 WeMos TTGO T-Base esp8266 Wi-Fi wireless module 4mb flash I2c for Arduino, for the connection with other devices
2) 1 Adafruit bno055 absolute orientation sensor as IMU
3) 2 black plastic boxes with dimensions 6,5 cmx4,5 cmx3,0 cm (2,56"x1,77"x1,18"), for the protection against falls, shocks and atmospheric agents
4) 1 FB75254 OHP battery (500 mAh and 3.7V) as electric surgent

All the materials above mentioned are shown in the Figure 2.1.
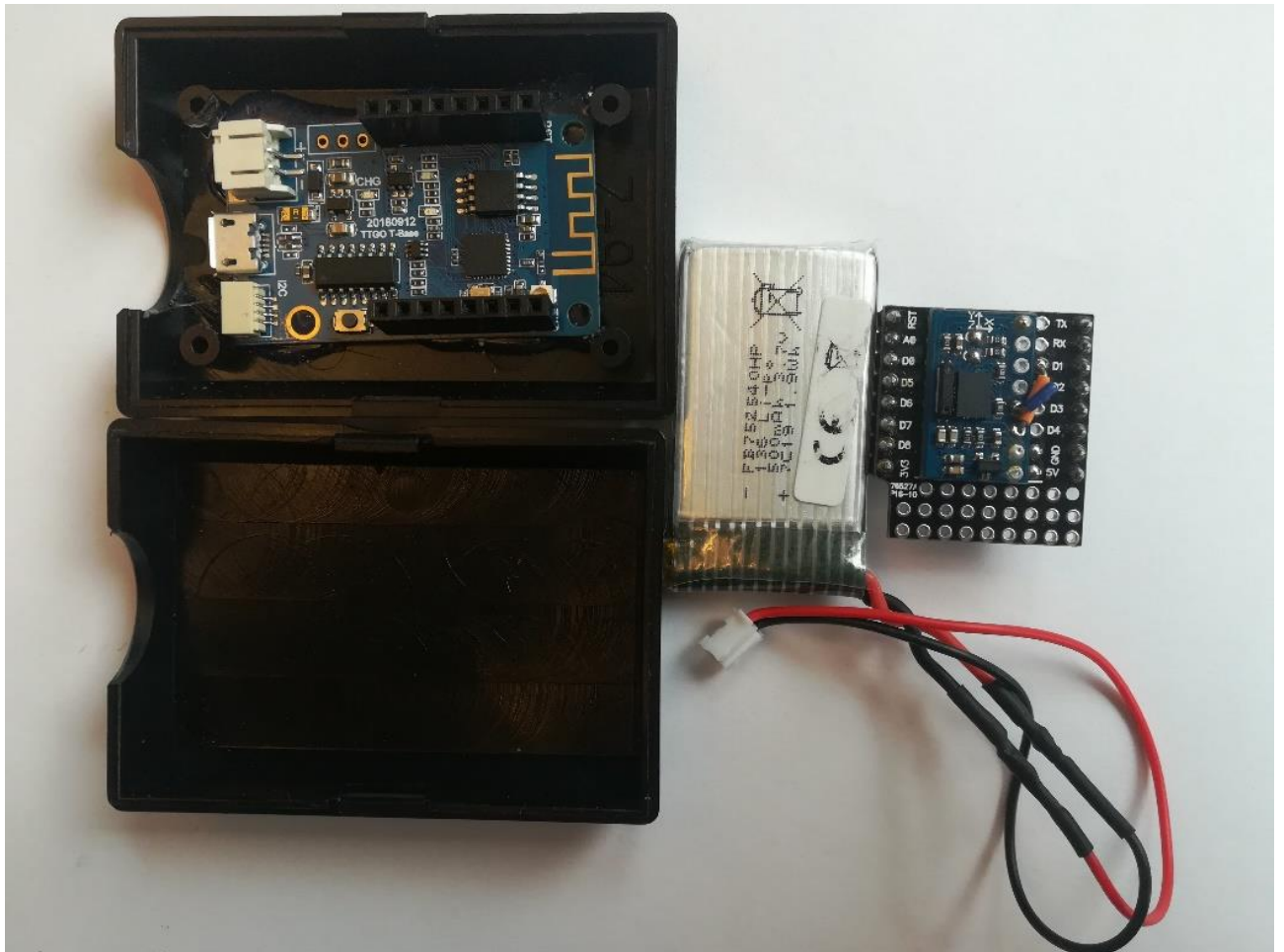
Figure 2.1 *All elements of Professor Lapaj's sensor. From left to right: a black plastic box empty (down), a black plastic box with esp8622 Wi-Fi board glued inside (up), FB75254 OHP battery and Adafruit bno055 absolute orientation sensor.*

All the commands that the board must do are included in a sketch, created with software Arduino IDE. When the sketch is upload on the board, via USB input, the code is compiled by esp8266 mini processor. A schematic diagram, with all the actions performed by these sensors,

is shown below. The functioning of the sensor can be assimilated to a switch: when the battery is plugged in, the sensors are connected to a Wi-Fi network and are sending data, independently if the app on the computer or the computer itself are ready to receive them. When there is no source to power the boards, they are completely switched off. Once loaded the sketch, the user does not have the possibility to modify the features as for example sample rate, Wi-Fi network or speed of transmission. The only way to modify the functioning is by uploading a new sketch, with different instructions, on the board. From a general point of view, we can distinguish, in all sensors, a sensitive part composed by an accelerometer, gyroscope and/or magnetometer and a processing part where all libraries are included, and all operations are performed. As specified in the chapter "Introduction", the sensitive part of most part of sensor have comparable performance (the sensitive part in black sensors is made with Bosh components), so we assumed that the accuracy of raw data are comparable with other commercial solution. What make a difference is the different approaches implemented in processing part. In our experimental solution all algorithm of sensor fusion are unknow because implemented directly by the use of Arduino libraries.

In Figure 2.2 shows how the sensor looks like with and without all protection, respectively.
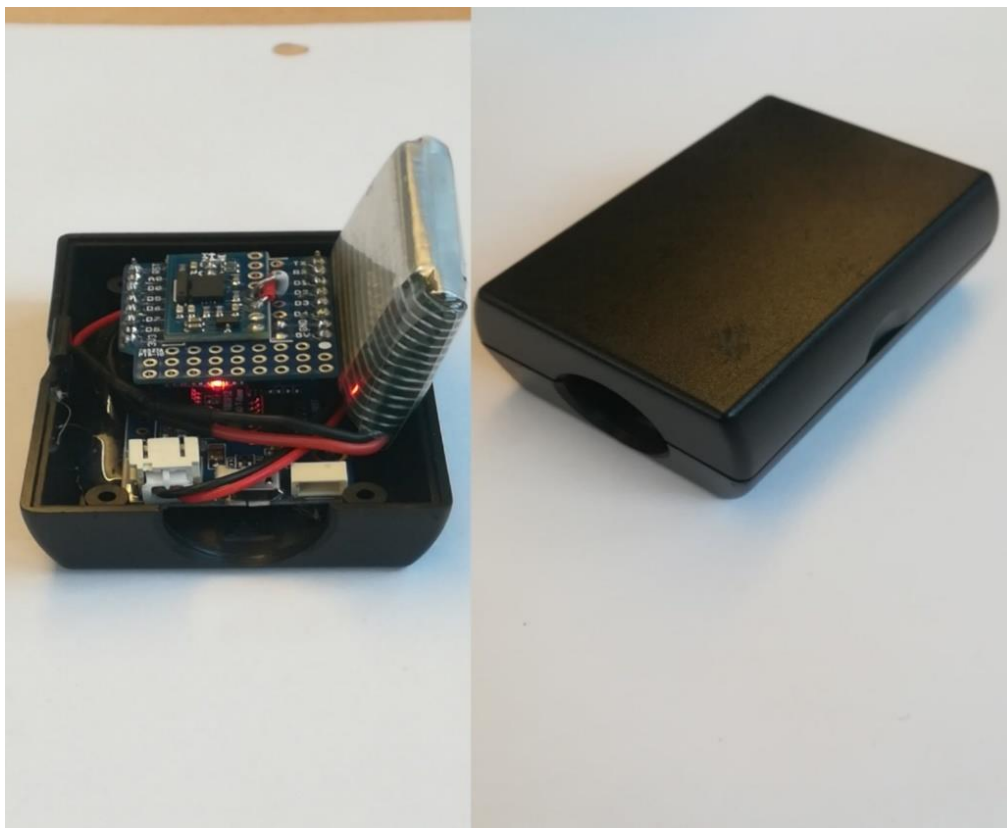
Figure 2.2 *Professor's Lapaj sensors assembled (on the left) and with all protection (on the right)*

2.2 Algorithm and Computer App

The app was created with the integrated development environmental Microsoft Visual Studio 2017 version 3.9 with which the user can select the type of internet connection, manage the streaming of data, (when it begins and ends), check if all sensors are connected and save the date received.

All these actions can be done thanks to the user-interface, shown in Figure2.3. The correct use of the app consists of 5 steps:

1) To select the type of network with the drop-down list under "Network". After that, the IP address and IP broadcast will appear besides "IP" and "bcast", respectively. During all tests performed in this project, we used a smartphone as hotspot, so the option "Wireless Network Connection" was chosen (Figure 2.4). However, the names on the list depend on the laptop where the app is used, it means that the same type of connection could have different names on different laptops.

2) To find connected devices. A necessary condition of this experimental set-up is that all sensors must be connected to the same Wi-Fi network. The app on the computer detects all the devices connected to the selected network, except the computer itself, and shows their IP addresses into the window "Console". If one of the sensors was missed, the user can repeat research with the button "Search". When all devices are connected, the app is ready for the data streaming.

3) To start data streaming with button "Start". These raw data, coming from all sensors, were displayed in different parts of the interface, especially in the window under "Incoming data counter". This version of the app was programmed to receive from the sensors the following output:

   - Eulerian angle respect X-axis (X)
   - Eulerian angle respect Y-axis (Y)
   - Eulerian angle respect Z-axis (Z)
   - Calibration of the gyroscope (gyr)
   - Calibration of the accelerometer (acc)
   - Calibration of the magnetometer (mag)
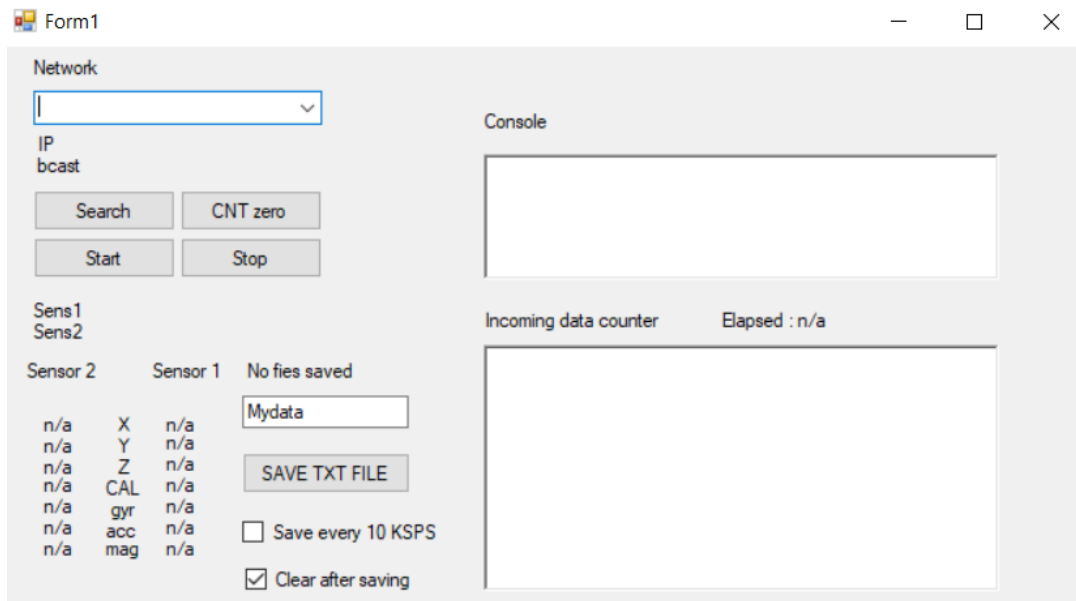
Figure 2.3 *Initial version of user interface professor Lapaj's computer app*

As reported by the official website of Adafruit (Adafruit, s.d.) [1]. "The BNO055 includes internal algorithms to constantly calibrate the gyroscope, accelerometer and magnetometer inside the device. The exact nature of the calibration process is a black box and not fully documented, but you can read the calibration status of each sensor using the ".**getCalibration**" function in the Adafruit_BNO055 library. The four calibration registers -- an overall system calibration status, as well individual gyroscope, magnetometer and accelerometer values -- will return a value between '0' (uncalibrated data) and '3' (fully calibrated). The higher the number the better the data will be".

In other words, the library allows having a scale of values, from 0 to 3, that shows to the user the inner level of calibration of each sensor and the user can check, in each sample, the status of accelerometer, gyroscope and magnetometer.
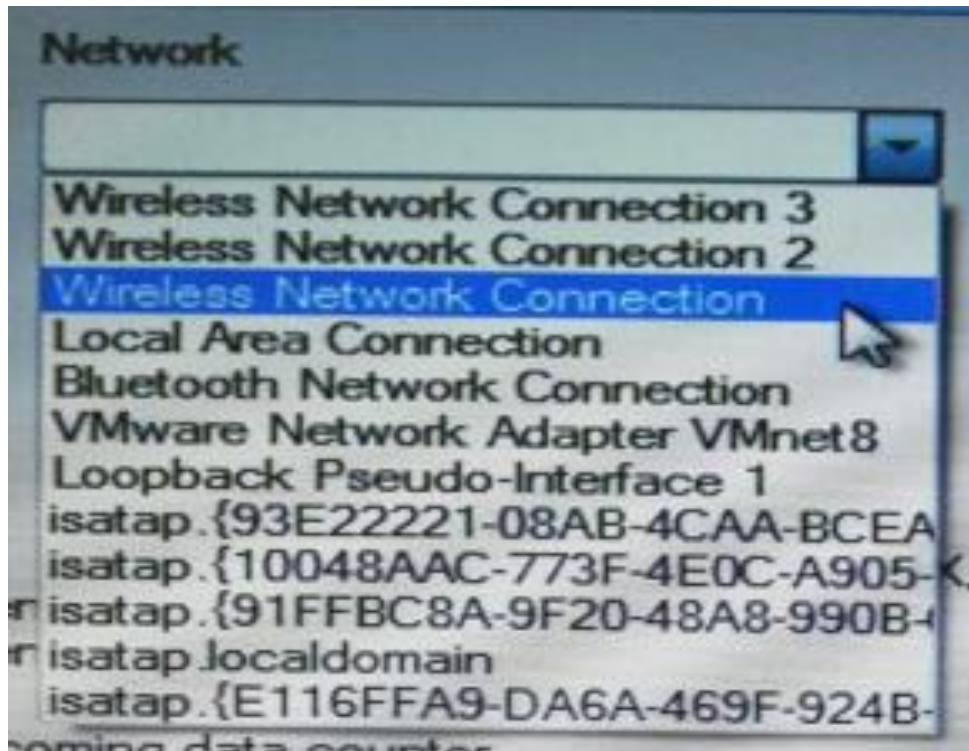
Figure 2.4 *An example of connections available on a computer*

The Euler angles, such as quaternions, are provided directly from the sensors thanks to Arduino library "utility/imumaths". They are calculated by an inner sensor-fusion algorithm that uses data from the gyroscope, accelerometer and magnetometer. Similar to the calibration procedure, this process is a not well-documented.

4) To end the acquisition with button "Stop".

5) To save the data in the window under "Incoming data counter" by pressing the button "SAVE TXT FILE". The name of the file can be changed by the user or it is automatically changed by the app to avoid the risk to overwrite the files. Professor Matthijs Lipperts shared with us his self-made algorithm created to analyse the results coming from commercial sensors GCDC Human Activity Monitor (HAM) that are a compact self-recording data logger available with several sensor variants. Data from the digital sensors are time-stamped using a real-time clock and stored to a microSD card in simple text format. When connected via the USB to a personal computer, the HAM appears as a standard mass storage device containing the comma-delimited data files and the user setup file. The HAM includes an internal 250mAh lithium-polymer rechargeable battery, which recharge using USB power. The sensors and their general features are shown below

Figure 2.5 *GCDC Human Activity Monitor (HAM) IMU sensors*

General Features of HAM-IMU

- Compact size (2.21" L 1.55" W 0.60" H, 0.9 oz)

- User selectable sample rates of 50, 100 and 200 Hz

- Accurate time stamped data using Real Time Clock (RTC)

- Data recorder to internal 8 GB flash memory

- Easily readable comma separated text data files

- Internal hardwired rechargeable Lithium-Polymer battery, charges via USB

- Data transfer compatible with Windows/Linus/mac via USB interface (no special software required)

- 3-axis accelerometer, gyroscope, magnetometer

- Quaternion orientation based on accelerometer and gyroscope data

The code of the algorithm is developed in the programming language MATLAB, version 9.4. The algorithm allows the extraction of the raw data in CSV format and, before the post-processing operations, as for example filtering and operations with quaternions, is performed on a preliminary stage for the synchronization between the sensors and the calibration on the subject. For each sample the outcome parameters given by GCDC HAM are tri-axial accelerations, tri-axial angular speed, tri-axial values of magnetic field and its quaternion, calculated by an inner algorithm based on the sensor fusion. The core of the elaboration is the

product between every quaternion and the first one, in order to obtain a new quaternion. As explained in the chapter "Introduction", this new quaternion represents the new position of the sensor in 3D space. Then is executed a conversion from quaternion to Euler angle is executed for each quaternion calculate in this way. This operation is done on both sensors. At the end of this part of the algorithm, the positions occupied by both sensors, in the subject's leg reference system, during all the duration of motion test are calculated and it is easily possible to add them or subtract them to calculate the subject's knee angle (the choice to add or to subtract the angles depends on the orientation of the sensor, in particular by the orientation of Z-axis. If the Z-axis of sensors have the same direction and, the angles will be subtracted, in the other case they will be added). An illustration about how the algorithm calculate knee angle is show in figure alongside.
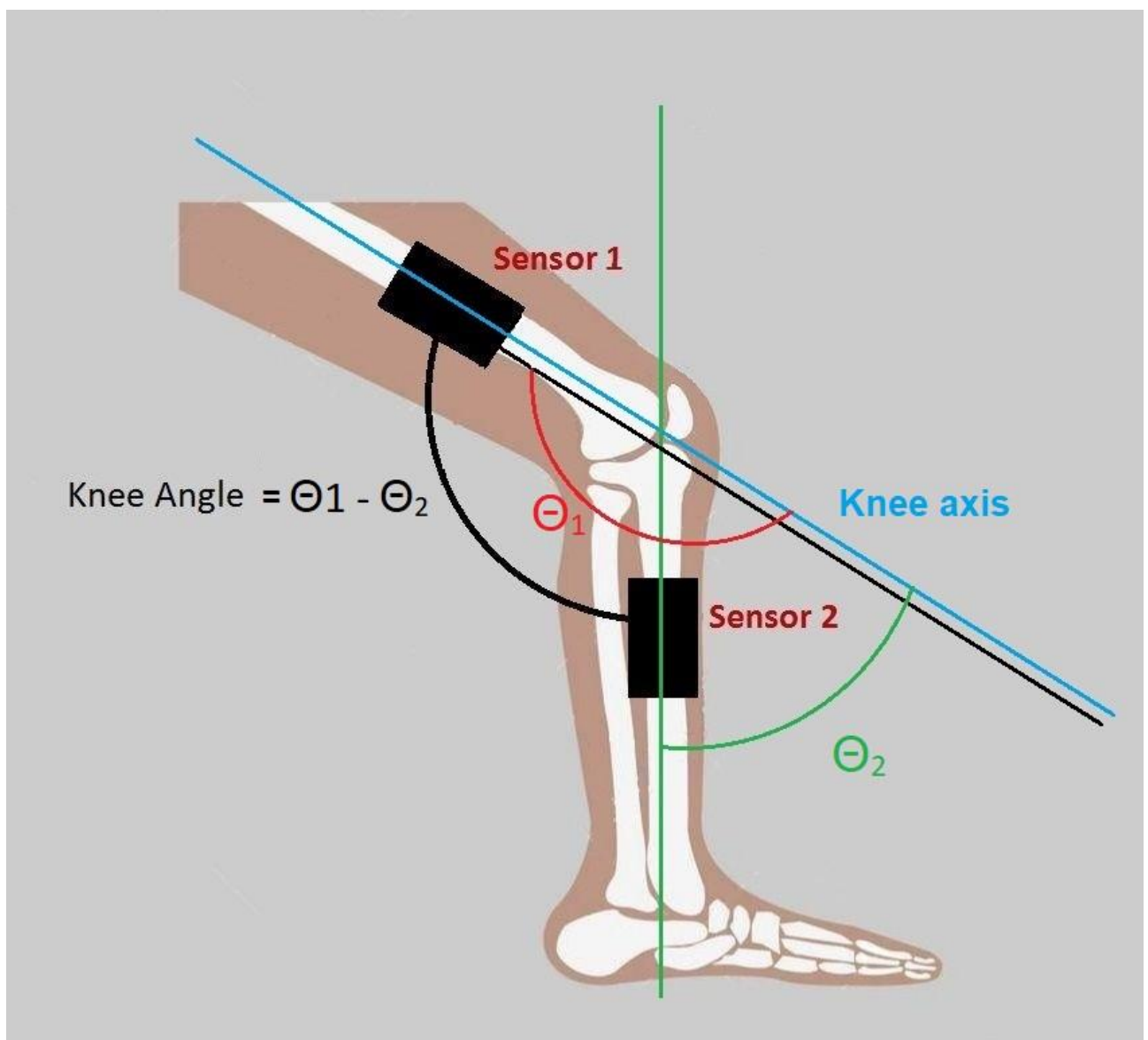
Figure 2.6. *Illustration procedure performed in Lipperts's algorithm*

2.3 Adaptation phase

We tried to combine these two different approaches in a unique solution to create a new experimental set up to achieve our purposes. We made changes in the Arduino Sketch, in the computer app and in the algorithm. A detailed list of all our changes, with their respective motivations, is reported in table below.

Table 2.1. *List of all changes made in Professor Lipperts and Professor Lipaj's solutions.*

New Elements	Where	Reason of the change
Sample rate (from 10 Hz to 63 Hz)	In the Arduino sketch	The continuous monitoring of movements requires higher sample rate than the one previously set, to avoid loss of information in faster movements
Output variables from sensors: • Timestamp • Triaxial accelerations • Triaxial angular speed • Quaternions • Inner calibration • Triaxial magnetic disturbs	In the Arduino sketch	We increased the number of output variables for two reasons: 1) to compare IMUs outcomes; 2) to use them in future upgrade of the algorithm. This argument is well explained in the section "Conclusion and future developments"

User Interface	In the Computer app	To make it more intuitive and easier to use for the user. The new version of the app can be seen in Figure 2.7
Saving data in CSV format	In the Computer app	The CSV format is easier to use not only with MATLAB but also with other programming language, as for example RStudio
Cleaning of previous acquisitions	In the Computer app	To the user is given the choice to hold the old data from previous acquisitions or to delete them to have a clean sheet with button "CLEAR ALL "
Adding of title	In the Computer app	In this way the user can immediately understand the meaning of the numbers that appear on the interface
Calibration on subject	In the algorithm	In professor Lipperts's algorithm there is a part dedicated to subject's specific calibration. A well-controlled movement, performed before any type of motion test, is used as reference, (in professor Lipperts's it is a slow squat performed in front of a wall). This part is missing in our set-up.
Offset elimination	In the algorithm	Because of their nature, quaternions take the initial position as system of reference, so the knee angle calculate with the algorithm always starts from 0°. To consider the real subject' knee angle in the erect position, it was calculated the offset between two signals, and it was removed.
Selection of data	In the algorithm	Since quaternions that IMU sent to computer app are the result of an inner combination of accelerometer, gyroscope and magnetometer data, if one of these tools is not well calibrated,

		the quaternion of that moment could be erroneous. For this reason, we established selection criteria for the samples: the value of inner calibration of accelerometer, gyroscope and magnetometer must be at least 2, in order to work only with quaternions coming from calibrated data.
Synchronization between sensors	In the algorithm	In professor Lipperts's algorithm, there is a part dedicated to synchronization between sensors. The user must perform a well-defined event, like a double tap on the sensors or a jump, before to start the motion test in order to easily identify it in the signal. In our set-up this part is completely automatic. Thanks to Arduino library "TimeClient", we synchronize inner clock of the sensors with Internet and then the algorithm finds the closest samples from two sensors.

Figure2.7. New version of professor Lapaj's app used in our project.

As can be seen on the above illustrated table, we adapted and changed the pre-processing part of Professor Lippert's algorithm because it was strictly linked to GCDC HAM-IMU, whereas we did not modify post-processing analyses. In order to clarify the functioning of the sensors in our project a little diagram with all steps performed, is reported below.

1° Step
- Writing of instruction on the Arduino sketch
- Upload sketch on the board via USB

2°Step
The micro-processor eps 8266 reads the list of instructions

3° Step
The micro-processor establish a Wi-Fi connection with Wi-Fi network indicated in sketch

4° Step
The micro-processor actives IMU in on the shield and sets the sample rate at value written in sketch

5°Step
The library " Adafruit_BNO055 " for the calcute of inner calibration and the orientation is enable

6° Step
The library "TimeClient" to set the inner clock to current time is enable

7° Step
The IMU, from the values of 3-axis accelerometer, gyroscope and magnetometer, calculate the orientation of the board in 3D space

8° Step
The IMU sends the values sampled and the quaternions, that describes the orientation, to laptop

Figure 2.8 *Diagram about functioning of home-made sensors (after adaptation)*

At the end of this adaptation process and fusion of different approaches, we developed our knee monitoring systems based on two IMUs, consisting of a hardware part (two sensors made with Arduino component by Professor Lapaj) and an adapted version from Matthijs' algorithm part.

From now on in this thesis work, we will refer to our experimental set-up (algorithm + sensors) as *black sensors* (because of the colour of their protection) in order to make notation lighter.

2.4 Validation

2.4.1 Plausibility test

In order to assess the goodness and the quality of the outcome coming from our solution, we made a preliminary test to control the plausibility of our results. We attached our sensor at the endings of a plastic goniometer. We attached the goniometer at the wall in vertical position, so

that between the sensors there was an angle of 180°, i.e. 0° in clinical system of reference. Then we moved the sensor attached at the upper ending of goniometer toward the other sensor, from 0° to 90° and from 90° to 0° in all human anatomical planes (frontal, sagittal, transverse) , in order to assess sensibility of our system and to simulate, only for the movement in sagittal plane, the physiological RoM of a human knee. In figure 2.7 are shown different moments of this test.
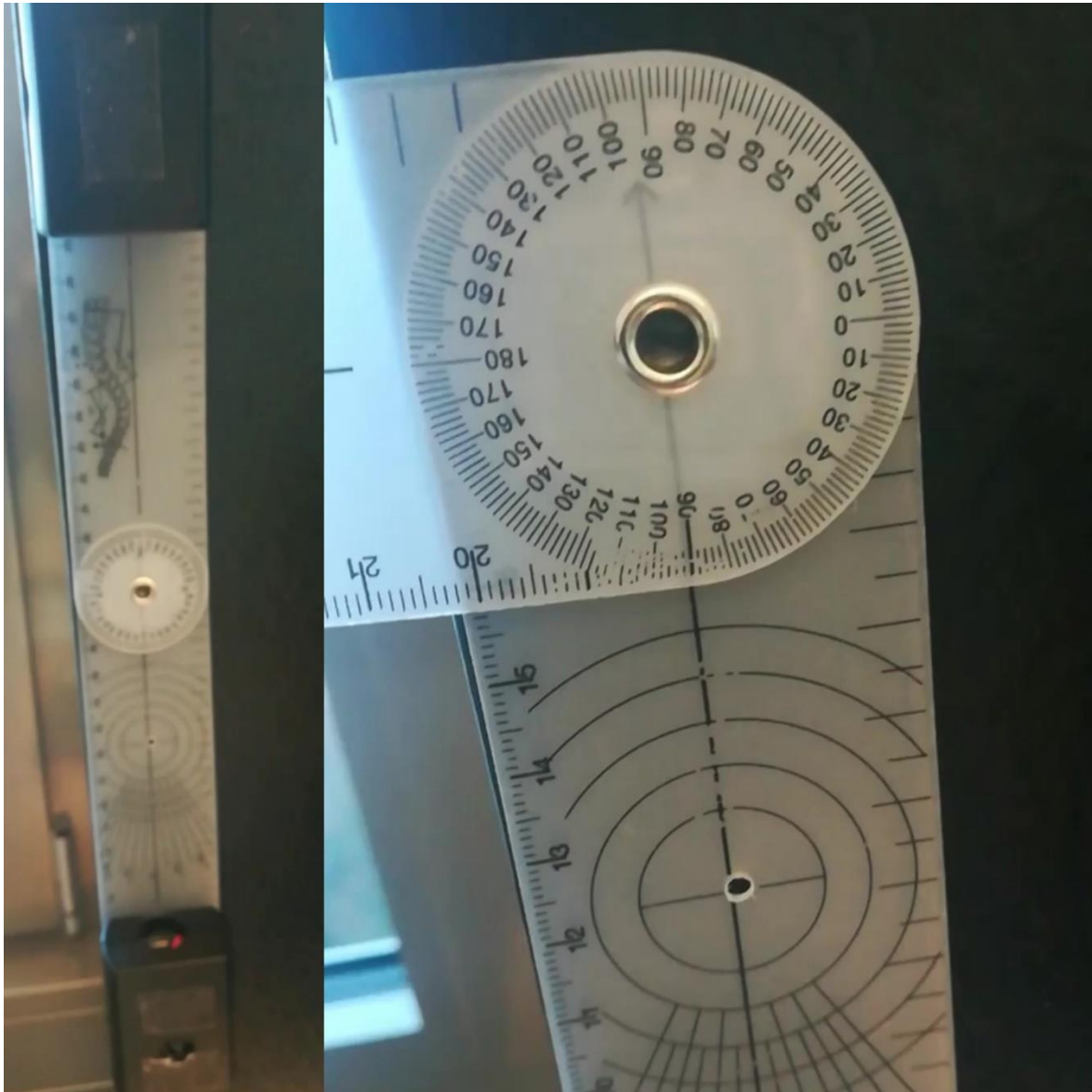
Figure 2.9. The position of sensors and goniometer while simulating stand up position (left), sit-down position (right)

2.4.2 Motion Tests

To assess the performance of our monitoring system, a series of very common daily movements were chosen. The movements selected are walking, squatting, sit-to-stand transitions, stair

climbing, going downstairs and running. With these movements we planned the following motion tests:

1. 5 squat and then 30 seconds walking
2. 1-minute sit-to-stand transitions with 3 seconds of rest after every change of position
3. 1-minute squatting changing every 3 squats the speed and intensity of movement
4. Stair climbing 4 steps, placing one foot on one step and the other foot on the next step
5. Stair climbing 4 steps, placing both feet on same step before to proceed to the next one
6. Going downstairs 4 steps, placing one foot on one step and the other foot on the next step
7. Going downstairs 4 steps, placing both feet on same step before to proceed to the next one
8. 1 minutes running at 10km/h speed

From now these tests will be called Motion Test 1 (MT1), Motion Test 2 (MT2), Motion Test 3 (MT3), Motion Test 4 (MT4), Motion Test 5 (MT5), Motion Test 6 (MT6) Motion Test 7 (MT7), Motion Test 8 (MT8), respectively. In all motion tests we assessed the sensibility of our solution, some of these tests were performed more than one time because we were also interested in the reliability of measurements. How many times each test was performed is shown in Table 2.

Table 2.2. *Little resume of all motion tests executed*

MOTION TEST	REPETITIONS
MT1	5
MT2	1
MT3	1
MT4	3
MT5	1
MT6	3
MT7	1
MT8	2

Figure 2.10 *Global view of sensor position*   **Figure 2.11** *Specific length of each segment*

It is important to specify that in the first repetition of MT8, the subject started the run on a treadmill from a standing position. After one minute, this repetition ended, and we started a new acquisition without stopping subject running. So, the second acquisition started while the subject was still running.

2.4.3 Position of sensors

We decided to attach the sensor on the right leg because is subject' dominant leg. We measured the length of the leg (80 cm), from the hip to the sole of foot, with a meter, as shown in Figure 2.8. We considered the total leg divided in two segments, upper (from the hip to the knee) and lower one (from knee to the foot). We measured the length of both, taking, respectively, as anatomic reference the distance lateral femoral epicondyle-anterior iliac spines, lateral femoral epicondyle-lateral malleolus (Figure 2.9). The black sensors were fixed at the same position on the segments, i.e. at 50% of length of single segment during all motion tests that corresponds at 20 cm from the lateral femoral epicondyle for upper segments and at 20 cm from the lateral femoral epicondyle for the lower one.

2.4.4 Motion Laboratory

The above-mentioned motion tests were performed in the human motion laboratory of Luxembourg Institute of Health (LIH) with a high-speed (200 Hz) motion analysis system consisting of four CX1 3D scanner units (CODAmotion, Charnwood Dynamics, UK) placed on all four sides of the treadmill. It was used to track knee and ankle joints as well as shoe/ground angles during the tests. The subject wore shoes that were pre-equipped with two markers on the calcaneus area and on the top of the shoe (base of shoelace). Two more markers were placed on the shoes on palpable anatomical locations at the 1st and 5th metatarsophalangeal joints. Ten markers (5 per leg were placed on the following anatomical landmarks: tibial and fibula malleoli, femoral condyles and greater trochanters. Finally, four rigid clusters equipped with four markers each were placed on the shanks and the thigh. A static calibration record was done using the full set of 34 markers with participant standing in a neutral pose. During all tests, only the clusters and the markers placed at the shoes (n=24) were tracked at 200 Hz. Kinematic data were analysed using Visual3D (V.5.02.19, C-Motion, USA). Joint angles were normalised with respect to the standing trial [2]. The knee flexion in sagittal, frontal and transvers plane was calculated.

2.5 Comparison and statistical analyses performed

Black sensors and motion laboratory estimated separately the knee angle. From these two signals, max knee flection and max knee extension were extracted for each single movement (i.e. a squat, a step, a gait cycle, etc.), in order to estimate the RoM. For each motion test, the values and time of these two parameters are compared. In the next chapter of this master thesis will be presented only the results about MT1, MT2 and MT8, in order to describe the quality of our monitoring system in three different condition of speed, (respectively: middle, low, high). Furthermore, a Bland-Altman plot is performed on the results of MT1 because is the motion test performed several times, in order to visualise the difference between our solution and the gold standard.

2.6 Usability

Another important parameter that was investigate in this project was the usability of the *black sensors*. We were interested about the usability of both hardware and software. In the scientific literature, there are a lot of questionnaires for the assessment of usability but, because of very low number of participants (n=2 for the app and n=1 for sensors) and lack of time, it was not deemed necessary submit one of them. We just limited to report the impressions and the

experience of the participant. To assess the usability of the app we took inspiration from Questionnaire for User Interaction Satisfaction (QUIS), developed in 1989 at the Human Computer Interaction Laboratory (HCIL), in the College Park of Maryland University by Kent Norman e Ben Schneiderman and the criteria selected by this questionnaire were:

- Screen design and layout
- Learnability
- Overall reaction to the software

To assess the usability of the sensors, we placed one sensor at 25%, 50% and 75% of the distance hip-knee and the other sensor 25%, 50% and 75% of the distance knee-foot. The measurements are illustrated in the following table

Table 2.3. Distance, in cm, at which the sensors were positioned during the usability tests

Segment of leg	25% of length	50% of length	75% of length
Upper (hip-knee)	10	20	30
Lower (knee-foot)	10	20	30

The sensors were worn by the subject for at least 4 hours in each position and he valued the comfort/discomfort during daily life activities. During the acquisition of experimental data, the placement of black sensors did not change, and we did not assess if sensor placement influence outcomes.

References

[1] Adafruit. (n.d.). Retrieved from https://learn.adafruit.com/adafruit-bno055-absolute-orientation-sensor/device-calibration

[2] Laurent Malisoux, P. G. (2017). Adaptation of running pattern to the drop of standard cushioned shoes: A randomised controlled trial with a 6-month follow-up. *Journal of Science and Medicine in Sport*, 734-739.

3 RESULTS

3.1 Results of plausibility test

When performing six distinct movements (ca. 90deg turns by hand in 3 orthogonal planes and in both directions) in sequence using the black sensor set-up mounted to a plastic goniometer, the output for the relative angle between both sensor units followed qualitatively and quantitatively the expected signal. In this stage of calibration, we were not interested to assess if our system was able to detect physiological movements, in fact only one movement could be considered physiological (from $0°$ to $-90°$ and go back), but rather its sensibility.
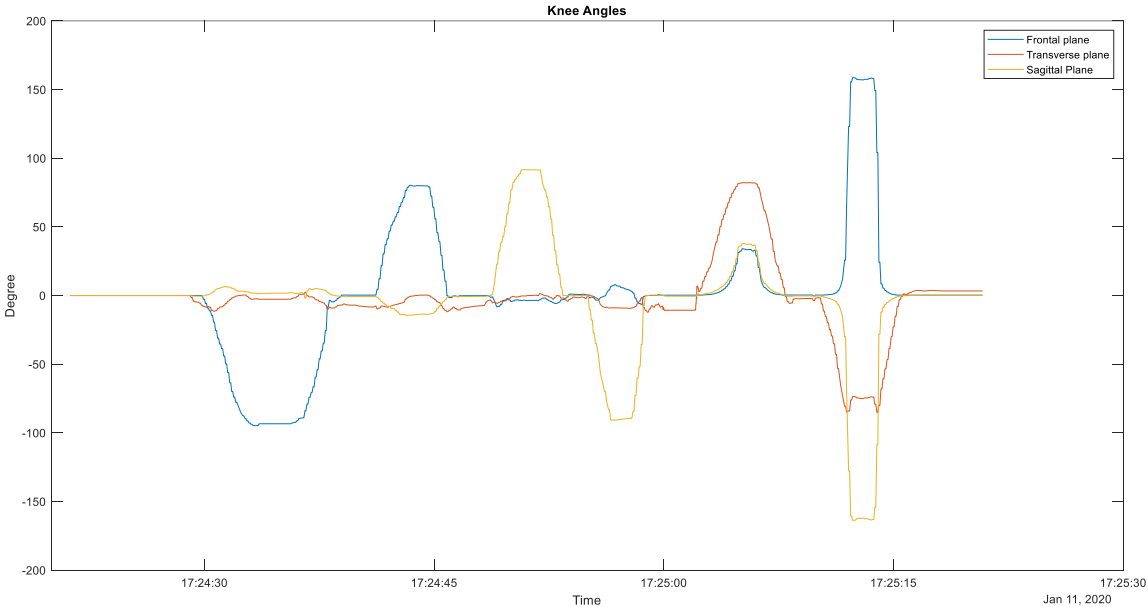
Figure 3.1 *Black sensor's knee angle output for various distinct movements as an initial plausibility test (no gold standard).*

As can be seen in Figure 3.1, black sensors outcomes followed the expected patterns, except for movements in transversal plane (they simulated the intra/extra rotations of knee). It is visible that, during the movements, in sagittal and frontal planes, there were large angular changes in values only in the expected plane.

A table with all range of motions (expected and calculated) is reported below.

Table 3.1. *Successive movements of the black sensors on a goniometer to compare output to the theoretically expected plausible value*

Type of Movement	Expected range in frontal	Expected range in sagittal plane	Expected range in transverse Plane

	frontal plane (degrees)	plane (degrees)	sagittal plane (degrees)	(degrees)	transverse plane (degrees)	(degrees)
0°to -90° in frontal plane	[-90,0]	[-94.75-0]	0	[0-6.37]	0	[-11.4,0]
-90° to 0° in frontal plane	[-90,0]	[-93.38-0]	0	[1.7-5.2]	0	[-6.6,2.3]
0°to 90° in frontal plane	[0,90]	[0, 80.32]	0	[-13.8, 0.72]	0	[-9.8,1.3]
90° to 0° in frontal plane	[0,90]	[0, 80.32]	0	[-13.7, -0.9]	0	[-1.2, -11.7]
0°to 90° in sagittal plane	0	[-8.13, -0.13]	[0,90]	[-0.6,91.3]	0	[-5.4,-0.55]
90° to 0° in sagittal plane	0	[-3, -1.82]	[0,90]	[0.11,91.3]	0	[-3.2, -0.7]
0°to -90° in sagittal plane	0	[-0.5, 6.7]	[-90,0]	[0.11, -90.63]	0	[-0.7, -8.4]
-90° to 0° in sagittal plane	0	[3.1, -0.7]	[-90,0]	[-89.34,0.21]	0	[-12.14, -8.7]
0°to 90° in transverse plane	0	[0.73, 34.09]	0	[0.57, 38]	[0,90]	[-10.56,81.8]
90°to 0° in transverse plane	0	[0.39,34]	0	[-0.57,36.8]	[0,90]	[-2.2, 82]
0°to -90° in transverse plane	0	[0.93, 158.6]	0	[-163.8, -0.29]	[-90,0]	[-2.2, -84]

-90°to 0° in transverse plane	0	[-158.1, 0.13]	0	[-163.4-0.13]	[-90,0]	[-85,3, 3]

To make the notation lighter from now on, we will refer to the movement made from 0 ° to 90 ° as "clockwise movement", while the other will be redefined as "counterclockwise movement".

For the discussion of the results of this initial test we distinguish two cases:

1. Angles calculated in the same plane in which the movement was made (eg sagittal angle in movements in the sagittal plane, etc.)
2. Angles calculated in planes perpendicular to that in which the movement was made (front and transverse angle in movement in the sagittal plane, etc.)

In the first case, the system has proven to be quite accurate. The absolute value of the difference between the expected angle and the estimated angle was less than:

- 2° in both movements in the sagittal plane
- 5 ° in the counterclockwise movement and 10 ° in the clockwise movement in the frontal plane
- 6 ° in the counterclockwise movement and 10 ° in the clockwise movement in the transverse plane

3.2 Results of motion tests

We are comparing the black sensor's angles for various movements to values generated simultaneously from an optical marker-based motion capture system (MoCap) used as gold standard (see Methods 2.4.4). For each motion test, results will be shown as:

1. Superimposition of both signals (black sensors, motion capture) against time
2. Scatter plot for maximum knee flexion values for both measurement methods
3. Scatter plot for maximum knee extension values for both measurements methods

After these plots, a table is reported containing the mean values of following parameters:

- Maximum knee flexion values for MoCap
- Maximum knee flexion values for black sensors
- Maximum knee extension values for MoCap
- Maximum knee extension values for black sensors
- Difference between MoCap and black sensors in maximum flection measurements

Difference between MoCap and black sensors in maximum extension measurements

During all the motion tests, only results concerning the sagittal plane of the subject were taken into consideration, since it is the main objective of this research project.

3.2.1 Squatting and walking

In this section we show the results of the five repetitions of MT1 (see Methods 2.4.2) performed by the subject. Because of the presence of two different movements in this test, in this subsection we will show also values for squatting and for walking.

MT1- 1° Repetition
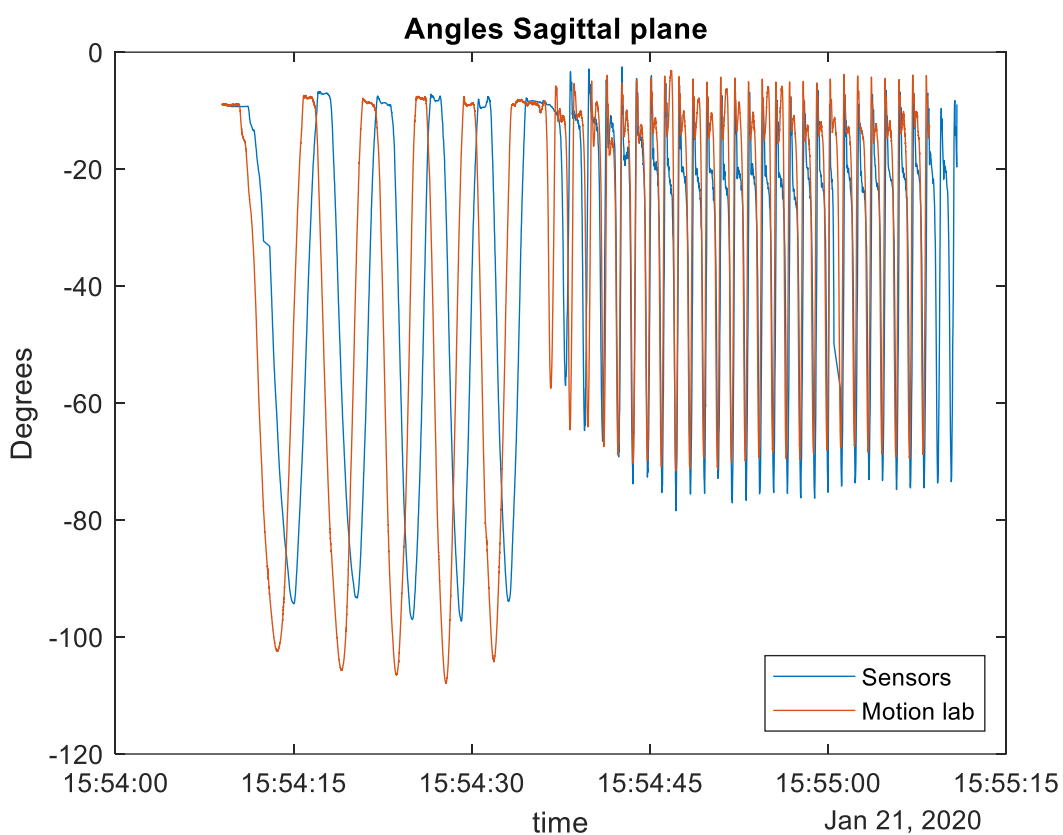
Figure 3.2 MoCap (red) and black sensors (blue) knee angle in MT1-1° Repetition for squatting followed by walking

Superimposition of the continuous signal traces from the black sensors and MoCap gold standard for squatting and walking show that the black sensors output qualitatively and quantitatively reflects the gold standard measurements. The deep and smooth squat movements are described as well as the sharper and lower flexion peaks during walking as a more dynamic movement. Both the shape of the curve and the difference between peak values allows the clear characterisation of the squatting and walking movement. One can also clearly

identify the increase of knee flexion during the first strides of walking on the treadmill until a gait rhythm and steady state is reached.

It can also be seen that over time no noticeable signal drift can be detected. There is only an initial delay (time shift) between the MoCap values and the black sensors angles trailing behind the gold standard measurements right from the start. The reason why this time shift exists and if or how it could be improved/removed, shall be treated in the discussion. This time shift is close to the stride time, so that the simultaneous knee flexion peaks during walking are indeed shifted by one stride. This delay is slightly increased during the motion test because black sensor's clock makes small leaps forward. An example can be seen in figure 3.2, obtained zoom-in the curve of previous figure. However, this behaviour is not common, and it can be found just few times in all motion test performed.
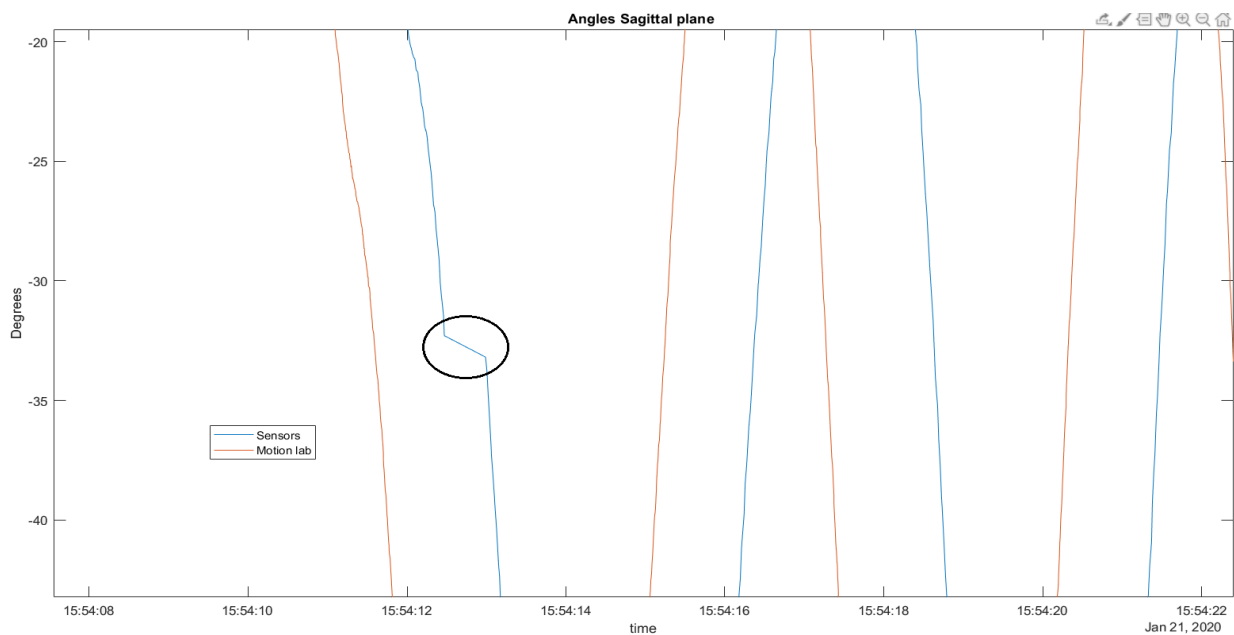
Figure 3.3 Temporal jump in black sensors in MT1-1° Repetition

The transition phase between squats is well defined in both systems and both the duration and value calculated by the two systems are very close.

When squatting, where knee flexion is large and slow, the black sensors peak values differ from MoCap peak values by a mean of 8.8 deg (see Table 3.2), whereas during walking the black sensors peak flexion angles differ by a mean of 5.6 deg (see Table 3.2).
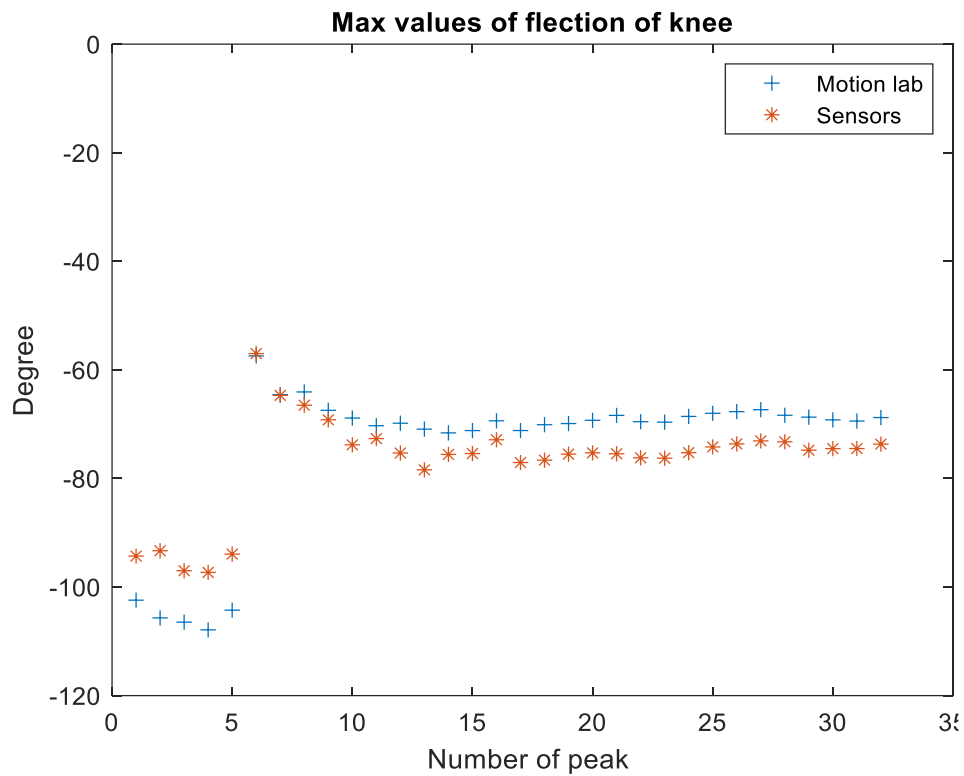
Figure 3.4 MoCap (blue) and black sensors (red) maximum values knee flection for each squat (5 values from left) or step in MT1-1° Repetition

At the end of each squat, where knee extension is maximum, the black sensors values are less by ca. 1 degree whereas during the midstance phase of gait, the difference between MoCap knee extension and black sensors knee extension become higher but still less than 10 degrees.
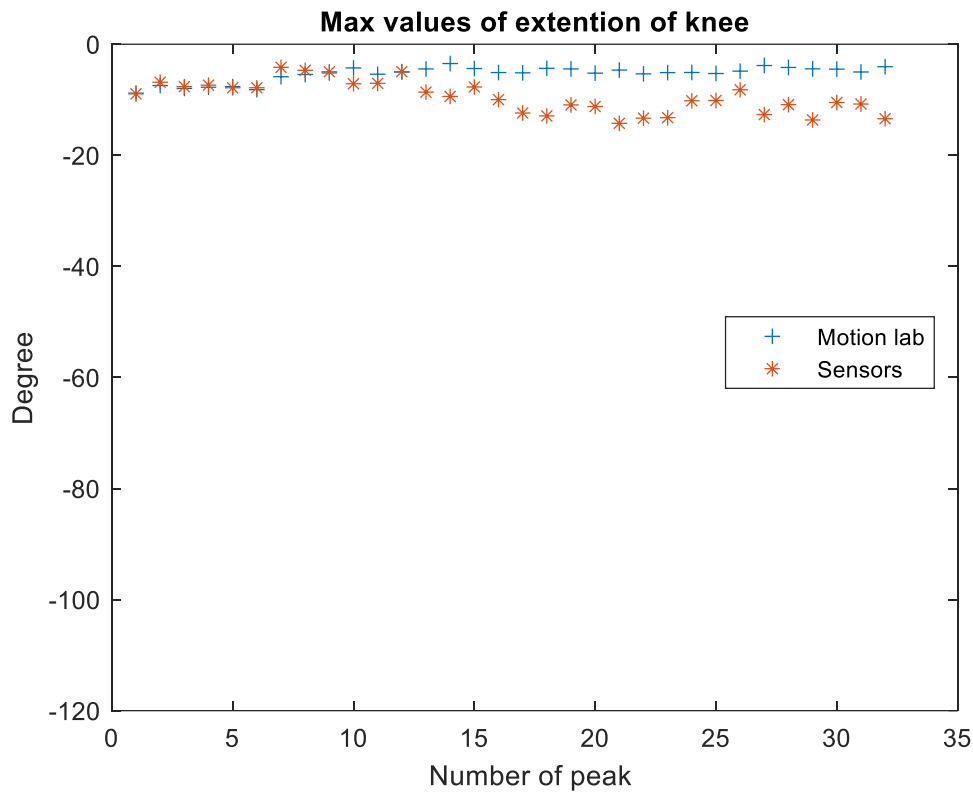
Figure 3.5 *MoCap (blue) and black sensors (red) maximum values knee extension for each squat or step in MT1-1° Repetition*

Table 3.2. *Mean values of experimental data, calculated by both system and compared, during MT1-1° Repetition*

Type of movement	Mean value of max knee flection in MoCap (degrees)	Mean value of max knee flection in black sensors (degrees)	Mean value of max knee extension in MoCap (degrees)	Mean value of max knee extension in black sensors (degrees)	Mean difference between MoCap and black sensors in max knee flection (degrees)	Mean difference between MoCap and black sensors in max knee extension (degrees)
Global	-74.3 ± 13.9	-76.8 ± 9.0	-5.2 ± 1.4	-6.7 ± 1.7	-5.7 ± 2.7	2.1 ± 1.3
Squatting	-110.9 ± 4.4	-100.4 ± 1.6	-7.2 ± 1.5	-8.3 ± 1.0	10.5 ± 4.0	1.3 ± 0.8
Walking	-68.4 ± 3.5	-71.0 ± 3.8	-4.4 ± 0.6	-5.6 ± 2.1	3.6 ± 1.6	2.0 ± 1.1

As can be noted by plots and by the values in Table 3.2, black sensors knee flexion is closer to MoCap values during walking and black sensors extension is closer to MoCap values during squatting. In this repetition, black sensors systematically underestimate knee flexion in slower movement (squatting), whereas systematically overestimating knee angle both in flection and in extension in faster movement (walking).

Since the variability of the results among all repetitions in this motion test is very low, we will present only the third and the fifth repetition, in order to show the temporal trend of our system. In fact, between the first and the third repetition, as well as the third and the fifth, at least ten minutes have passed.

MT1- 3° Repetition
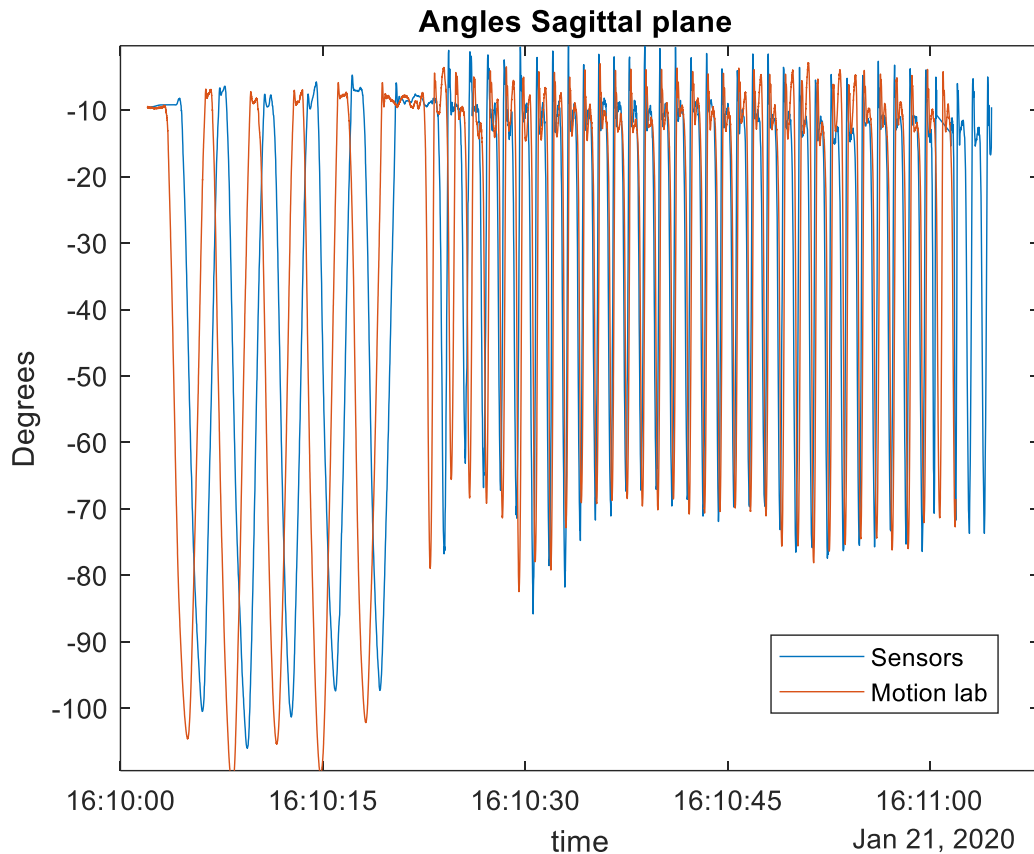
Figure 3.6 *MoCap (red) and black sensors (blue) knee angle in MT1-3° Repetition*

Also in this case, the continuous knee angle signal traces from the black sensors and MoCap gold standard are very similar both qualitatively and quantitatively. As in the previous repetition, there is an initial temporal delay between two knee angle signals but this time black sensor' clock worked perfectly. So, the initial temporal delay has not been increased and all peaks, both in extension and in flection, are closer to each other.

Even during this repetition, the different system accuracy depending on movement. The black sensors better estimate the flection peak during walking, whereas the system extension values have a higher accuracy during the squatting. Moreover, as can be seen by Table 3.4, the absolute mean difference, both in maximum knee flexion and in maximum knee extension, is lower that MT1-1° repetition
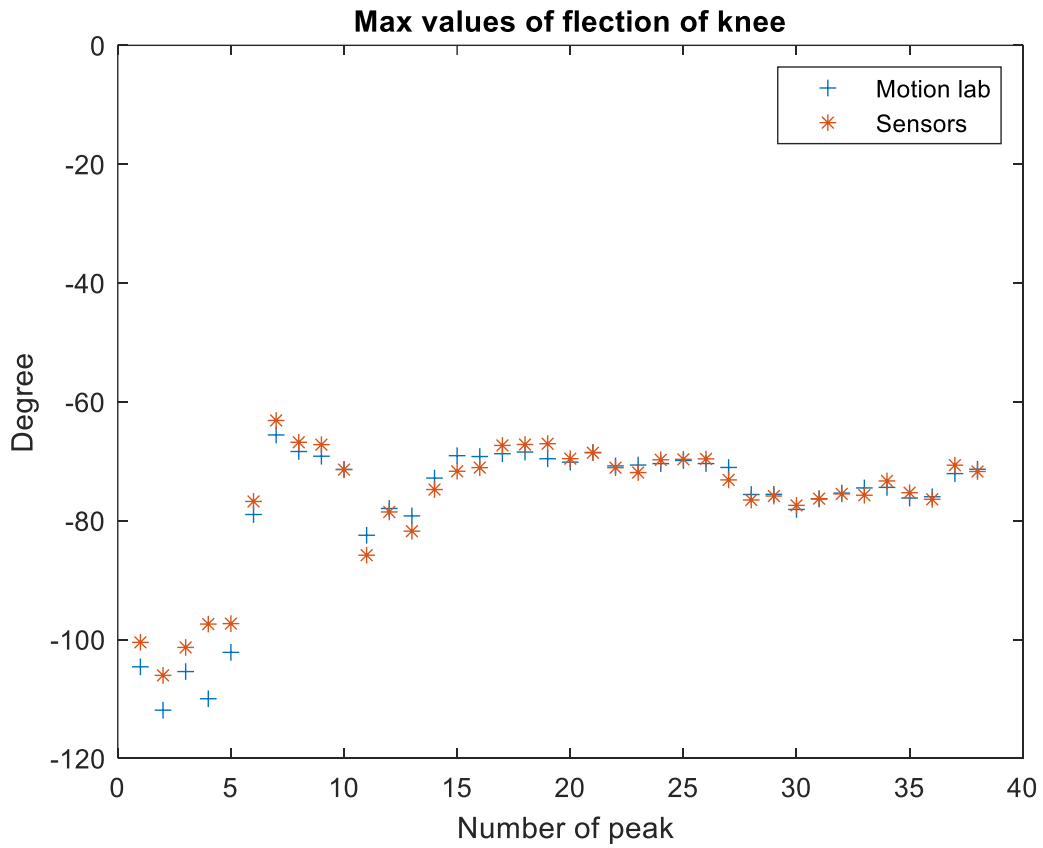
Figure 3.10. *MoCap (blue) and black sensors (red) maximum values knee flection for each squat (peak 1-5) or step (peaks >6) in MT1-3° Repetition*
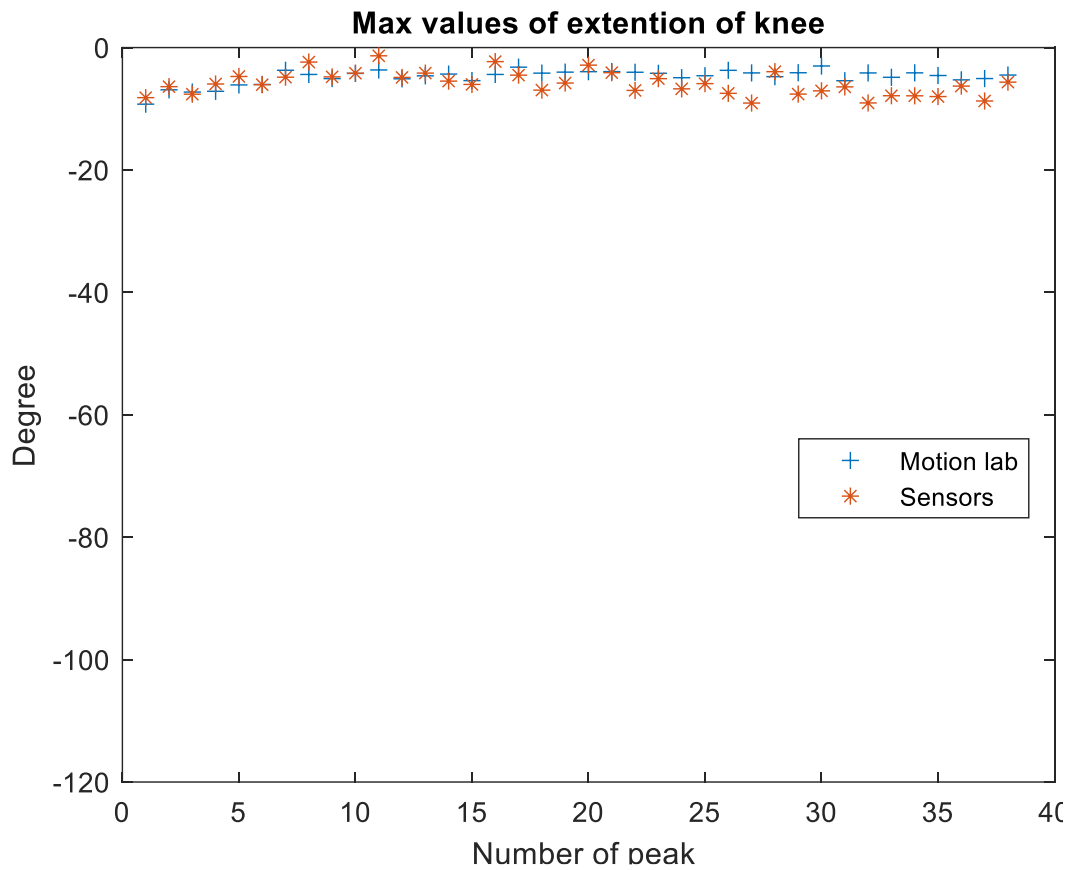
Figure 3.11 *MoCap (blue) and black sensors (red) maximum values knee extension for each squat (peak 1-5) or step (peaks >6) in MT1-3° Repetition*

Table 3.4. *Mean values of experimental data, calculated by both system and compared, during MT1-3° Repetition*

Type of movement	Mean value of max flection in MoCap (degrees)	Mean value of max flection in black sensors (degrees)	Mean value of max extension in MoCap (degrees)	Mean value of max extension in black sensors (degrees)	Mean difference between MoCap and black sensors in max flection (degrees)	Mean difference between MoCap and black sensors in max extension (degrees)
Global	-77.1 ± 12.4	-76.3 ± 10.6	-4.6 ± 1.3	-3.1 ± 2.1	1.9 ± 2.3	1.8 ± 1.1
Squatting	-106.8 ± 4.0	-100.5 ± 3.6	-7.2 ± 1.3	-6.5 ± 1.4	6.3 ± 3.6	0.8 ± 0.4
Walking	-72.7 ± 4.0	-72.7 ± 4.8	-4.2 ± 0.7	-2.6 ± 1.6	1.2 ± 0.9	1.9 ± 1.1
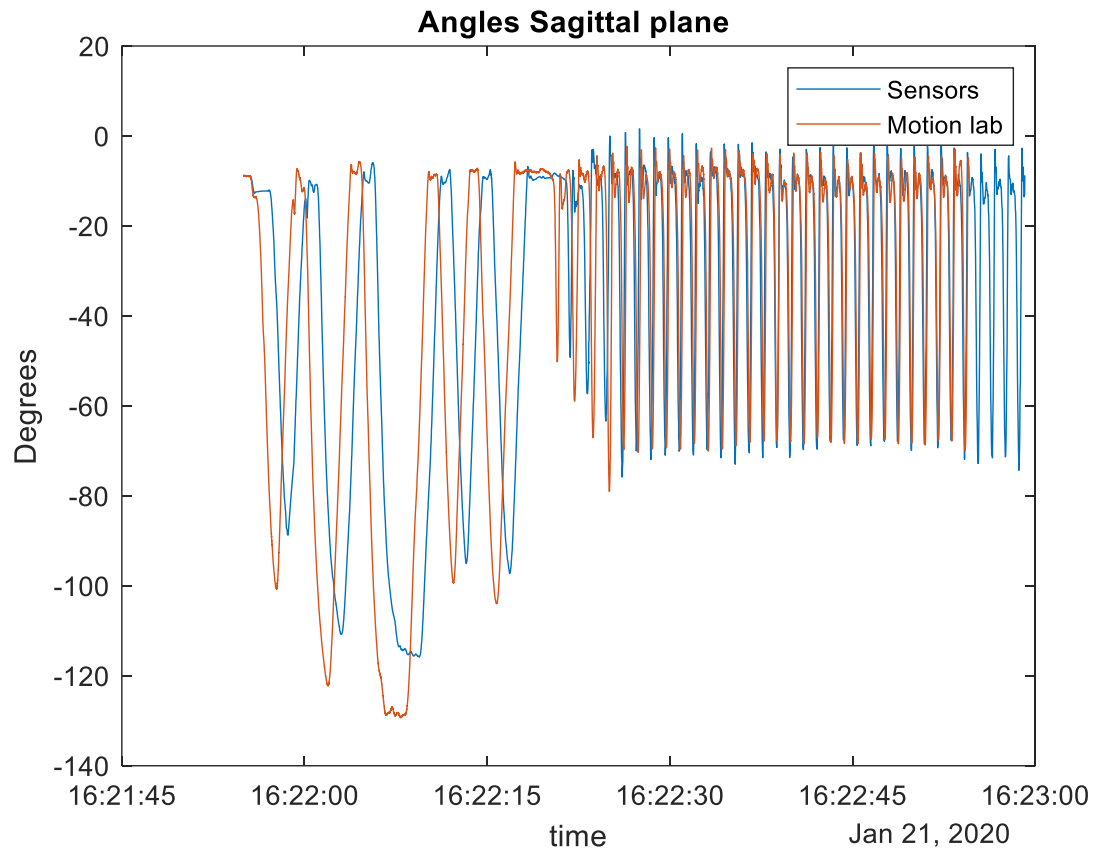
Figure 3.12 *MoCap (red) and black sensors (blue) knee angle in MT1-5° Repetition*
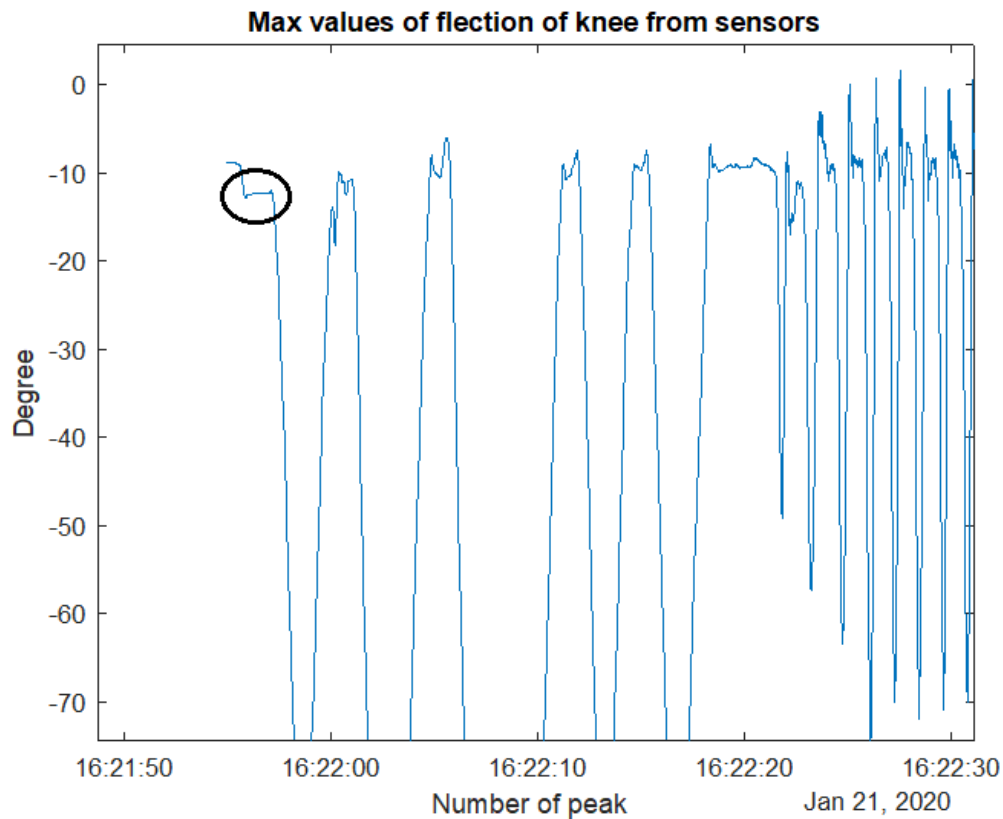
Figure 3.13 *Time jump in black sensors in MT1-5° Repetition*

In the fifth, and last, repetition of this trial performed in MT1, one can observe the same features as during previous two repetitions. As with the first repetition, the black sensor system curve presents a temporal jump forward, at the beginning of acquisition (Figure 3.13). From figure 3.12, it is more evident than the others that the two knee angle curves differ this by a systematic error, since before the time jump the two curves were superimposed. The plateau of maximum knee flexion during squat 3 and the variations occurring holding this position as shown by the gold standard method are represented also in the IMU black sensor system.

The trend, coming out during previous two repetitions, to estimate flexion peaks with minor error during the walking is confirmed also here.

The plateau of maximum knee flexion during squat 3 and the variations occurring holding this position as shown by the gold standard method are represented also in the IMU black sensor system.
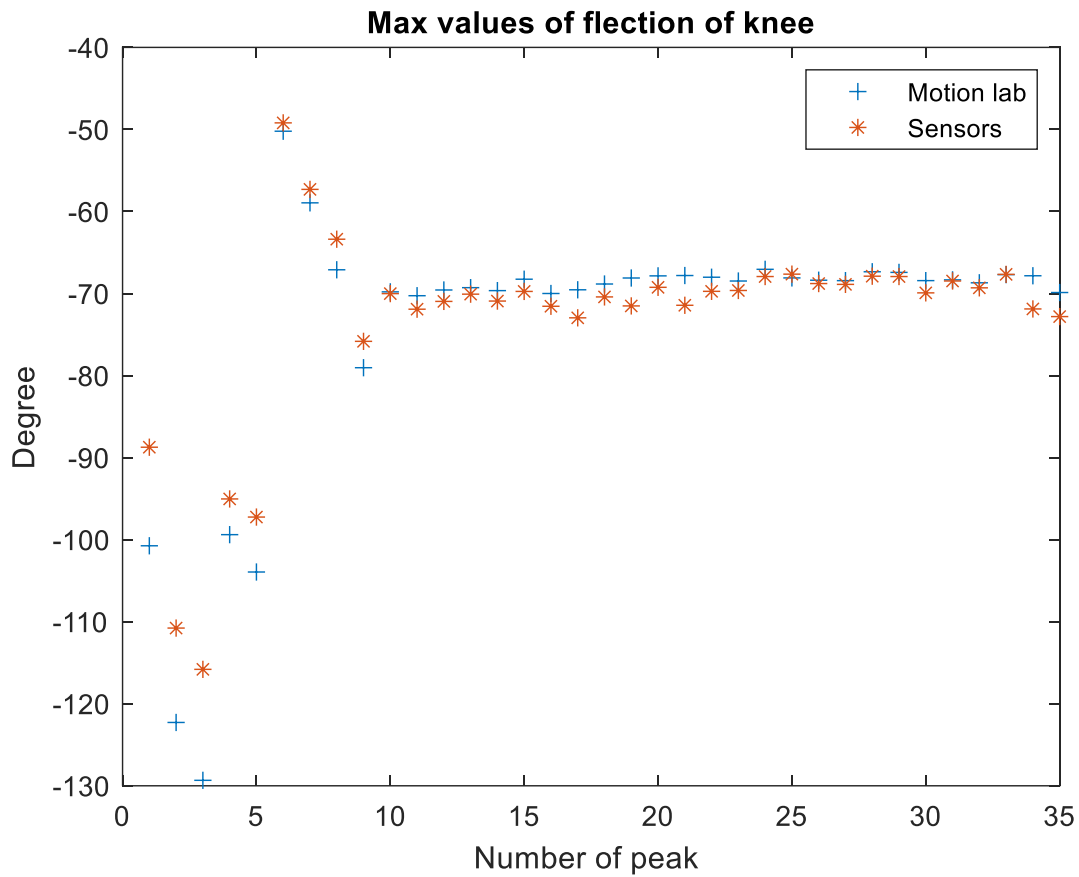
Figure 3.14. *MoCap (blue) and black sensors (red) maximum values knee flection for each squat (peaks 1-5) or step (peaks >=6) in MT1-5° Repetition*

The knee extension values have been estimated with smaller absolute error during squatting than during walking, as had already happened in the first and in the third repetition. However, mean values of the absolute error both in max knee flection and in max knee extension decreases respect the first repetition of MT1 presented, showing an improvement of system performance.
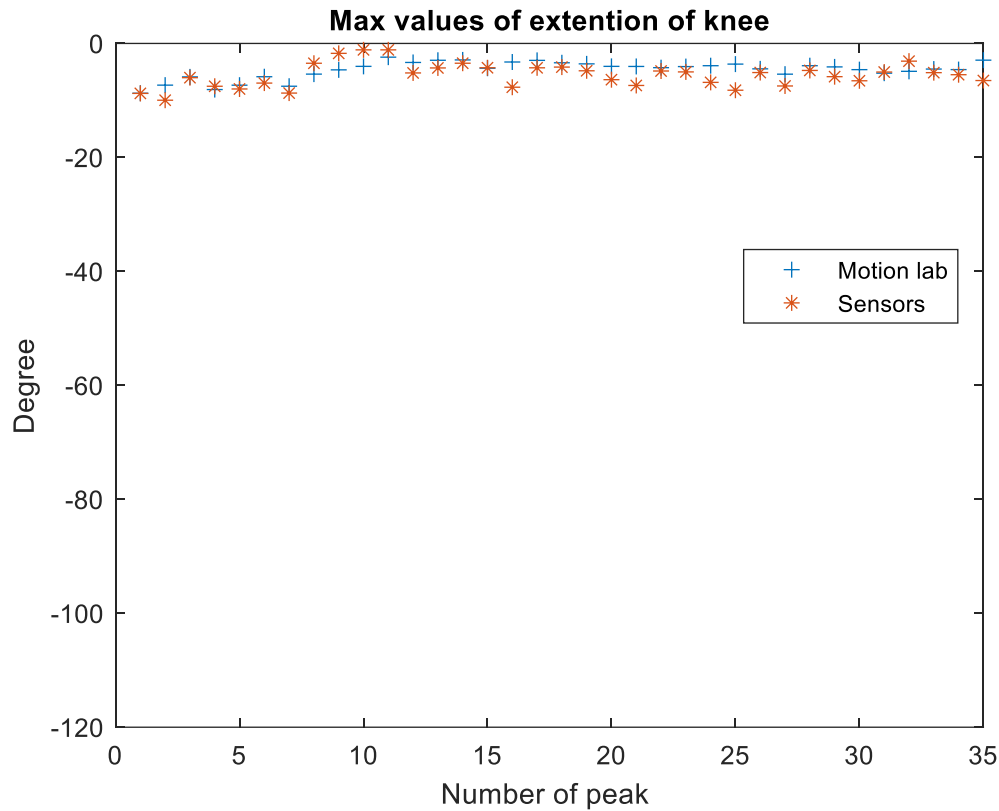
Figure 3.15. *MoCap (blue) and black sensors (red) maximum values knee extension for each squat or step in MT1-5° Repetition*

Table 3.6. *Mean values of experimental data, calculated by both system and compared, during MT1-5° Repetition*

Type of movement	Mean value of max knee flection in MoCap (degrees)	Mean value of max knee flection in black sensors (degrees)	Mean value of max knee extension in MoCap (degrees)	Mean value of max knee extension in black sensors (degrees)	Mean difference between MoCap and black sensors in max knee flection (degrees)	Mean difference between MoCap and black sensors in max knee extension (degrees)
Global	-74.1 ± 16.5	-73.5 ± 13.1	-4.5 ± 1.6	-3.1 ± 2.8	2.7 ± 3.3	1.8 ± 1.2
Squatting	-111.1 ± 13.7	-101.5 ± 11.3	-7.4± 1.1	-7.9 ± 1.5	9.6 ± 3.9	0.7 ± 1.1
Walking	-67.9 ± 4.4	-68.9 ± 4.9	4.0 ± 1.1	-2.3 ± 2.0	1.6 ± 1.2	2 ± 1.2

3.2.2 Sit-to-stand-to-Sit transitions

In this section we show the results of the only repetition of MT2 (see Methods 2.4.2) performed by the subject.

MT2
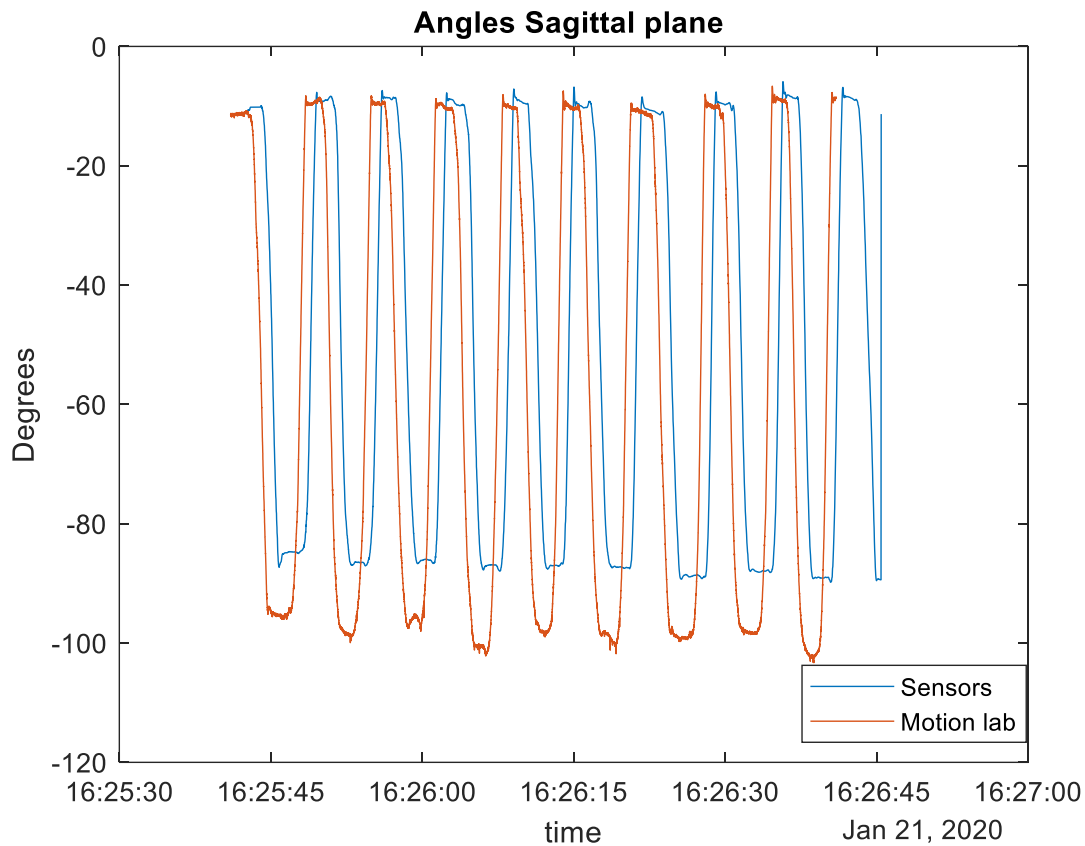
Figure 3.15. *MoCap (red) and black sensors (blue) knee angle in MT2*

In this motion test is possible the sensibility of black sensor system. Zooming in the first stand-to-sit cycle, one can note two little peaks in both signals, one in the moment of sitting and the other when the subject is fully stand (Figure 3.16).
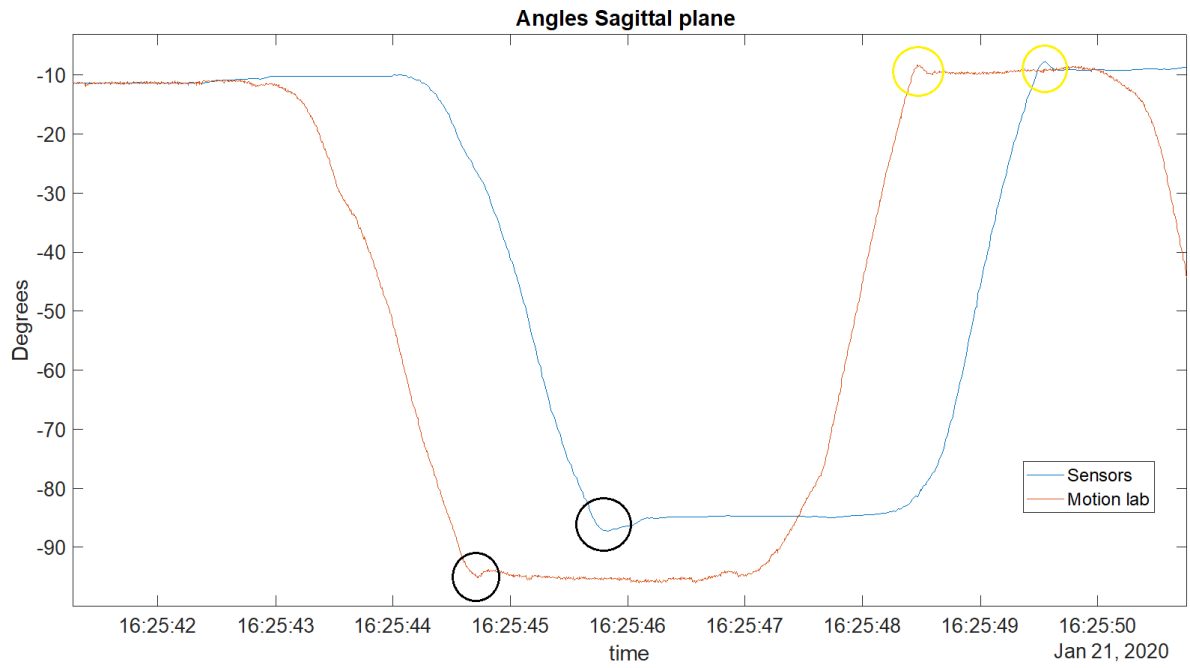
Figure 3.16. *Little motion features at the end of sitting (black circle) and at the end of standing (yellow circle) in both knee angles curves*

This is a small detail which both systems capture showing that this is a distinct movement feature. That means that black sensor system is also able to detect such small features which may be part of a real-life monitoring assessment of sit-to-stand movements.
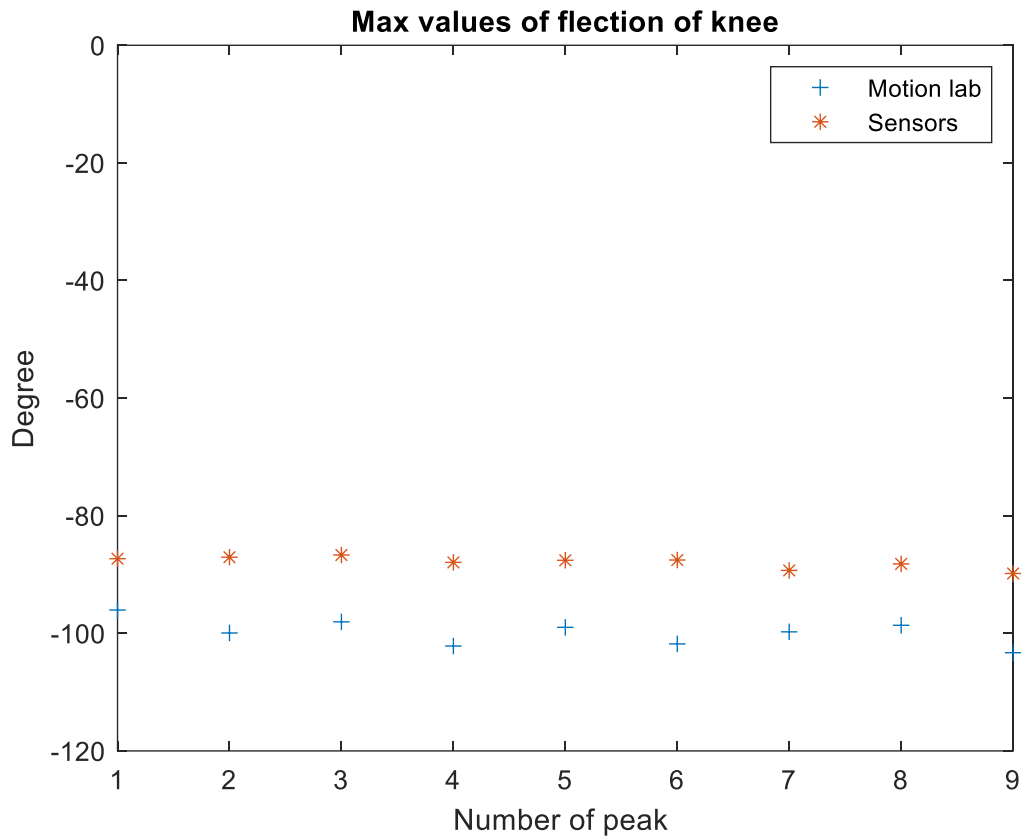
Figure 3.17. *MoCap (blue) and black sensors (red) maximum values knee flexion for each squat or step in MT2*

In the slow movements, our experimental set up significantly underestimated flection values, as can be seen in figure 3.15. Nevertheless, knee angle curve of black sensors system strictly follows the MoCap knee angle curve. The estimation of extension values was performed very well by black sensors system, since the mean difference is less than 1 degree.
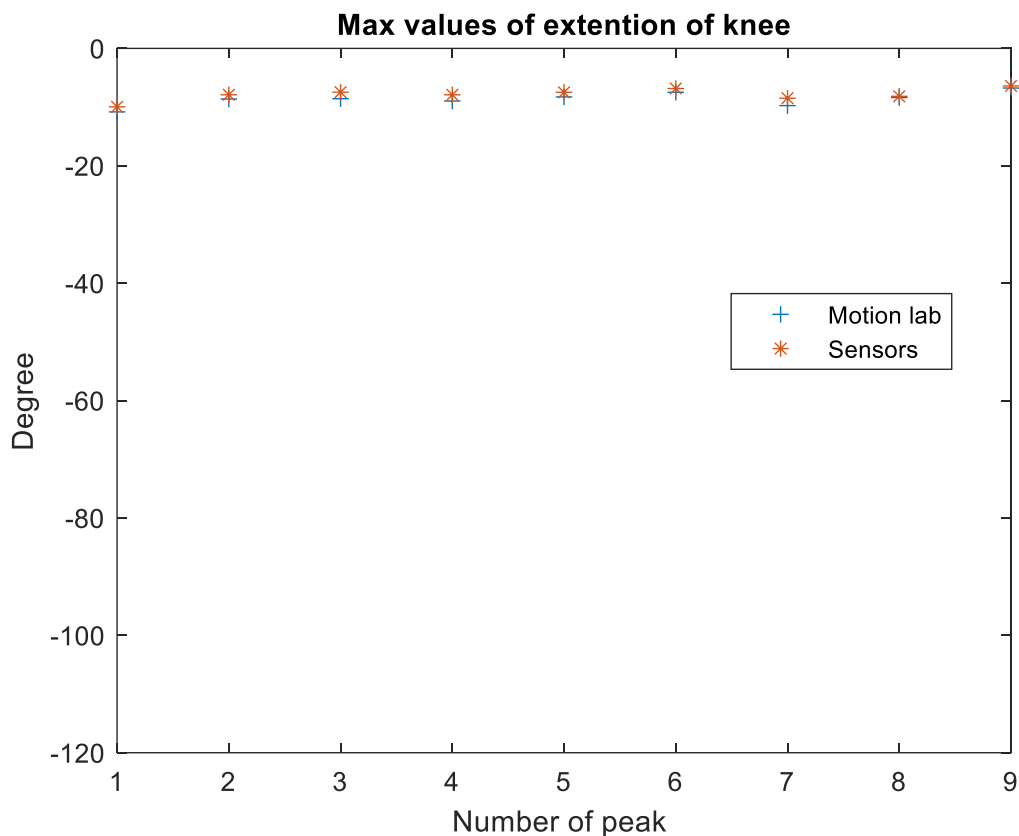
Figure 3.18. *MoCap (blue) and black sensors (red) maximum values knee extension for each squat or step in MT2*

Table 3.7. *Mean values of experimental data, calculated by both system and compared, during MT2*

Mean value of max flection in MoCap measurements (degrees)	Mean value of max flection in black sensors measurements (degrees)	Mean value of max extension in MoCap measurements (degrees)	Mean value of max extension in black sensors measurements (degrees)	Mean difference between MoCap and black sensors in max flection measurements (degrees)	Mean difference between MoCap and black sensors in max extension measurements (degrees)
-99.9 ± 2.3	-87.9 ± 1.0	-8.4 ± 1.2	-7.6 ± 1.1	11.9 ± 1.9	0.8 ± 0.2

3.2.3 Running

In this section we show the results of the two repetitions of MT8 (see Methods 2.4.2) performed by the subject. The two repetition of these motion test belong to the same test run.

MT8-1° Repetition (Starting from a standstill)
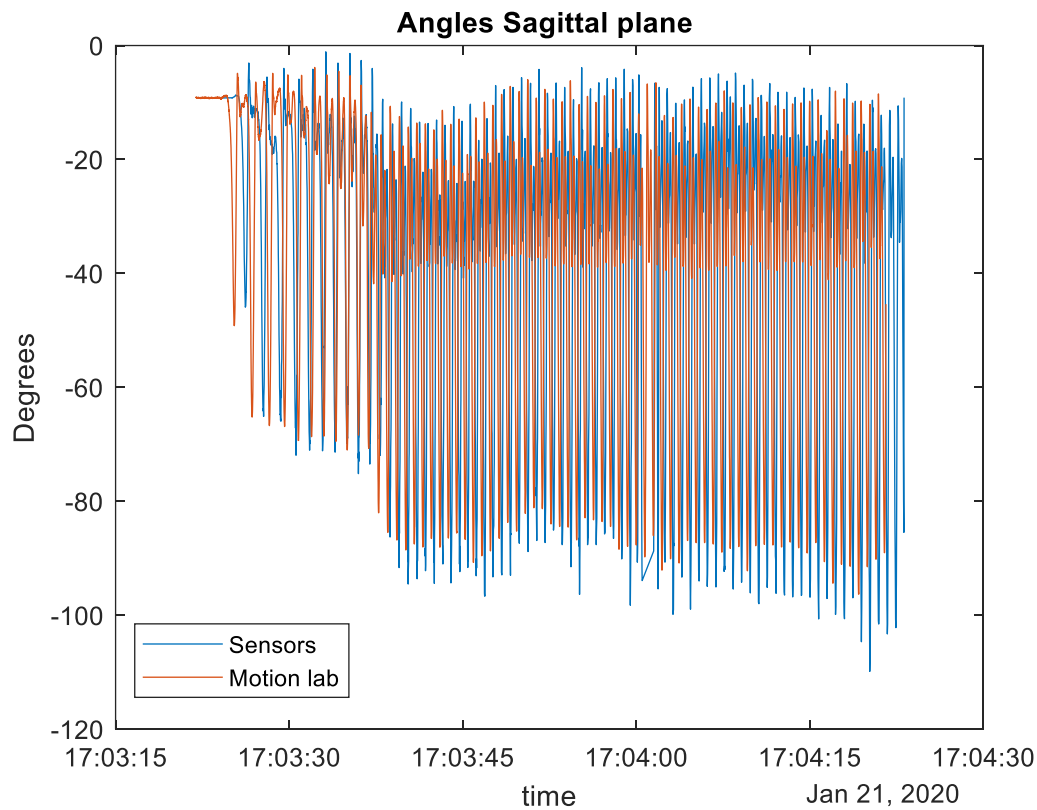
Figure 3.19. MoCap (red) and black sensors (blue) knee angle in MT8-1° Repetition

Due to the high number of samples, the curves can be difficult to read, which is why we have zoomed in the first 15 seconds in order to give a general idea of the patterns of both curves.

One can also clearly identify the increase of knee flexion during the first strides of running on the treadmill from standstill including the transitions from walking to fast walking to slow running and fast running, until a rhythm and steady state is reached. By peak flexion values, by peak-to-peak distance and other features one can identify all these categories and surely identify walking and running and transitional phases.

In this test it is clearly visible that all knee flexion peaks calculated by black sensors were overestimated during the running, whereas, during the transition phase from fast walking to running, black sensors knee flection peak values were closer to the MoCap ones.
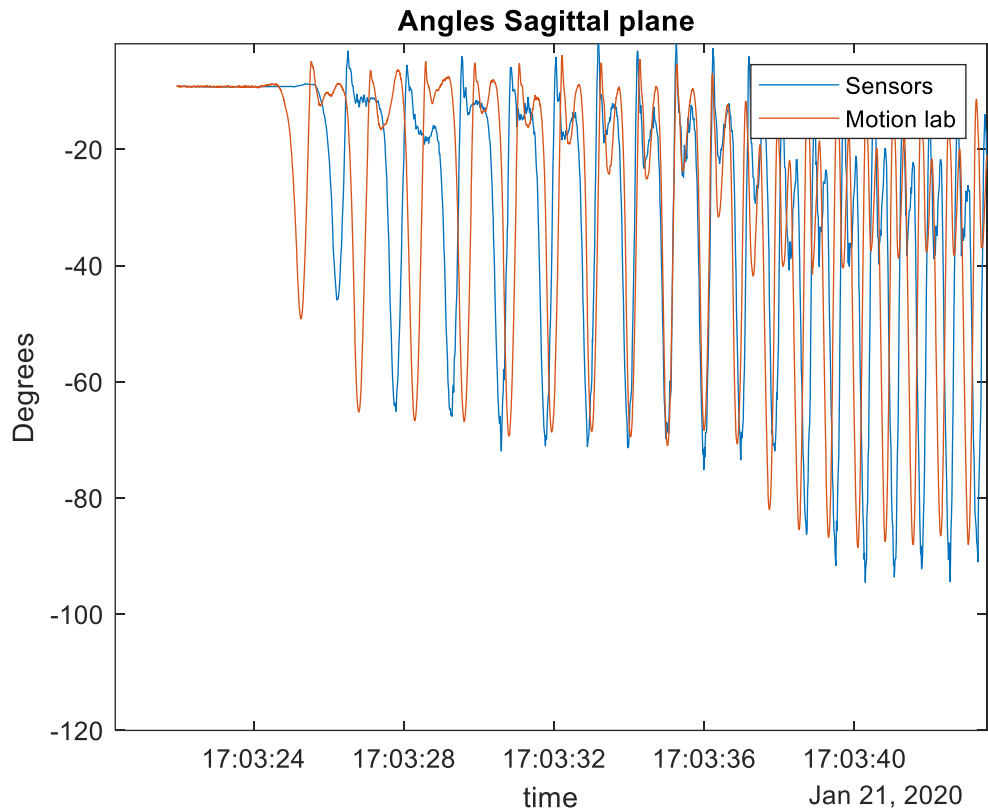
Figure 3.20. *Sagittal angles (knee flexion) during treadmill running from standstill for the first 15 seconds of MT8-1° Repetition*
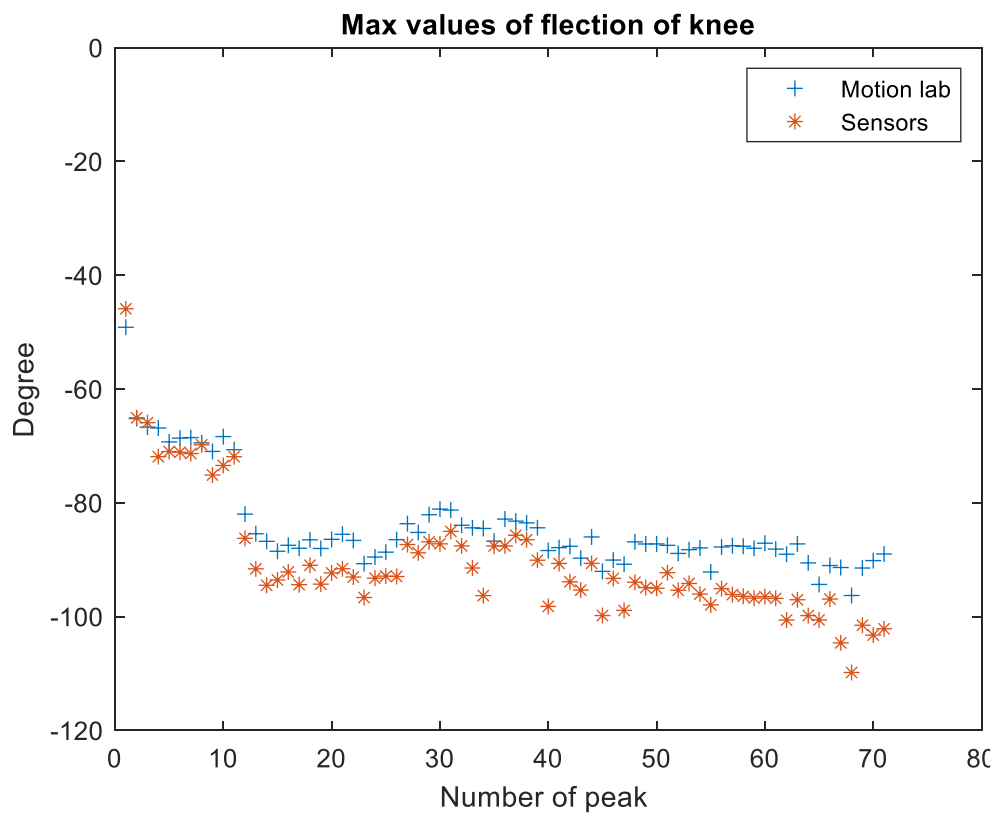
Figure 3.21. *MoCap (blue) and black sensors (red) maximum values knee flection each squat (peak numbers) or step (peak numbers, can we label walking/running) in MT8-1°Repetition*
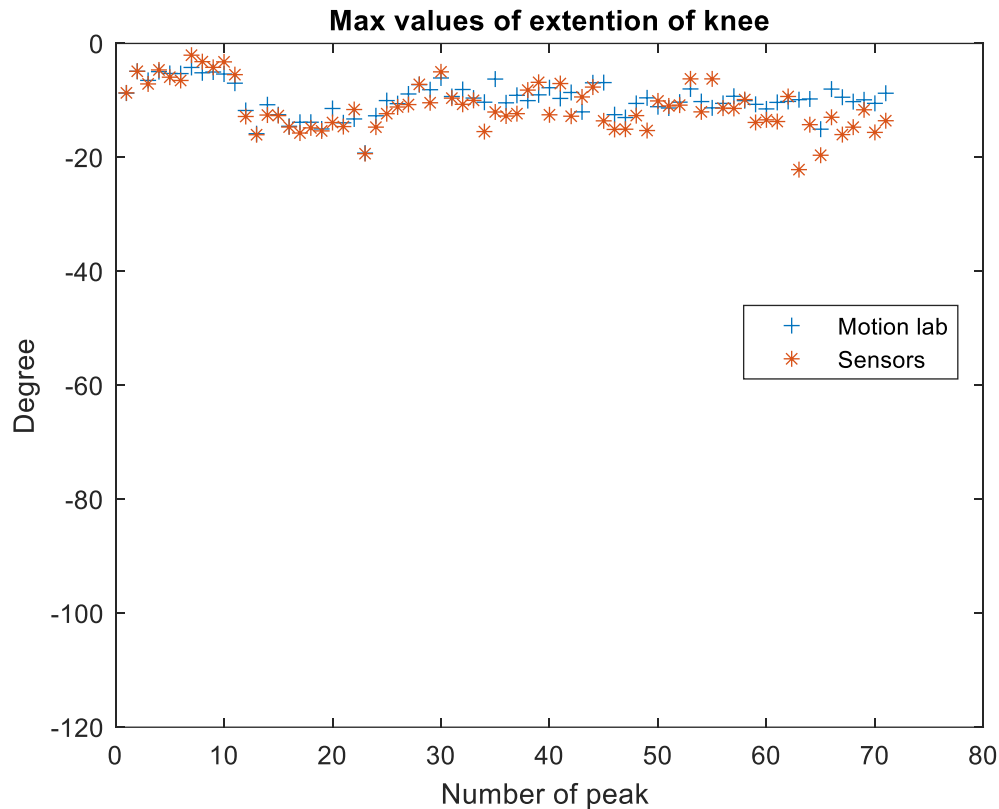
Figure 3.22. *MoCap (blue) and black sensors (red) maximum values knee extension for each squat or step in MT8-1°Repetition*

Table 3.8. *Mean values of experimental data, calculated by both system and compared, during MT8-1° Repetition*

Mean value of max flection in MoCap measurements (degrees)	Mean value of max flection in black sensors measurements (degrees)	Mean value of max extension in MoCap measurements (degrees)	Mean value of max extension in black sensors measurements (degrees)	Mean difference between MoCap and black sensors in max flection measurements (degrees)	Mean difference between MoCap and black sensors in max extension measurements (degrees)
-84.3 ± 8.4	-90.2 ± 10.9	-9.7 ± 2.9	-7.9 ± 3.4	6.1 ± 3.1	2.1 ± 1.3

MT8-2° (Started running)

Contrary to MT 8-1 ° repetition, it is visible that the blue curve, while continuing to qualitatively follow the pattern of the curve of the MoCap system, underestimates the angle of the knee. Due

to the large number of samples, as in MT8-1°, the first 15 seconds of both signals were zoomed in. This time, black sensors clock made two mistakes, introducing a time delay.
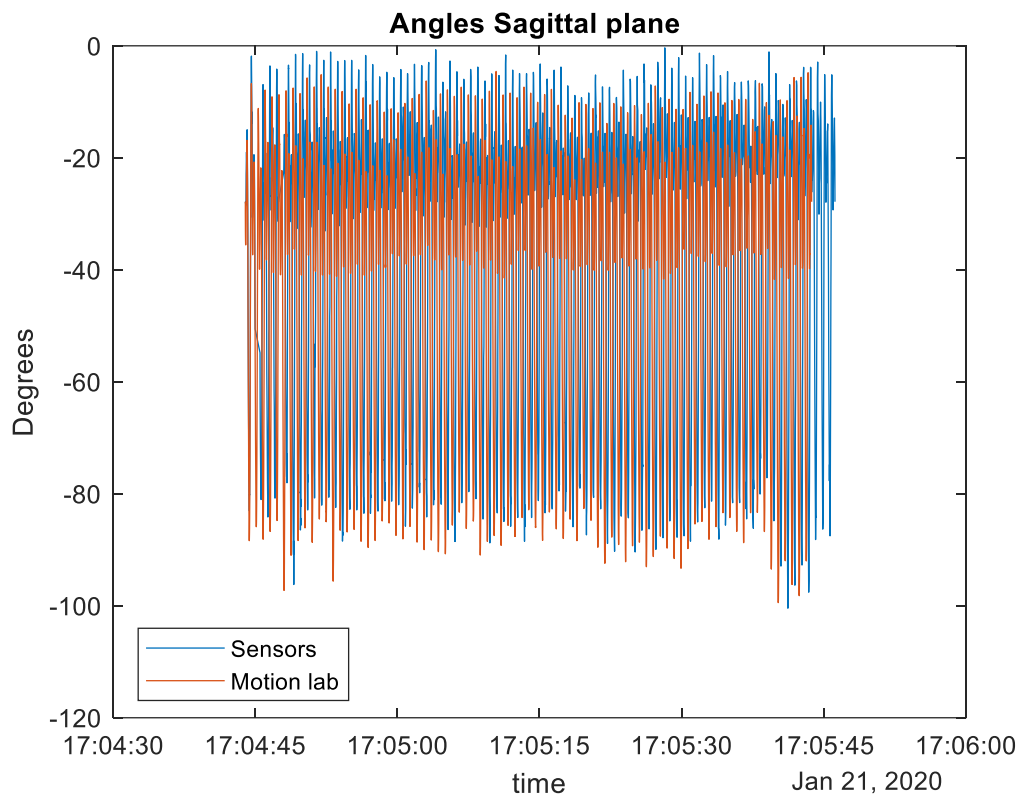
Figure 3.23. *MoCap (red) and black sensors (blue) knee angle in MT8-2° Repetition*

As the previous repetition of this test, in order to make it easier to evaluate we have zoomed in the first 15 seconds of this motion test.
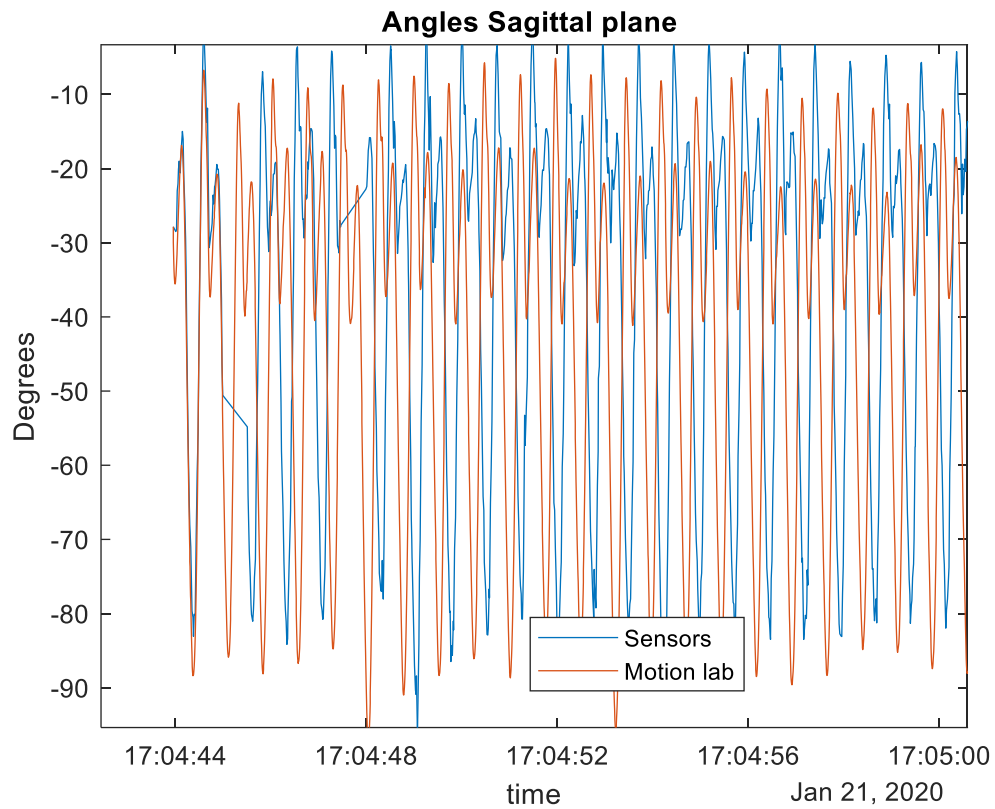
Figure3.24. *First 15 seconds of MT8-2° Repetition*
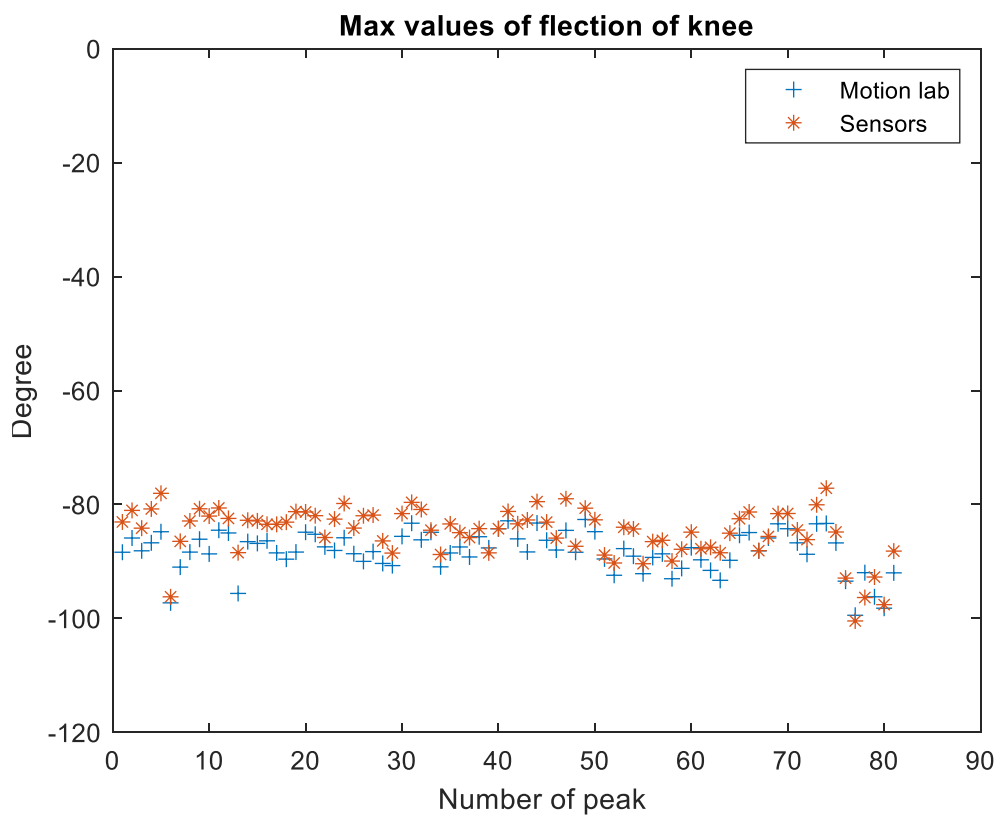
Figure 3.25. *MoCap (blue) and black sensors (red) maximum values knee flection for each squat or step in MT8-2°Repetition*
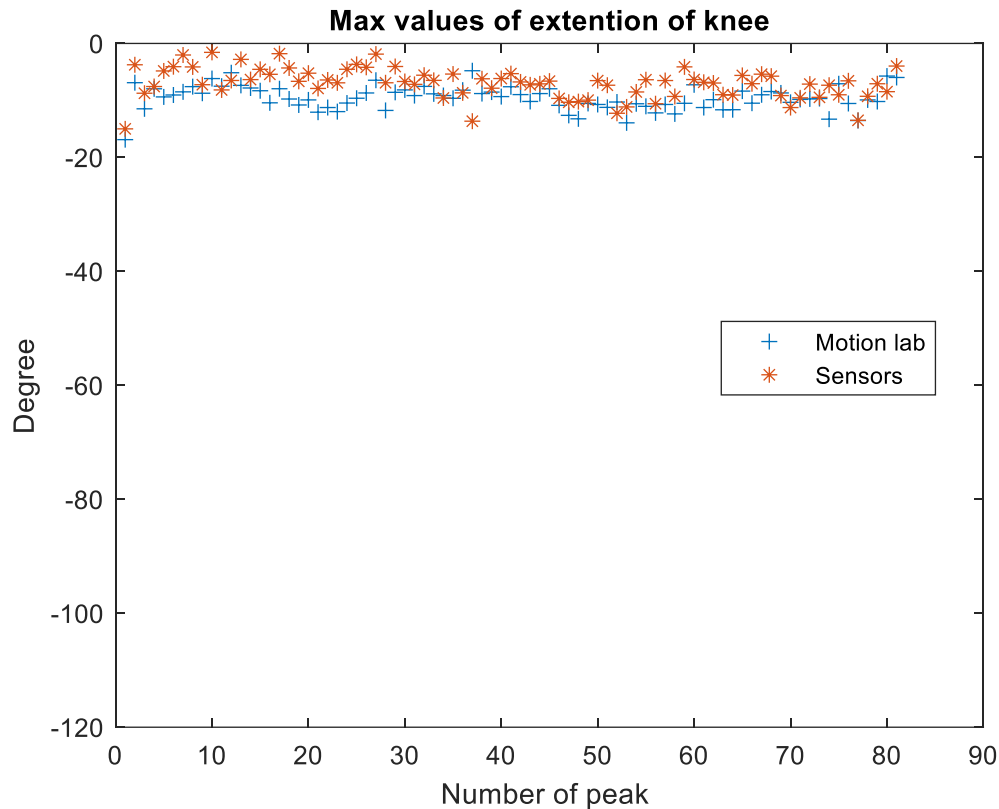
Figure 3.26. *MoCap (blue) and black sensors (red) maximum values knee extension for each squat or step in MT8-2°Repetition*

Table 3.9. *Mean values of experimental data, calculated by both system and compared, during MT8-2° Repetition*

Mean value of max flection in MoCap measurements (degrees)	Mean value of max flection in black sensors measurements (degrees)	Mean value of max extension in MoCap measurements (degrees)	Mean value of max extension in black sensors measurements (degrees)	Mean difference between MoCap and black sensors in max flection measurements (degrees)	Mean difference between MoCap and black sensors in max extension measurements (degrees)
-88.2 ± 3.6	-84.9 ± 4.4	-9.4 ± 2.1	-4.7 ± 2.4	3.5 ± 1.9	4.8 ± 1.5

3.3 Results of statistical analyses

From the parameters extracted in each repetition of MT1, we calculated the RoM in each single movement (i.e. a squat, a step, a gait cycle, etc.). All these values are collected in two tables

with size 32x5 (32 RoMs calculated for each repetition, 5 repetitions performed). In order to build the Bland-Altman plot, we calculated the mean of each row of each table and we reported it in Table 6.11 in the Appendix.

From Table 6.11, we calculated:

$$x\ axis = (\log_2(\text{Mean values from MoCap Table})$$
$$+ \log_2(\text{Mean values from Motion Sensor Table}))/2$$

$$y\ axis = \log_2(\text{Mean values from MoCap Table})$$
$$- \log_2(\text{Mean values from Motion Sensor Table})$$

$$Mean = mean(y\ axis)$$

$$Upper\ limt\ of\ Agreement = Mean + 1.96 * standard\ deviation\ (y\ axis)$$

$$Lower\ limt\ of\ Agreement = Mean - 1.96 * standard\ deviation\ (y\ axis)$$

The results are shown in Figure 3.26.

There are some very important features, in clinical terms, in this Bland-Altman plot. First, the distribution of points is not casual, and this gives us information about the systematic over- and underestimation. Then, the mean difference between systems (i.e. bias) is very close to the zero and most parts of points lie close to the bias line. It means that there is a high level of agreement between the MoCap system and black sensor system. Also, the limits of agreement are not wide that gives us information on interchangeability. It does not seem to be a trend in the scattering of points. A deeper discussion about the information given by the Bland-Altman plot is reported in   the   next   chapter.
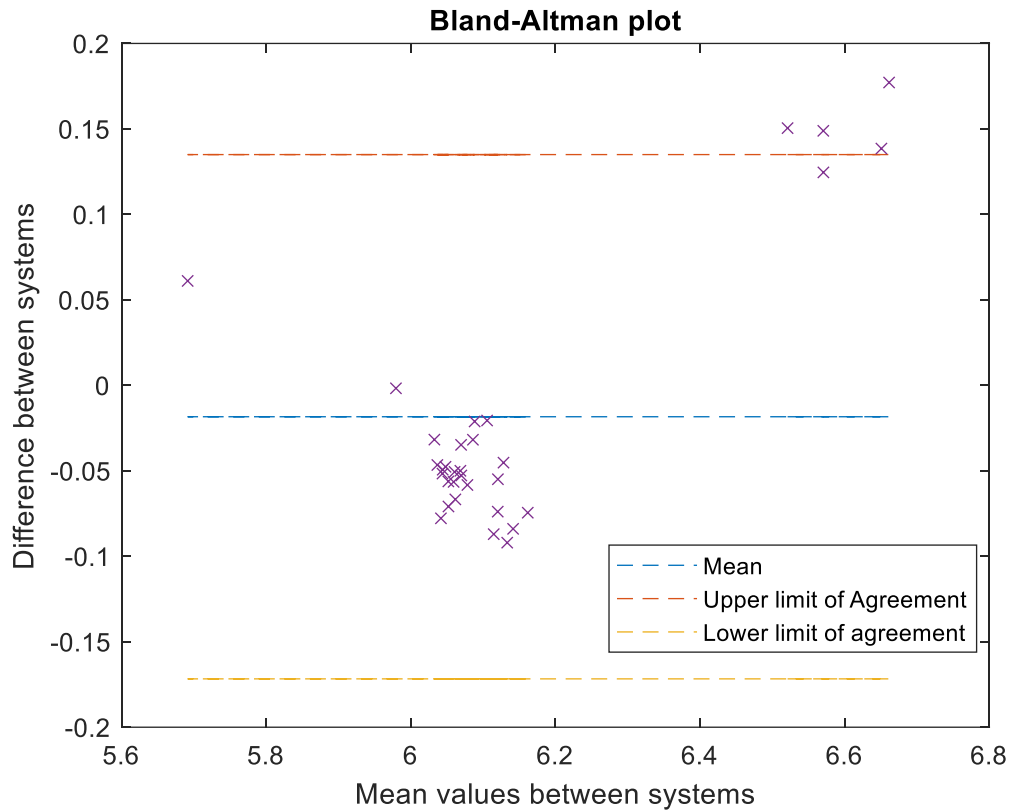
Figure 3.27. *Bland-Altman plot of all repetitions performed in MT1*

3.4 Results of usability test

The usability of both the software and hardware parts of our experimental system has been evaluated.

The usability of the software was assessed by two operators experienced in the analysis of movement who did not attend the adaptation phase of the app. From here on they will be indicated as operator A and operator B. This evaluation was carried out using the criteria selected and mentioned previously (see Methods 2.6). Operator comments are followed under their respective criteria.

1) **Screen Design and layout**

> *Operator A: "Appropriate, clean interface, all relevant information displayed, self-explanatory operating button"*

Operator B: "*Efficient screen design, technical layout for a professional operator, self-explanatory to some but not all degree, could be improved by stepped advise or prompts*"

2) **Learnability:**

Operator A: *"very easy to master for naïve experimenters, accommodation time less than 5 minutes"*

Operator B: *"Not fully self-explanatory but easy to learn. Quick-Start instructions may help to refresh user experience*"

1) **Overall reaction to the software**

Operator A: "it serves the purpose of data acquisition well"

Operator B: *"Purposeful, lean, contains required plus some additional features, good solution at this prototype stage and a good basis for further development*"

As for the wearability of the sensors, it was assessed by the same subject of the acquisitions. The sensors were worn under informal clothing in the way which is described in the methods chapter (see methods 2.6). The first assessment of wearability was carried out by placing both sensors 30 cm from the lateral femoral epicondyle (i.e. 75% of the length of the upper and lower segments).

The subject experienced after an initial sensation of discomfort, which continued for about 30 minutes. Later, he began not to perceive the presence of sensors during static daily activities (sitting for a long time, lying down, etc.). Instead, in dynamic activities (walking, climbing stairs, etc.) it happened that the hand hit the sensor located in the upper segment of the leg, due to its arm swinging movement.

During the subsequent evaluations, carried out respectively at 20 cm and 10 cm (i.e. at 50% and 25% of the length of the upper and lower segment), the subject had a lower discomfort time interval (i.e.

15 minutes). In these two evaluations, there were no difficulties in movements, both static and dynamic, due to the sensors.

The only problem common to all assessments of wearability occurred during the dressing and undressing of the subject, due to the attachment to the skin used to limit the movement of the sensors themselves.

As a final assessment, the subject said he was more comfortable when the sensors were placed 20 cm from the lateral femoral epicondyle.

4 DISCUSSION

A prototype knee monitor was build using 2 IMU units and an adapted algorithm to measure knee joint angles during motion based on the quaternion outputs. The new system was evaluated in a plausibility test, in a gait laboratory against gold standard 3D video motion capture and in a usability survey all showing feasibility, acceptable motion feature recognition and accuracy for some movement parameters and limitations for others for which solutions appear possible and are partially suggested.

4.1. Plausibility Test

What was expected, during the execution of the plausibility test, is that our experimental system followed the angles that were formed between the two sensors. What emerged from the results is that the sensors managed to qualitatively and quantitatively describe the movement made, albeit with varying degrees of accuracy for which in this simple test no ground truth value was measured but was assumed by position. It should be borne in mind that the theoretically intended movement paths between the sensors was performed by a human operator, which introduces some deviations and slight inaccuracy due to handshake. During sagittal plane movements, the "black sensors" estimated the angles in that same plane with a minimum difference between measurement output and intended movement, (less than 2 °), which, in our simulation, represents the flexion/extension angle of the patient's knee, the most important degree of freedom the "black sensors" system is designed to capture and monitor.

During sagittal plane movements, our knee monitoring system calculated also the angles in frontal and in transverse plane. The values expected in these two planes were very close to $0°$ but, instead, we have maximum angle measurements recorded for the frontal and transversal plane, during the movement above mentioned. They were less than $9°$. Due to sagittal plane movement is performed manually, there will be some movement also in the two other planes as the devices are not mounted on a fixed arm or robot. Thus, some part of this value is true, and the plausibility test showed that this aspect can be captured at plausible values, but how much of this is due to error cannot be calculated without a ground truth.

In the angles calculated during the movements performed in the frontal plane, the system showed a slightly lower accuracy (an error <5 ° in the range of the frontal plane and an error <12 ° in the ranges of the other two planes). Our experimental system failed to correctly calculate angles in the sagittal and frontal plane during movements in the transverse plane,

especially in the counterclockwise movement. During manual operation, one would create some rotations in the other axis but not that high in the transversal plane. The cause of this is due to the way the angles in the gyroscope are calculated. In fact, in the gyroscope, the angles are calculated in a range from -180 ° to 180 °. This issue is called influences the calculation of the quaternions and, consequently, the estimate of the angle.

In the literature there are several articles that present algorithms capable of overcoming the "flip" issue due to the -180 to 180 degrees definitions, starting from raw data of accelerometer, gyroscope and magnetometer. A possible solution for a better estimate of the angles during movements in the transverse plane would be to implement one of these particular algorithms. In fact, using the Arduino library, all quaternions describe angles in the range [-180°, 180°], instead, with the implementation of one of these particular algorithms, the quaternions leaving our knee monitoring system will describe angle in a range [0°, 360°], giving to the user (clinicians, physiotherapists) a more intuitive idea of knee angle.

However, some movements paths manually simulated in this test, such as excursion of ± 90 ° in the transverse plane reflect completely unnatural pathways and could only in theory be caused by a severe traumatic event. Considering this, we identified this particular issue as a secondary system error and less relevant for the intended solution and clinical needs, which thus did not significantly affect the performance in our system invalidation during tests.

4.2 Motion tests

4.2.1 Qualitative features

In general, our experimental system managed to give a probable estimate of the angles assumed by the patient's knee during all the motion tests performed. The black sensors output proved to closely follow the changes in motion patterns characteristic for each movement and the transition between them (for example from squatting to slow walking, from slow walking to fast walking or from fast walking to running). Moreover, the capacity of the black sensor system to also capture e.g. near-static posture such as a deep-flexion position during a squat (as for example the 3° squat during MT1-3° Repetition), including the variations during holding the postures, indicate that the system in a real-life monitoring situation could classify and /or count these situations as behaviour and analyse the stability of it as a potential digital mobility biomarker of knee function during a demanding task. The results show that the "black sensors" system possesses the characteristics and sensitivity required for monitoring the knee angle. From its knee angle curve both general parameters, (maximum knee flexion, maximum knee

extension, RoM, etc), and more specific events, (as for example the little peaks highlighted in MT2), can be detected. Moreover, all movements performed during the motion test are clearly recognizable as well as the transition phases between them. In real-life monitoring this could be very helpful e.g. in recovery or return-to-sports. While the knee flexion angle curves of the black sensor system qualitatively follow the gold standard well in shape and acceptably well in peak values, they are apparently slightly asynchronous, a feature explained in more detail under 4.3. limitations. From the plots and angle values calculated in the sagittal plane, our measurements do not seem to be affected by the drift problem. At least two hours have passed between the start and the end of the acquisitions,(as can clearly be seen from the plots timestamps), and even in the latest motion tests performed in chronological order (MT8-1° Repetitions and MT8-2° Repetitions), the black sensor system signal does not show any particular slope or anomalous value. The main reason of the lack of drift in values, but not the only one, is the direct use of the data coming from the gyroscope in the quaternions, without any integration process. The absence of this problem in our calculations avoids further post-processing operations and/or control procedures on the results. However, we cannot assume that "black sensors" system will be totally not affected by the values drift problem in longer acquisitions but, based on these results, we may suppose that if this problem will appear in future acquisition it will have a less impact on the quality of outputs.

There is a drift problem in the time vector of black sensors, but this aspect is treated in details in the "4.3. Limitations".

4.2.2 Quantitative features

A measure of how quantitatively close the two systems are, is given by the average absolute mean difference calculated, both in extension and in flexion, in each motion test. What emerged clearly from the results of the acquisitions is that the calculation of the knee extension by the black sensor system is not influenced by the movement speed. In fact, for this parameter, the absolute mean difference between the two systems is less than 5 ° in all the motion tests performed. On the other hand, the accuracy of knee flection estimation is linked to movement speed. Indeed, during slow movements (squats and sit-to-stand-to-sit transitions), the absolute mean difference between values of MoCap system and black sensors system becomes higher than in fast movements (walking and running).

The best estimation by black sensors system of maximum knee flexion was in walking, where the mean absolute difference is less than 4°. The estimation of this parameter is the better in walking than in running probably because during the running the vibrations and skin artifacts are more consistent and that compromise the goodness of measurements

More generally, one can notes that knee angle flexion peaks are systematically underestimated in slower movements and knee angles values, both in flexion and in extension, are systematically overestimated in all motion tests performed.

The reasons of this behaviour are unclear. A possible cause of this behaviour could be the placement of the sensors on the subject's body segments, which could make the system very sensitive to speed movements. Another possible cause could be the lack of any filtering process, which could make the results too influenced by noise at low and high frequencies. In this case, the results could improve after applying an appropriate filter (i.e. a 4 order Butterworth low pass filter or a band-pass filter). Finally, a reason of this behaviour could be the Arduino quaternions, since we do not know how they are calculated from BNO055. In this case the implementation of quaternion calculation in our algorithm could reduce or even solve the problem. However, this behaviour must be studied in the subsequent stages of the project development, in order to fully understand the cause and look for optimal solution.

4.2.3 Inner calibration features

Looking at the values of the absolute mean errors reported in the tables below the tests, it can be deduced that the performances of black sensors prototype system have improved with time. In fact, the calculated average error, both in flexion and in the extension of the knee, decreased with the succession of tests. Increasing of absolute mean errors in MT8, the last motion test performed in time, is caused by artificial shaking during running. This trend is because the accelerometer, the gyroscope and the magnetometer inside each sensor achieve better calibration if they are kept in motion. The accelerometer, the gyroscope and the magnetometer are able to keep the level of calibration achieved for long time. We do not investigate the time request to lose one (or more) "level" of inner calibration (we remember that the inner calibration status is expressed between a scale from 0 to 3 in which 0 means "no calibration" and 3 means " fully calibrated"), so we can only discuss about what happened during our acquisitions in gait laboratory. The maximum level of inner calibration was achieved by all tools in IMU unit after

few minutes from the turning on the sensors and before the beginning of MT1-1° Repetition. During motion tests, all levels of inner calibration never decreased because the subject moved the dominant leg, where the sensors were attached, also when he was not performing a motion test. In our opinion, little movements are enough to keep the accelerometer, gyroscope and magnetometer in BNO055 well calibrated. Moreover, these three tools can recalibrate themselves, so any calibration loss is not a problem in long activity monitoring applications. Better internal calibration of the single instruments implies a better calculation of the quaternions and, consequentially, a more precise evaluation of the knee angle. Performance improvement over time is a feature that perfectly matches with needs of knee monitoring in daily life.

4.2.4 Statistical features

A further evidence about the goodness of our new system comes from statistical analyses performed through Bland-Altman plot. The proximity of most points in the graph to the bias line indicates that there is a good agreement between two methods, i.e. gold standard MoCap system and our experimental black sensors system for the knee kinematic movement parameters chosen (maximum knee extension, maximum knee flexion and range-of-motion per movement cycle). The concentration of points in specific areas of plot indicates some movement specific systematic error beyond the random effect and confirms that the two methods are not interchangeable. We aim to create a continuous knee monitoring system that is as valid as the optical motion capture systems, but which does not replace them.

The last aspect investigated during motion test was the duration of battery life. Battery life was tested both during acquisitions and outside the analysis laboratory. The result was that the battery, if at maximum charge, kept the device on for at least 16 consecutive hours.

4.3 Limitations

Currently, our experimental system suffers some limitations, as can also be seen from the acquisitions, both at a design and performance level. At this stage, the variability introduced by various subjects was not a priority as the principles to be developed and studies here are sufficiently well represented by a single test subject and a certain number of tests and repetitions.

The first limitation of black sensors system is the inability to correctly measure the subject's turning during the activities. Fast and sudden turning are wrong-calculated by black sensors because of the above-mentioned "flip" angle issue (from -180° to 180°). Turning is a very common event in daily life and it is evident that representing angles in this range is completely unsuitable for daily activity monitoring. Moreover, turning events modify the reference system against which the knee angle is calculated, so the movement estimation after turning is compromise. There are no problems in estimating the angle of the knee if the turning is performed very slowly or you remain motionless for a few seconds before restarting any activity

As it has been widely shown in the "Results" section, the second limitation is the time delay between the two signals. To clearly explain the origin of this problem, the diagram in Figure 4.1. was created.

The time shift seen in the graphs is caused by two factors:

1) the lack of synchronization between the clock of the motion analysis laboratory and that of the sensors
2) from an anomaly that sometimes occurs in one of the sensors.
   a) Furthermore, it is sometimes increased by the "time jumps" that occur in the black sensors' timeline.

As previously explained in the methods chapter, when the sensors acquire a sample, they also record the time in HH: MM: SS format. As already explained in table 2.1, (see "Methods- 2.3 Adaptation phase"), the black sensors timeline is calculated starting from the capture moments of the two sensors. Since the sketches are loaded into the two sensors at different instants, the clocks of the two sensors are not synchronized. We have this situation:

$$Timestamp\ from\ Sensor\ 1 \neq Timestamp\ from\ Sensor\ 2$$

For this reason, we created an artificial timestamp taking the mean time from each sample of each sensor. Of course, this operation introduces an error in comparison with MoCap signal. The anomaly in the timeline of the black sensors consists in an incorrect recording of the time at which date is sampled. The cause of this anomaly remains unclear for now. This malfunction of the microprocessor could be due to the high number of operations required in a few milliseconds. The error committed every time this anomaly occurs is <1 second and the combination of these factors determines an incorrect calculation of the timeline vector of our experimental system. While this non-constant (thus linearly non-correctable), time shift affects the exact timing of specific events, this is of less or no interest/effect in long-term monitoring,

where activity classification is central and the timing of events refers to their duration which remains highly accurate and not on their exact clock time. Thus, the black-sensor system as is, seems usable for monitoring applications.

```
                        ┌─────────────────────┐
                        │     TIME DELAY      │
                        └─────────────────────┘
```

┌─────────────────────┐   ┌─────────────────────┐
│   No synchronization │   │   black sensor's │
│   MoCap-black sensor │   │   timeline vector │
└─────────────────────┘   └─────────────────────┘
                                              ┌─────────────────────┐
                                              │ no synchronization │
                                              │ Sensor 1 - Sensor 2│
                                              └─────────────────────┘
                                              ┌─────────────────────┐
                                              │ black sensors 's clock│
                                              │   jump forward   │
                                              └─────────────────────┘
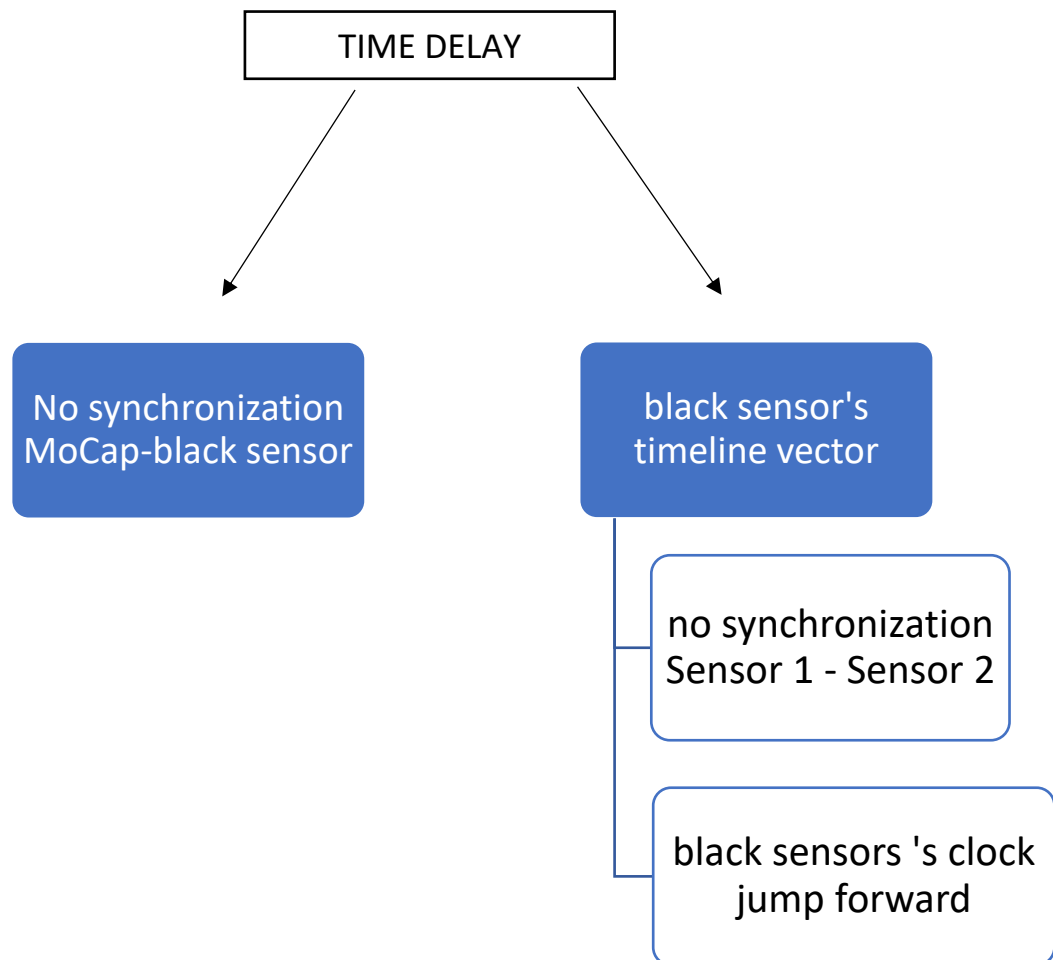
Figure 4.1. *Diagram to schematize the time delay problem*

From a general point of view, the two major limitations that prevent using this prototype in monitoring daily activities are:

• the dependence of a wi-fi network

• the lack of a storage system for the data collected

These two problems are closely related since the need to establish a Wi-fi connection for the transmission of data from the sensors to the computer arises from the lack of memory inside the sensors. The flash EPROM memory built into the microprocessor board is too small (4 MB)

to be useful for this project. Due to the high number of samples stored every second, the card would run out of memory space within a few seconds. Besides, saturating the EPROM memory would make the entire card unusable.

4.4 Possible solutions to our problems and future works

As it is possible to see the definition of the angles in the gyroscope between -180 and 180 causes problems and inaccuracies both in the estimate you need intra / extra rotational movements and in turning. To redefine the angle range, in order to delete the "flip" issue", through the implementation of a new algorithm for calculation of quaternions could solve both, increasing the performance of the black sensors monitoring system.

As part of a monitoring project such as ours, having a correct timing of events is very important for evaluation. It is essential to avoid the possibility that the shift over time between the two systems increases. The problem of temporal mismatch between the MoCap system and the black sensors has been carefully analysed, and several possible approaches have been proposed. It is necessary to implement a synchronization procedure between the two systems so that the time difference is reduced or even cancelled. The "time jump forward" problem could be solved in the post-processing phase. The designed solution consists of a function inserted within the Matlab algorithm, which has as input the raw timeline coming from the sensors and as output a new timeline without this calculation error. The function should recognize the presence of a "time jump" and replace it with a new time. The new time can be obtained through interpolation between the time preceding the anomaly and the following one. In order to eliminate the dependence on the computer, it was thought to implement a 64 GB micro-SD card. The implementation of this solution required the change of some hardware components and the addition of new components. The WeMos TTGO T-Base esp8266 board has been replaced by LOLIN D1 mini, a mini wifi board with 1MB flash based on ESP-8266EX, shown in figure 4.1. This new card, smaller in size than the previous one, has the following characteristics:

• 11 digital IO, interrupt / pwm / I2C / one-wire supported (except D0)

• 1 analog input (3.2V max input)

• a Micro USB connection

• Compatible with MicroPython, Arduino, Nodemcu

• Size: 34.2x25.6 mm

• 1M Bytes FLASH inside

• Weight: 3 g

Figure 4.1. *The new Wi-fi board LOLIN D1 mini*

The new components that we used to build the new version of our monitoring system are:

1) **A micro SD card shield**
2) **Dual base shield for Wemos D1 mini**
3) **2 male connectors**
4) **A battery shield with following features:**
   a) Charging Voltage: max: 10V, recommend: 5V
   b) Charging Current: max: 1A
   c) Lithium Battery voltage: 3.3-4.2V
   d) Boost Power Supply: 5V (max: 1A)

In Figure 4.2 is shown how the new version of our experimental sensors looks like.
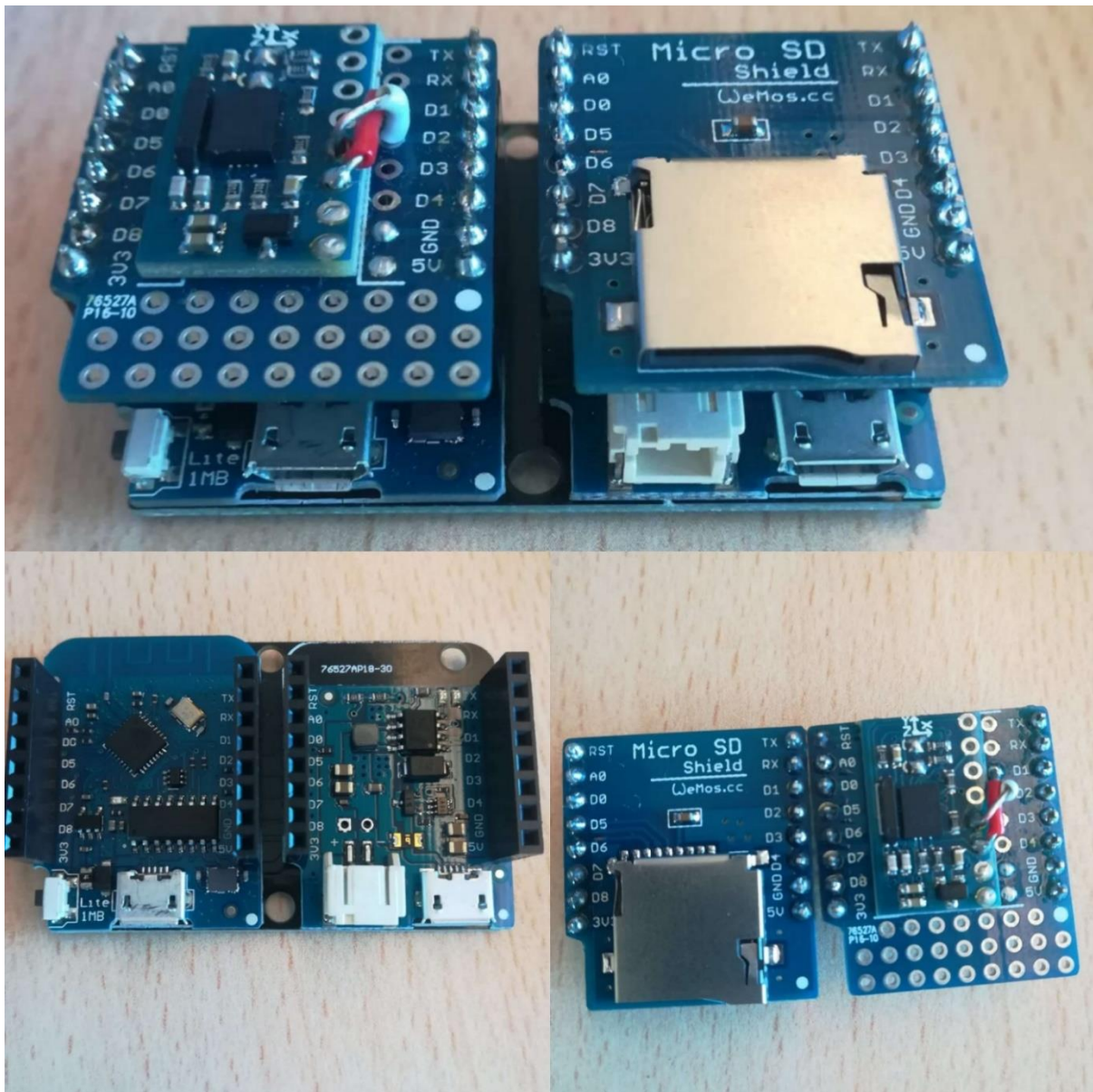
Figure 4.2. Lolin D1 mini and the battery shield welded on dual base shield (left down) with 2 male connectors, the Adafruit BNO055 absolute orientation sensor and the micro SD shield (right down), all component assembled together (up)

With the elimination of the Wi-fi connection, the Arduino sketch was also changed. The part that managed the sending of data to the computer has been replaced with lines of code that allow writing the data directly on the micro-SD card. This solution will allow storage capacity compatible with the needs of long-term monitoring, making the use of an additional device unnecessary. Unfortunately, it was not possible to test this new version of the experimental system in the context of this thesis project. The experimentation of this new set-up will be

carried. Furthermore, it can be assumed that by reducing the number of operations entrusted to the microprocessor, the "time jump" events are also significantly reduced.

However, the dimensions of this new prototype of the knee angle monitoring system black sensors are too large to allow comfortable and prolonged use by the subjects. sensor miniaturization is one of the next objectives. Nevertheless, the black sensors system developed here was meant as a low cost, highly adaptable platform for algorithm development and validation and not yet a commercial product, so that these usability aspects do not matter yet as much.

The black sensors' performance will be tested in free-living environmental with a high number of subjects. Despite we tested during our acquisitions the most part of daily life movements, we tested them separately and in well-defined way. Indeed, in daily life conditions, there are rapid and sudden changes in motion patterns, as well as long periods of rest (sleep) that have not been simulated in our motion tests. So, the next step of validation process of this knee angle monitoring system will be the assessment of performance in real life conditions with a wide number of subjects. Once the problems listed above have been resolved, the performance of the black sensor monitoring system will also be evaluated on the frontal and transverse planes, to be able to perform a complete and 3D analysis of the movement of the knee. The next step will be the design of support for the assessment of knee motion. Once the black sensor system will be able to record the variations on all three anatomical planes, an algorithm for recognizing specific events (steps taken, stopovers, sitting-standing transitions, running) or events abnormal in the patient's motor activity (turns, falls, reduction for prolonged periods, hyperextensions) will be elaborated. This will provide clinicians and physiotherapists an additional tool for assessing knee mobility.

4.5 Discussion about usability

The computer app was rated positively by the two experts. From the reported comments (see Results 3.4), the design and organization of the user interface have been deemed clear and efficient. The system proved to be very easy to use, although not completely intuitive, thanks to the button descriptions. The system did not generate any problems for the operators at the time of use. Despite the positive opinion, the usability of the app can be improved by using prompts and pop-ups in the various stages of use. As for the usability of the sensors, it depends on the positioning on the subject's leg. Although they did not limit or obstruct daily physical

activities, they aroused a feeling of discomfort in the subject, especially when the sensors were closer to the hip and ankle. This is a problem related exclusively to the design and shape of the sensors, it can be solved in the subsequent phases of the project, with the miniaturization of both the hardware components of the sensors and the protections.

However, there is a need to perform a more objective and accurate assessment of the usability of our experimental system. This can be done using standardized questionnaires and the increase in the number of users.

5 Conclusion

The aim of this thesis was to show the development and results achieved in the initial phase of a project for the development of a new knee monitoring system. The goal in this initial phase of the project was to create a knee monitoring system that had performance comparable to the MoCap system in a wide range of daily activity and specific movements. In this thesis work the bases on which the project was developed, and the subsequent adaptation phases were explained. Finally, the results obtained following the validation phase were exposed and discussed. The new experimental system designed has been evaluated concerning the current gold-standard reference instruments and has managed to obtain, in any movement performed on the sagittal plane, comparable results, especially in evaluating the extension of the knee in any movement performed, with an absolute error less than 5°.

Although these results relate to acquisitions on a single subject, they provide promising indications on the possible applications and performances that the new experimental system can obtain. The prototype of the black sensor system has numerous aspects that must be developed both in the software part (such as the creation of the time vector, the implementation of a low-pass/band-pass filtering and subject-specific self-calibration procedures) and in the hardware part (miniaturization of components, waterproofing of sensors, improvement of battery life). In the future, this device could also be validated for further populations, adapted to be used for the monitoring of other joints and further developed in order to operate even without calibration and adaptation

The final goal is to create a tool for daily monitoring of knee activity in daily living conditions that is reliable and that can help correct any errors. The areas in which the use of this tool is applied are rehabilitation, but also, shortly, that of prevention.

6. APPENDICE

6.1 Quaternion theory

A quaternion is an extension of complex numbers. As is known, a complex number is made up of two components, that is, a real part and an imaginary part; it can be mapped in a Cartesian plane and therefore represented as a vector. If you have a complex number of type x + i·y in a plane you will get the value x as the coordinate of the abscissa, as the value y is ordered. Operations between these numbers are performed with the known rule $i^2 = -1$. Quaternions are an extension of complex numbers to the purpose of mapping the space, only that unlike the complex field, the dimensions used are four, one real and three imaginaries. This peculiarity makes them difficult to visualize in their entirety since they consist of a four-dimensional abstraction that satisfies properties similar to those related to complex numbers. A quaternion can be described by the formula:

$$t + x \cdot i + y \cdot j + z \cdot k$$

where t, x, y and z are real numbers and i, j and k are imaginary components. If y and z are equal to 0, an imaginary number is trivially obtained, while if x, y and z are equal to 0 there is a real number. Sum and product of two quaternions are defined taking into account the relations:

$$i^2 = j^2 = k^2 = -1$$

$$i \cdot j = k$$

$$j \cdot k = i$$

$$k \cdot i = j$$

$$j \cdot i = -k$$

$$k \cdot j = -i$$

$$i \cdot k = -j$$

Can be seen from the previous expression the analogies with the rule $i^2 = -1$, which governs complex numbers. Unlike these, the product of quaternions is not, in general, commutative, precisely for the rules which indicate a very precise order in the operations to be performed.

Quaternions have many characteristics similar to complex numbers, such as the norm and the conjugate, however they differ in not having a commutative product as mentioned above. The main properties of the quaternions are shown below:

1. **Non-commutative product.** The product can be applied to two quaternions considering them as polynomials. In general, considering two quaternions q1 and q2, the product of q1 by q2 usually differs from the product of q2 by q1 ($q1 \cdot q2 \neq q2 \cdot q1$). Since the product of the quaternions before the simplifications of the imaginary components always have the same structure, the resulting quaternion can be obtained directly by immediately operating on parameters a, b, c and d, therefore if we consider for example the quaternions:

$$Q_1 = t_1 + x_1 \cdot i + y_1 \cdot j + z_1 \cdot k, \quad Q_2 = t_2 + x_2 \cdot i + y_2 \cdot j + z_2 \cdot k$$

$$Q_1 \cdot Q_2 = Q_{ris} = t_{ris} + x_{ris} \cdot i + y_{ris} \cdot j + z_{ris} \cdot k$$

With

$$t_{ris} = t_1 \cdot t_2 - x_1 \cdot x_2 - y_1 \cdot y_2 - z_1 \cdot z_2$$

$$x_{ris} = t_1 \cdot x_2 + x_1 \cdot t_2 + y_1 \cdot z_2 - z_1 \cdot y_2$$

$$y_{ris} = t_1 \cdot y_2 + y_1 \cdot t_2 + z_1 \cdot x_2 - x_1 \cdot z_2$$

$$z_{ris} = t_1 \cdot z_2 + z_1 \cdot t_2 + x_1 \cdot y_2 - y_1 \cdot x_2$$

This product definition is extremely convenient from the computational point of view since it allows to obtain a direct result without further refinements.

2. **Associativity**

This feature does not only concern the product of quaternions, but can also be extended to the sum, in fact the quaternions can be added and multiplied with each other like complex numbers (as long as the order of the multipliers is maintained in the product as it is not commutative) and they enjoy the associative property with respect to these two operations, so given three quaternions Q_1, Q_2, Q_3 we can say that:

$$Q_1 + (Q_2 + Q_3) = (Q_1 + Q_2) + Q_3$$

and that

$$Q_1 * (Q_2 * Q_3) = (Q_1 * Q_2) * Q_3$$

3. **Identity**

Consider a particular type of quaternion useful in multiplications, that is the quaternion with a real part equal to 1 and imaginary parts equal to 0 (therefore comparable to the real number 1). A quaternion thus formed is referred to as identity and is formulated through the following writing:

$$Q_{id}=1+0{\cdot}i+0{\cdot}j+0{\cdot}k$$

This quaternion has the characteristic of being the neutral element for multiplication, that is, for any quaternion, it is valid that:

$$Q_{id} *Q = Q* Q_{id} =Q$$

4. **Conjugate**

A conjugate quaternion is defined as following

$$Q= t - x{*}i - y{*}j - z{*}k$$

that is, the sign of the parameters of the imaginary components is inverted. from this, it can be understood that the conjugate produces a contrary rotation of the quaternion from which it derives.

5. **Norm**

The norm of a quaternion is thus defined:

$$|Q|=\sqrt{t^2 + x^2 + y^2 + z^2}$$

Unit quaternions will be considered later, and this subset will be referred to. There are also formulas for using normal quaternions for rotations, only that they will not be taken into consideration since their operation is similar to that reported for the unit subset.

The fixed reference system depends on the initial position of the sensor, and that the system integral with the platform has the x, y and z axes defined directly by the hardware.

The gyroscope, when scanned, simultaneously provides measurements of rotations of the 3 axes. This data can be transformed into yaw, pitch and roll rotation angles. The order of insertion of the rotations is a crucial point for obtaining the correct quaternion, in fact, if you first insert a rotation in one axis (e.g. a rotation of yaw) and then a rotation in another axis (of roll) you get a different quaternion than what would be obtained if the order were reversed. In this regard, it is necessary to have an insertion formula (and then, as we will see, its extraction) that can manage these values simultaneously. The formula for all the Arduino platforms is similar to that for the Eulerian angles, it differs only from the position of the X, Y, Z axes of reference of the Cartesian space as mentioned above. Given the yaw, pitch and roll rotation angles, we define the following intermediate angles:

$$p = pitch/2 \quad y = yaw/2 \quad r = roll/2$$

we also define the following intermediate results, useful for obtaining the rotation formulas:

$$a = \cos(p) \cdot \cos(y)$$

$$b = \sin(p) \cdot \cos(y)$$

$$c = \sin(p) \cdot \sin(y)$$

$$d = \cos(p) \cdot \sin(y)$$

Formulas that transform rotation into angles into a quaternion are defined as:

$$t = a \cdot \cos(r) + c \cdot \sin(r)$$

$$x = a \cdot \sin(r) - c \cdot \cos(r)$$

$$y = b \cdot \sin(r) + d \cdot \cos(r)$$

$$z = b \cdot \cos(r) - d \cdot \sin(r)$$

The system created in this project will provide the position of the sensors in the form of a quaternion that will be elaborated and reconverted in eulerian angles through the formulas inverse to those shown.

6.2 Results of other motion tests

MT1-2° Repetition
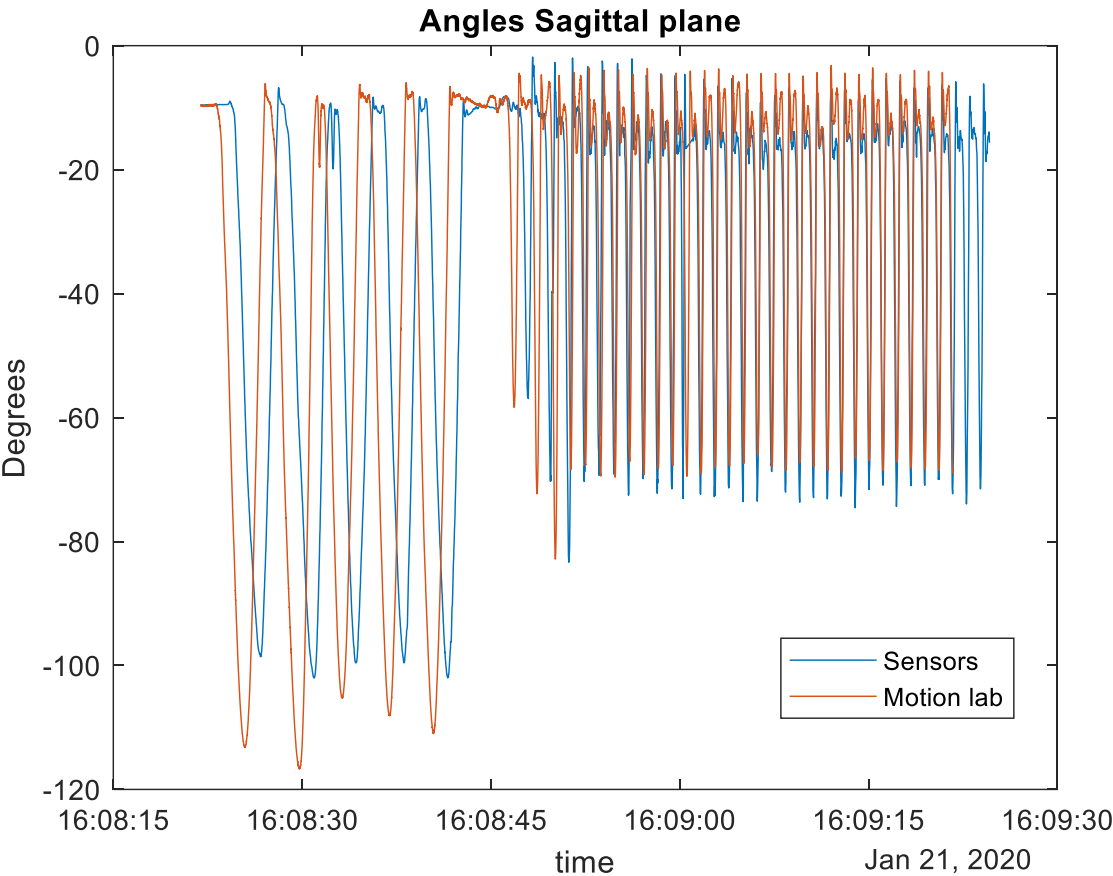
Figure 6.1. *MoCap (red) and black sensors (blue) knee angle in MT1-2° Repetition*

In this motion test there are not significative differences respect the previous one. Despite this time black sensor' clock worked perfectly, a delay between two signals still remains. The shapes of knee angle signals remain qualitatively very close. Even in this repetition, during squatting, black sensors knee sensors peak values underestimate the real values of knee angle by ca. 10 degrees
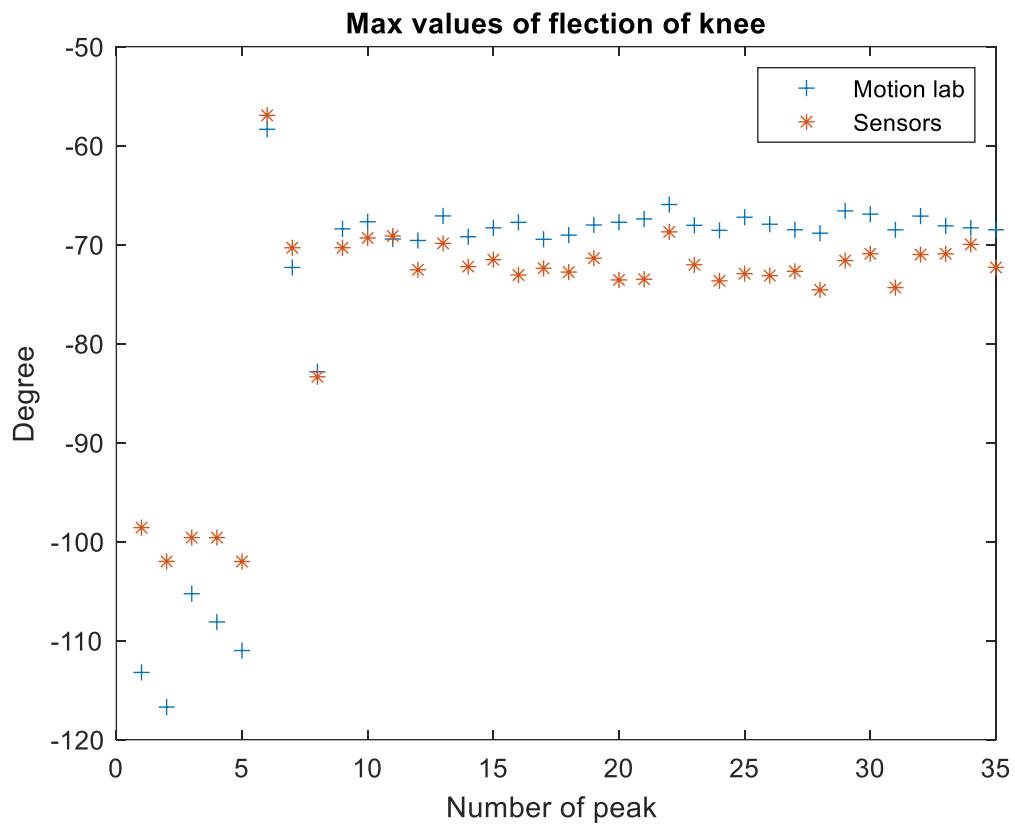
Figure 6.2. *MoCap (blue) and black sensors (red) maximum values knee flection for each squat (peak 1-5) or step (peaks >6) in MT1-2° Repetition*
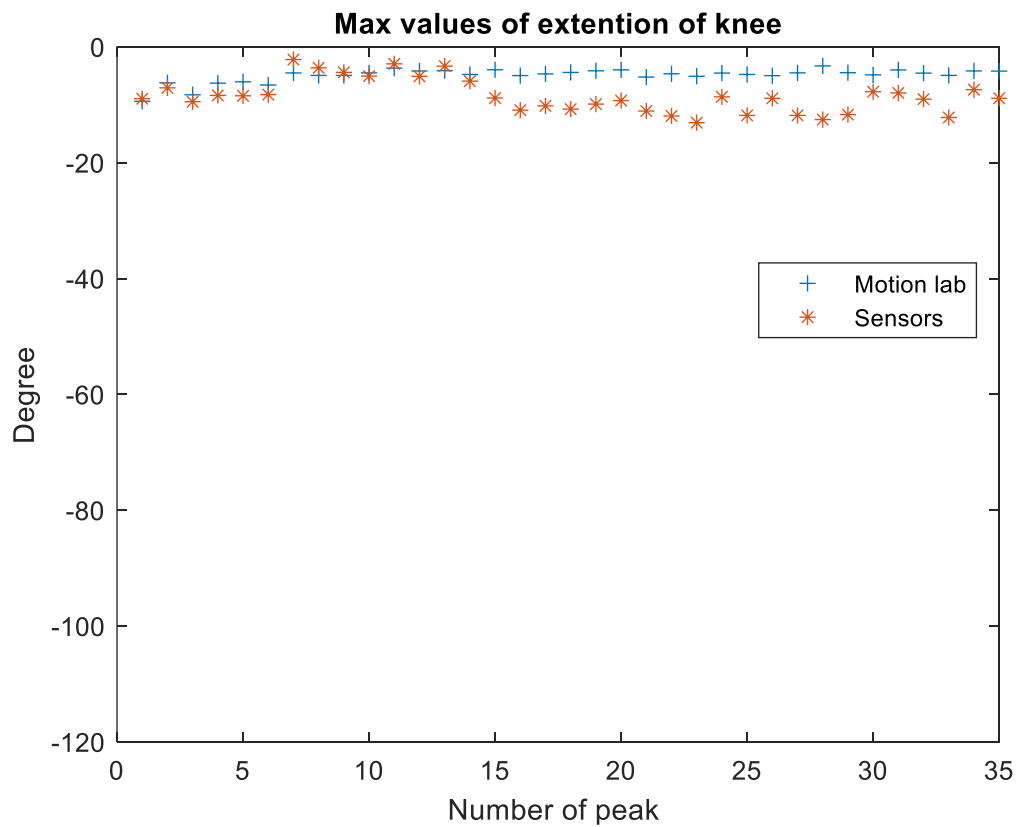
Figure 6.3. MoCap (blue) and black sensors (red) maximum values knee extension for each squat (peak 1-5) or step (peaks >6) in MT1-2° Repetition

Table 6.1. *Mean values of experimental data, calculated by both system and compared, during MT1-1° Repetition*

Type of movement	Mean value of max knee flection in MoCap (degrees)	Mean value of max knee flection in black sensors (degrees)	Mean value of max knee extension in MoCap (degrees)	Mean value of max knee extension in black sensors (degrees)	Mean difference between MoCap and black sensors in max knee flection (degrees)	Mean difference between MoCap and black sensors in max knee extension (degrees)
Global	-74.5 ± 15.5	-75.8 ± 10.8	-4.8 ± 1.3	-6.0 ± 2.2	4.6 ± 3.2	1.9 ± 1.1
Squatting	-110.9 ± 4.4	-100.3 ± 1.6	-7.2 ± 1.5	-8.3 ± 1.0	10.5 ± 4.0	1.1 ± 1.1
Walking	-68.4 ± 3.5	-71.7 ± 3.8	-7.2 ± 1.5	-8.3 ± 1.0	3.3 ± 2.1	1.2 ± 2.0

MT1- 4° Repetition
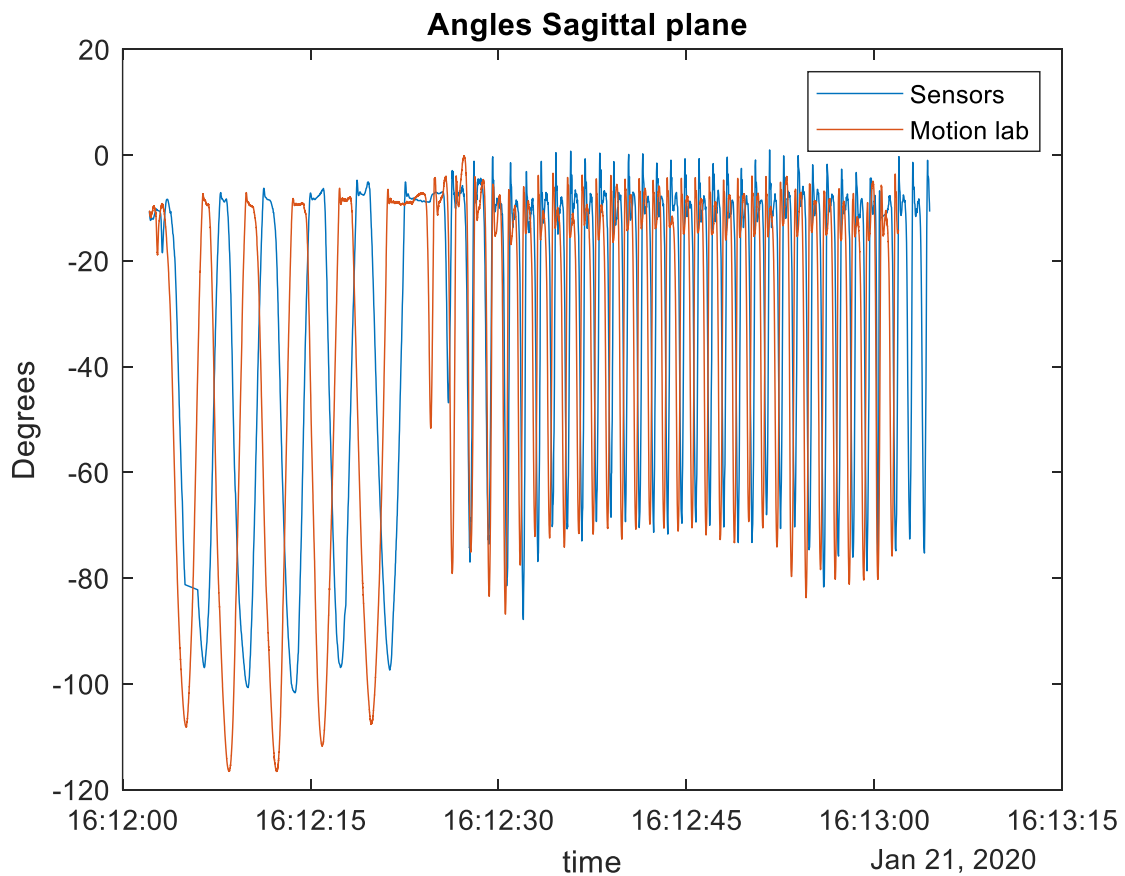
Figure 6.4 *MoCap (red) and black sensors (blue) knee angle in MT1-4° Repetition*
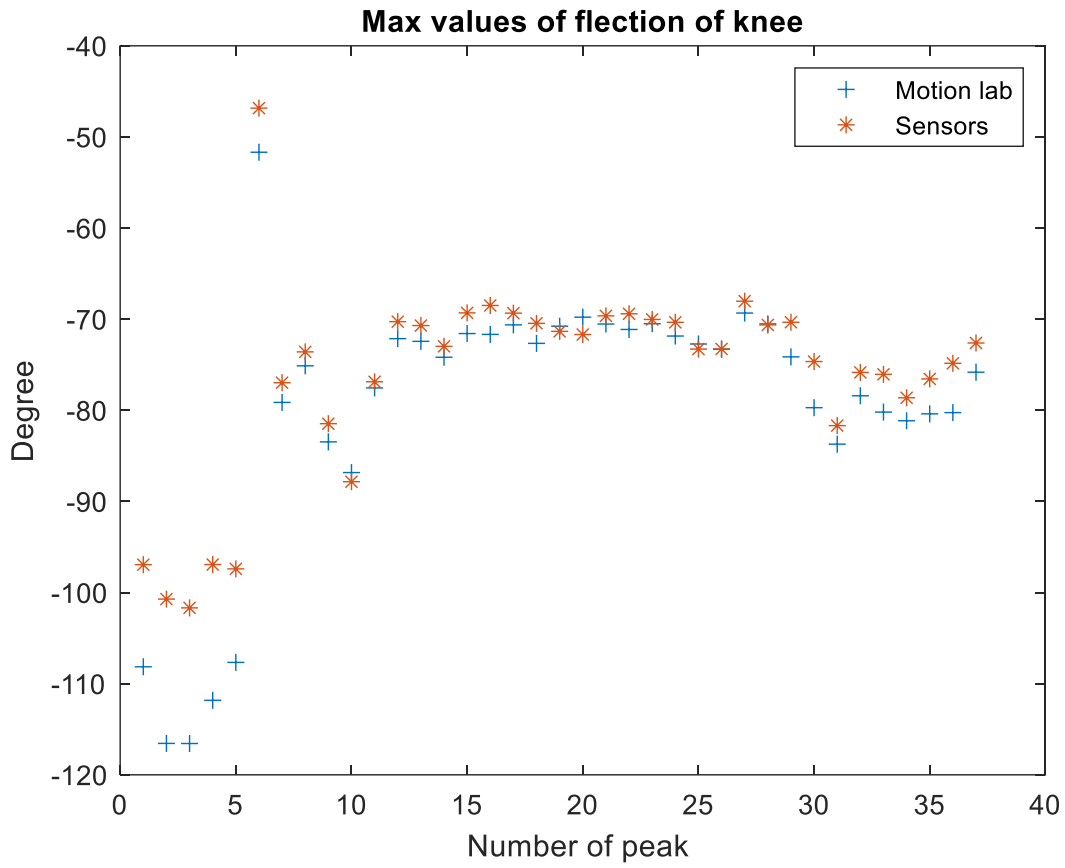
Figure 6.5. MoCap (blue) and black sensors (red) maximum values knee flection for each squat (peak 1-5) or step (peaks >6) in MT1-4° Repetition
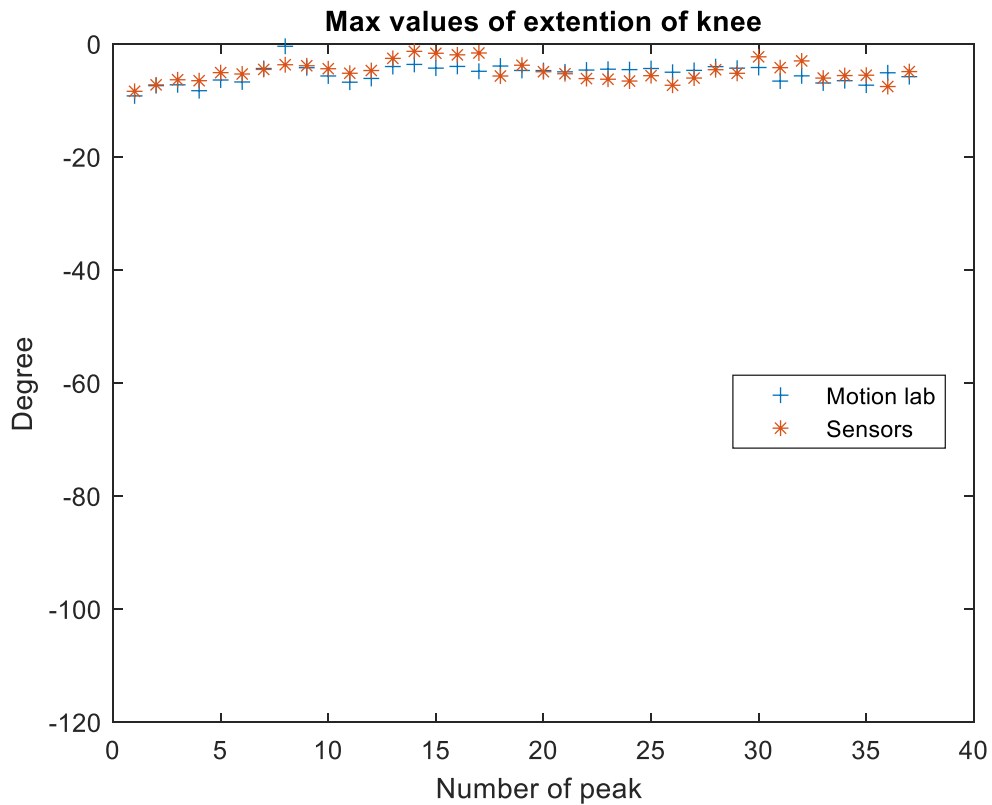
Figure 6.6. MoCap (blue) and black sensors (red) maximum values knee extension for each squat (peak 1-5) or step (peaks >6) in MT1-4° Repetition

Table 6.1. *Mean values of experimental data, calculated by both system and compared, during MT1-1° Repetition*

Type of movement	Mean value of max knee flection in MoCap (degrees)	Mean value of max knee flection in black sensors (degrees)	Mean value of max knee extension in MoCap (degrees)	Mean value of max knee extension in black sensors (degrees)	Mean difference between MoCap and black sensors in max knee flection (degrees)	Mean difference between MoCap and black sensors in max knee extension (degrees)
Global	-79.6 ± 14.4	-76.2 ± 10.9	-5.1 ± 1.6	-2.1 ± 2.5	3.6 ± 4.2	3.2 ± 1.3
Squatting	-112.1 ± 4.3	-98.7 ± 2.3	-7.6 ± 1.1	-6.6 ± 1.3	13.4 ± 2.5	1.0 ± 0.7
Walking	-74.5 ± 6.3	-72.6 ± 6.5	-4.7 ± 1.3	-1.4 ± 1.7	2.1 ± 1.4	3.5 ± 1.0

MT3

MoCap system failed the acquisition in this motion test. A numeric comparison is not possible for these motion test. Otherwise, the qualitative pattern can be evaluated by blue curve of black sensor system.
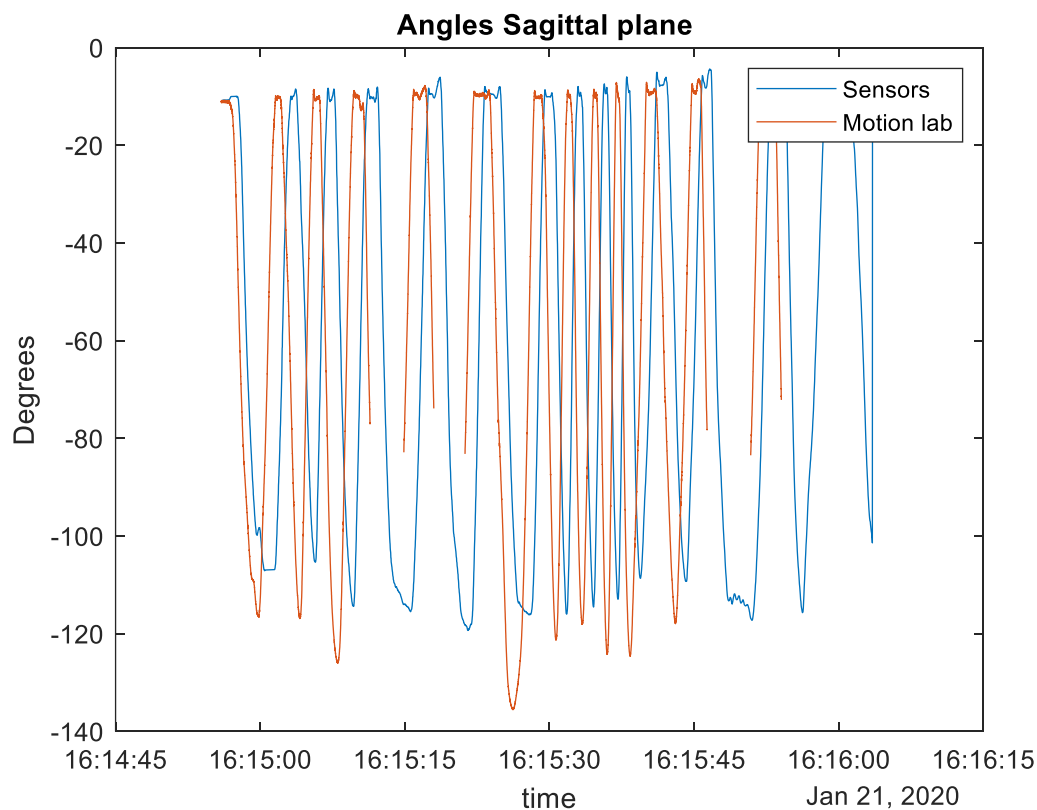
Figure 6.7. MoCap (red) and black sensors (blue) knee angle in MT2

MT4- 1° Repetition
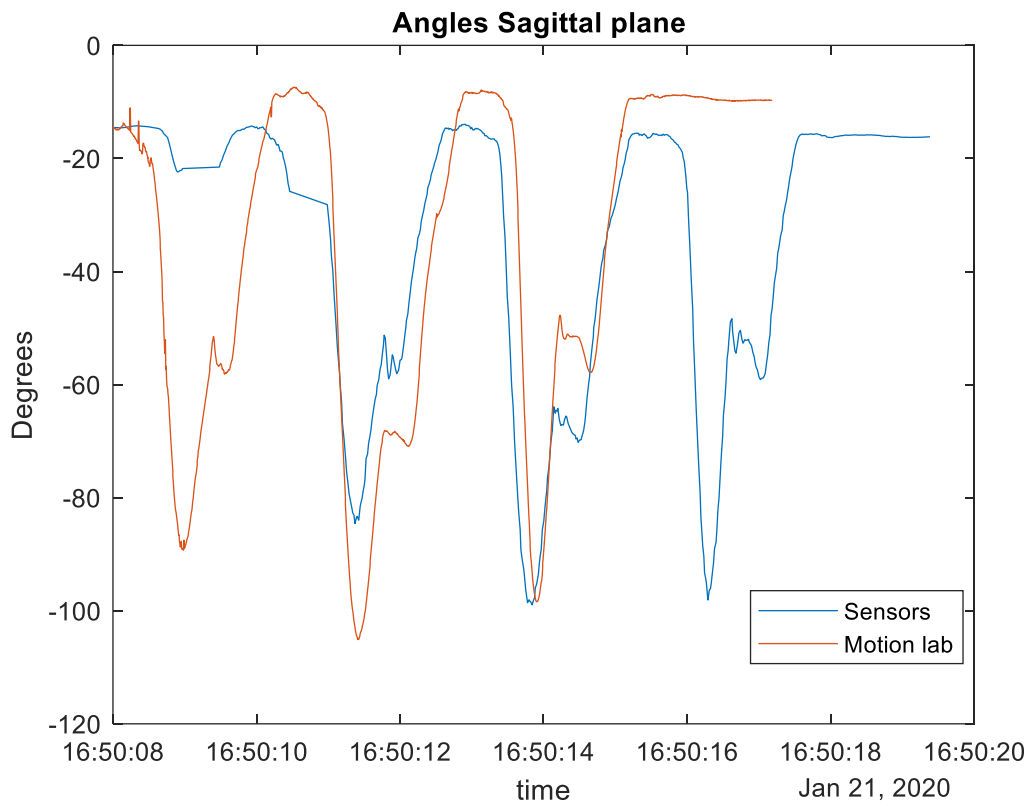
Figure 6.8. MoCap (red) and black sensors (blue) knee angle in MT4-1°Repetition
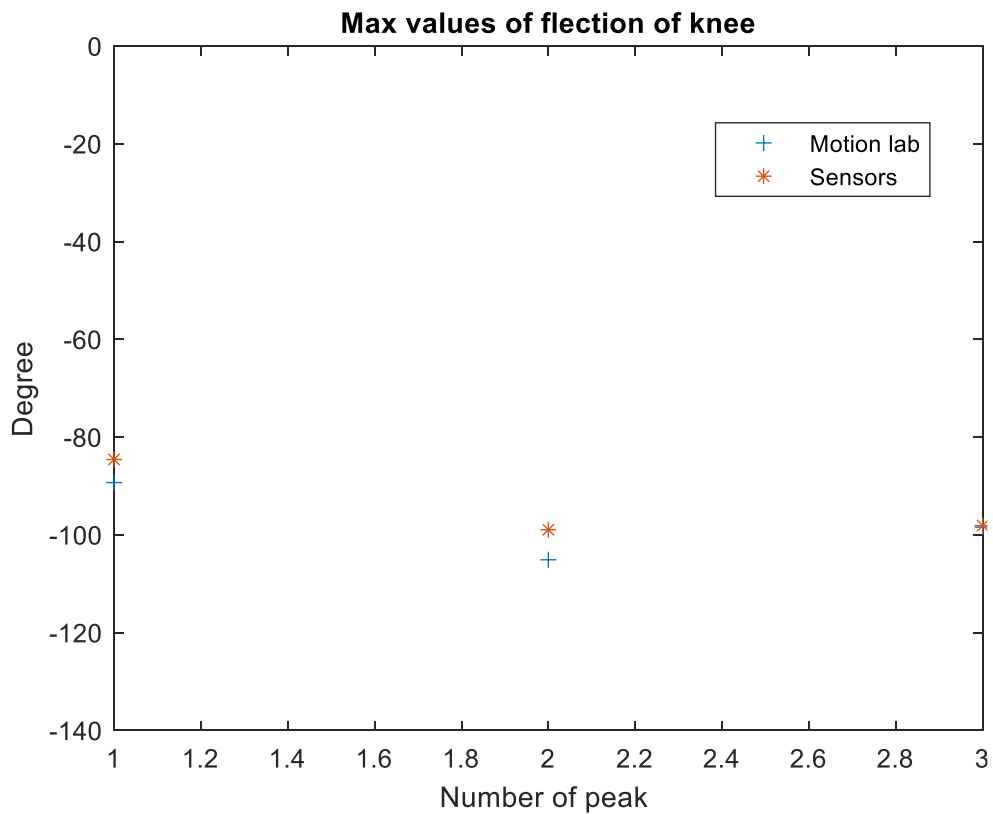
Figure 6.10. *MoCap (blue) and black sensors (red) maximum values knee extension for each step in MT4-1°Repetition*

Table 6.2. Mean values of experimental data, calculated by both system and compared, during MT4-1° Repetition

Mean value of max flection in MoCap measurements (degrees)	Mean value of max flection in black sensors measurements (degrees)	Mean value of max extension in MoCap measurements (degrees)	Mean value of max extension in black sensors measurements (degrees)	Mean difference between MoCap and black sensors in max flection measurements	Mean difference between MoCap and black sensors in max extension

				(degrees)	measurements (degrees)
-97.6 ± 7.9	-93.8 ± 8.1	-8.8 ± 2.0	-1.4 ± 0.9	3.7 ± 3.0	5.8 ±2.3

MT4- 2° Repetition
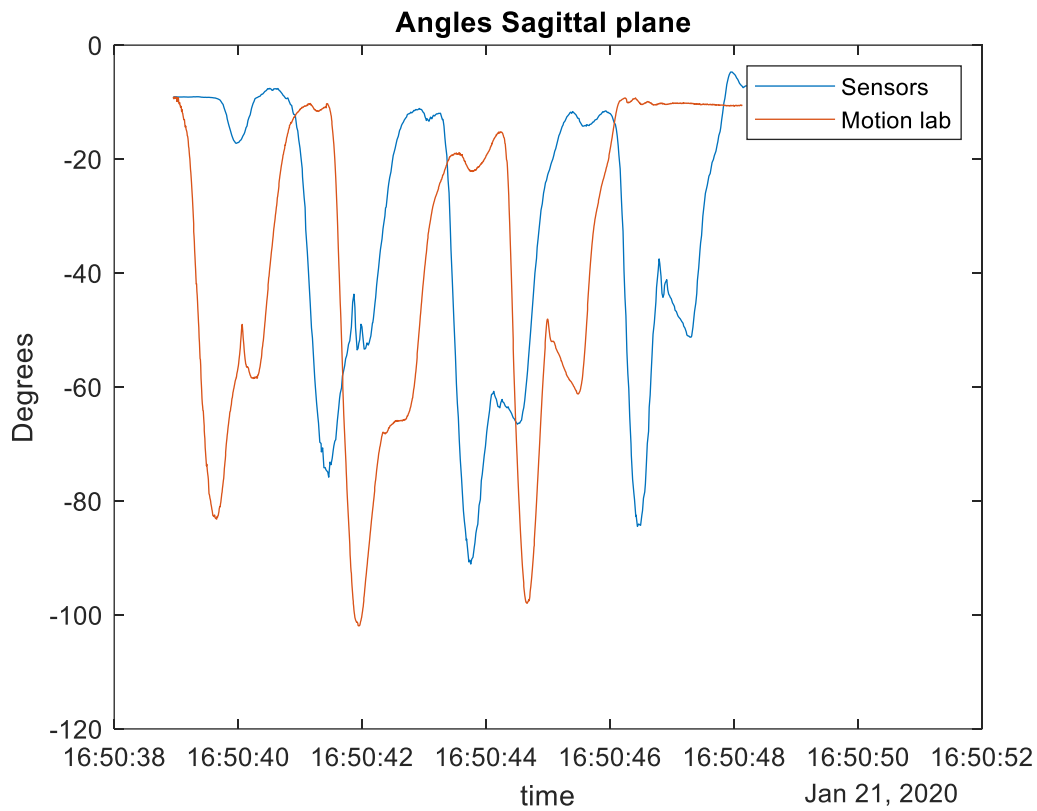
Figure 6.11. MoCap (red) and black sensors (blue) knee angle in MT4-2°Repetition
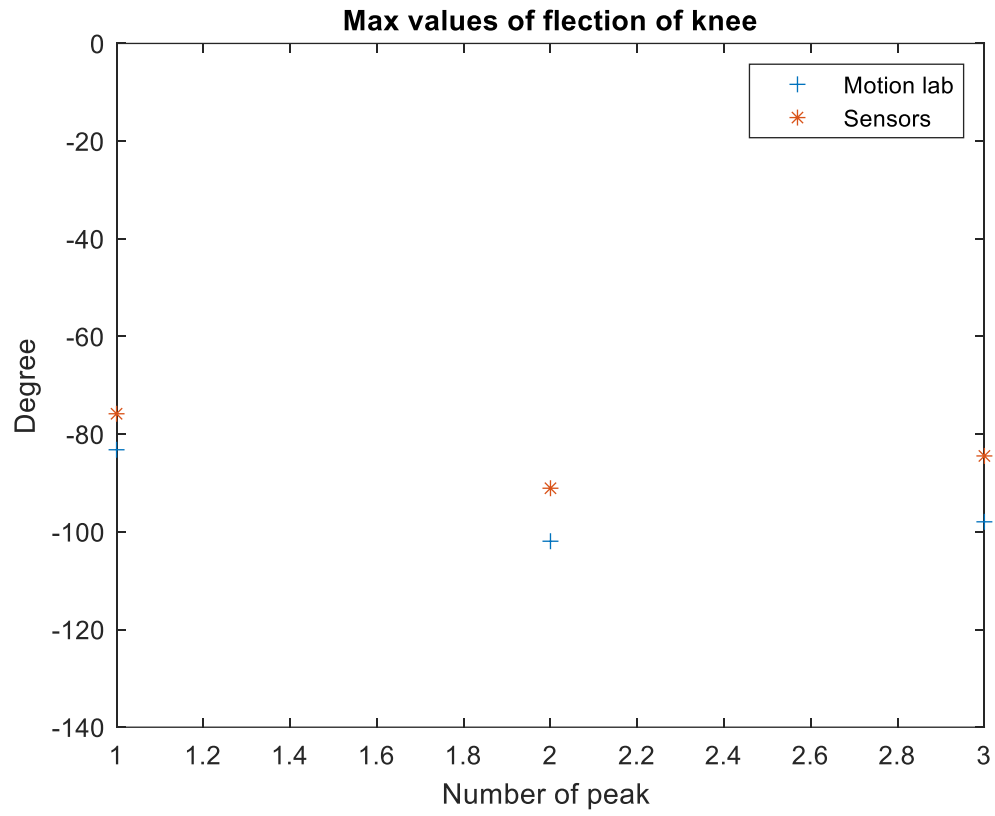
Figure 6.12. *MoCap (blue) and black sensors (red) maximum values knee flection for each step in MT4-2°Repetition*
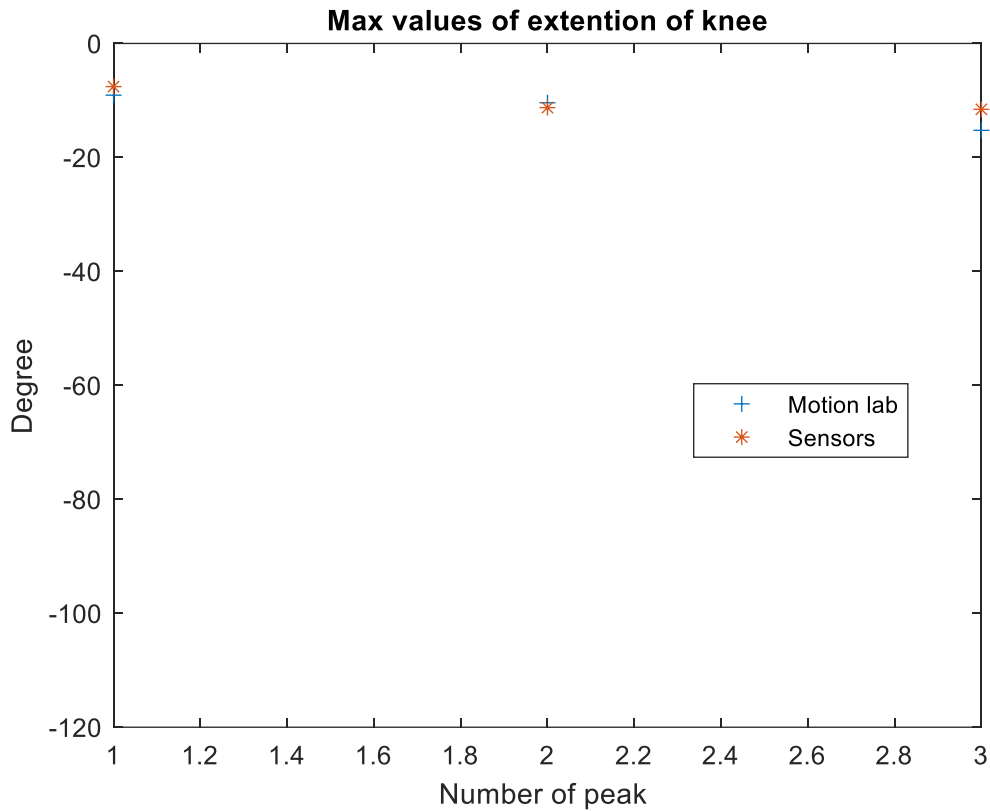
Figure 6.13. *MoCap (blue) and black sensors (red) maximum values knee extension for each step in MT4-2°Repetition*

Table 6.3. *Mean values of experimental data, calculated by both system and compared, during MT4-2° Repetition*

Mean value of max flection in MoCap measurements (degrees)	Mean value of max flection in black sensors measurements (degrees)	Mean value of max extension in MoCap measurements (degrees)	Mean value of max extension in black sensors measurements (degrees)	Mean difference between MoCap and black sensors in max flection measurements (degrees)	Mean difference between MoCap and black sensors in max extension measurements (degrees)
-94.4 ± 9.9	-83.8 ± 7.6	-11.5 ± 3.3	10.1 ± 2.2	10.6 ± 3.1	2.0 ± 1.5

MT4- 3° Repetition
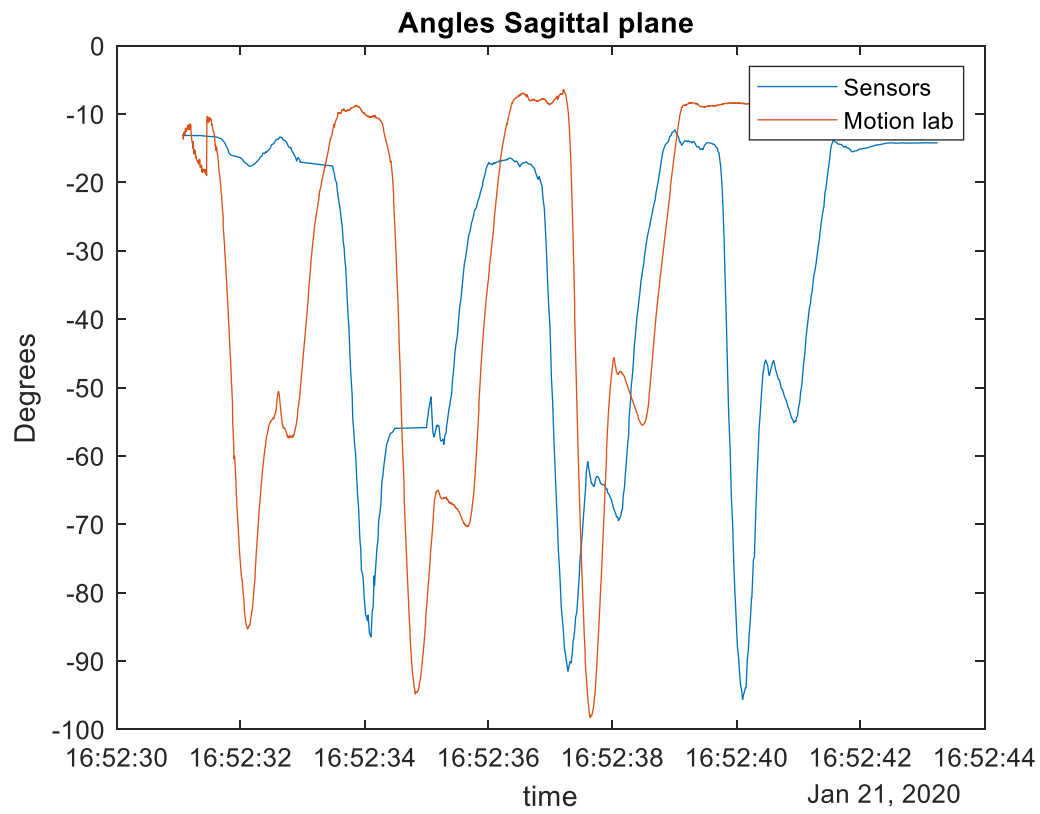
Figure 6.14. *MoCap (red) and black sensors (blue) knee angle in MT4-1°Repetition*
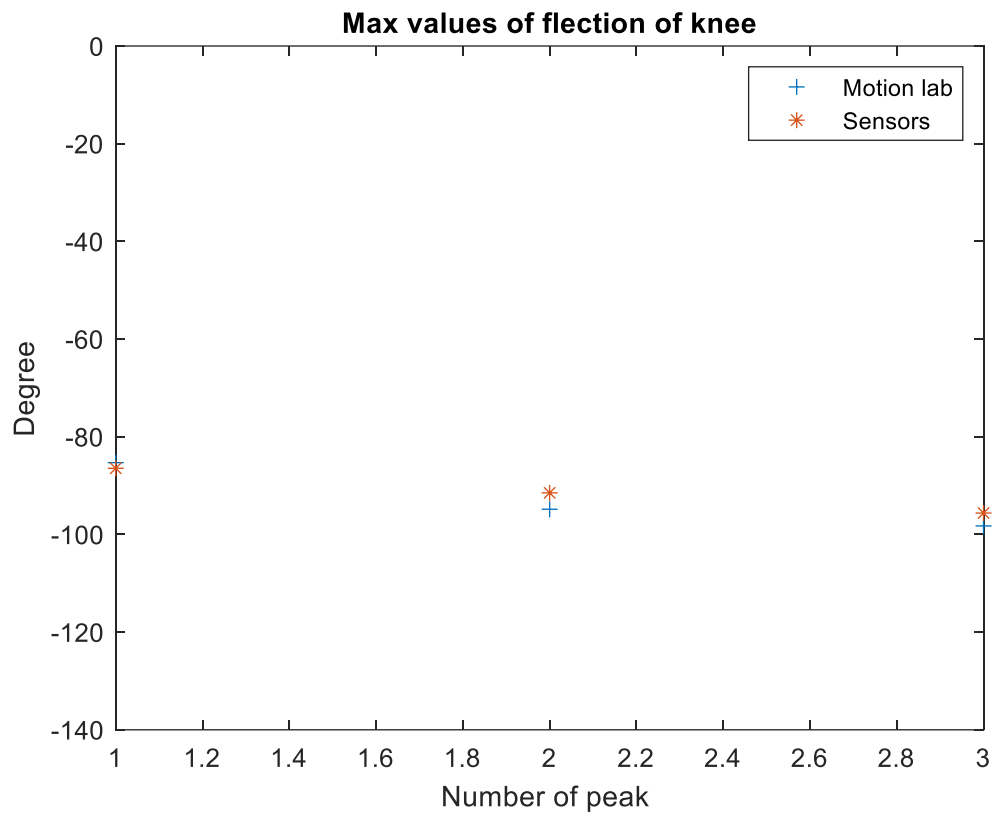
Figure 6.15. *MoCap (blue) and black sensors (red) maximum values knee flection for each step in MT4-3°Repetition*
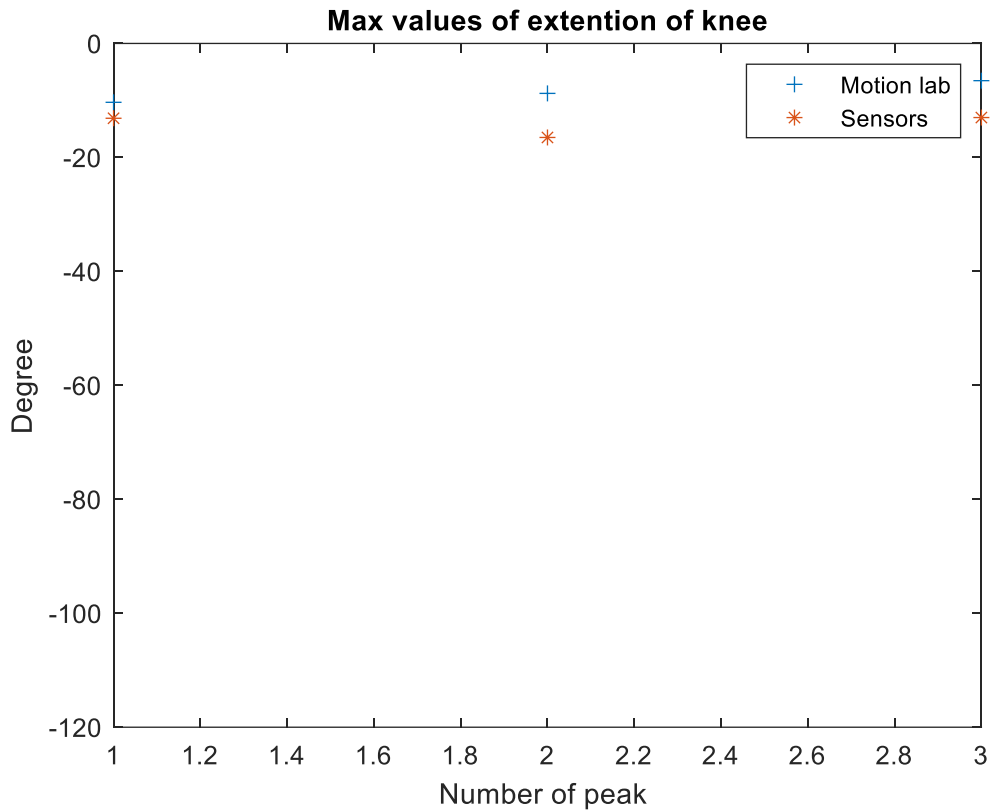
Figure 6.15. *MoCap (blue) and black sensors (red) maximum values knee extension for each step in MT4-3°Repetition*

Table 6.4*. Mean values of experimental data, calculated by both system and compared, during MT4-3° Repetition*

Mean value of max flection in MoCap measurements (degrees)	Mean value of max flection in black sensors measurements (degrees)	Mean value of max extension in MoCap measurements (degrees)	Mean value of max extension in black sensors measurements (degrees)	Mean difference between MoCap and black sensors in max flection measurements (degrees)	Mean difference between MoCap and black sensors in max extension measurements (degrees)
-92.8 ± 6.7	-91.2 ± 4.6	-8.5 ± 2.0	-14.0 ± 2.2	2.4 ±1.1	5.5 ± 2.5

MT5
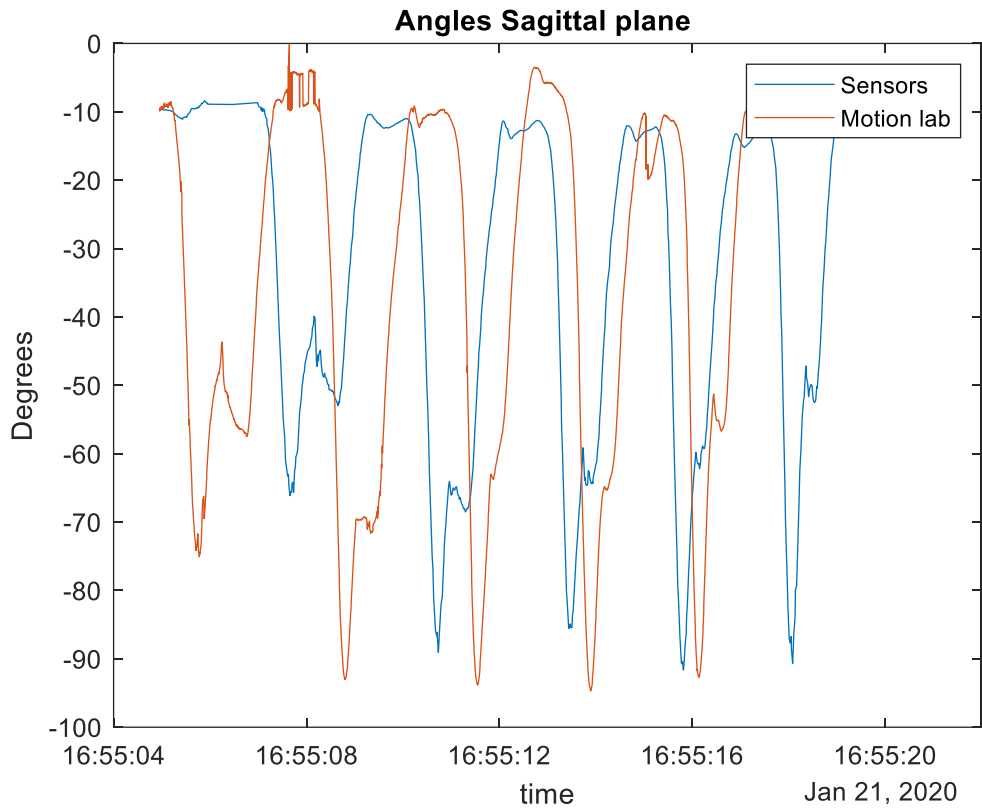
Figure 6.17. *MoCap (red) and black sensors (blue) knee angle in MT5*
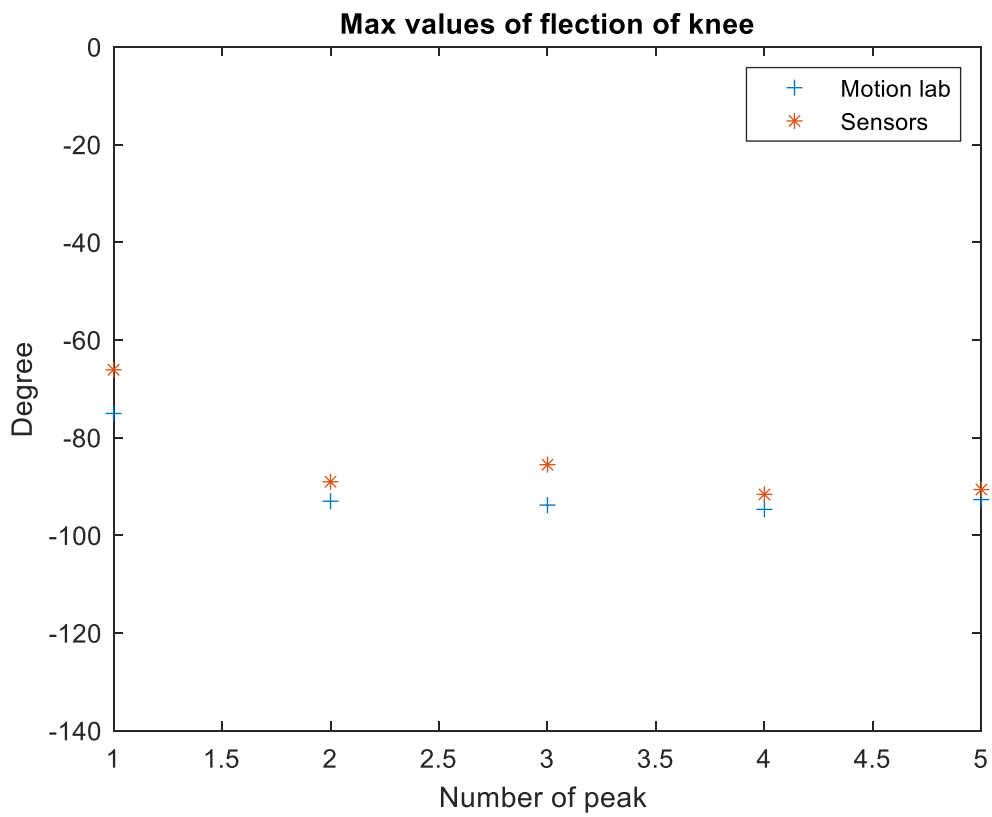
Figure 6.18. MoCap (blue) and black sensors (red) maximum values knee flection for each step in MT5
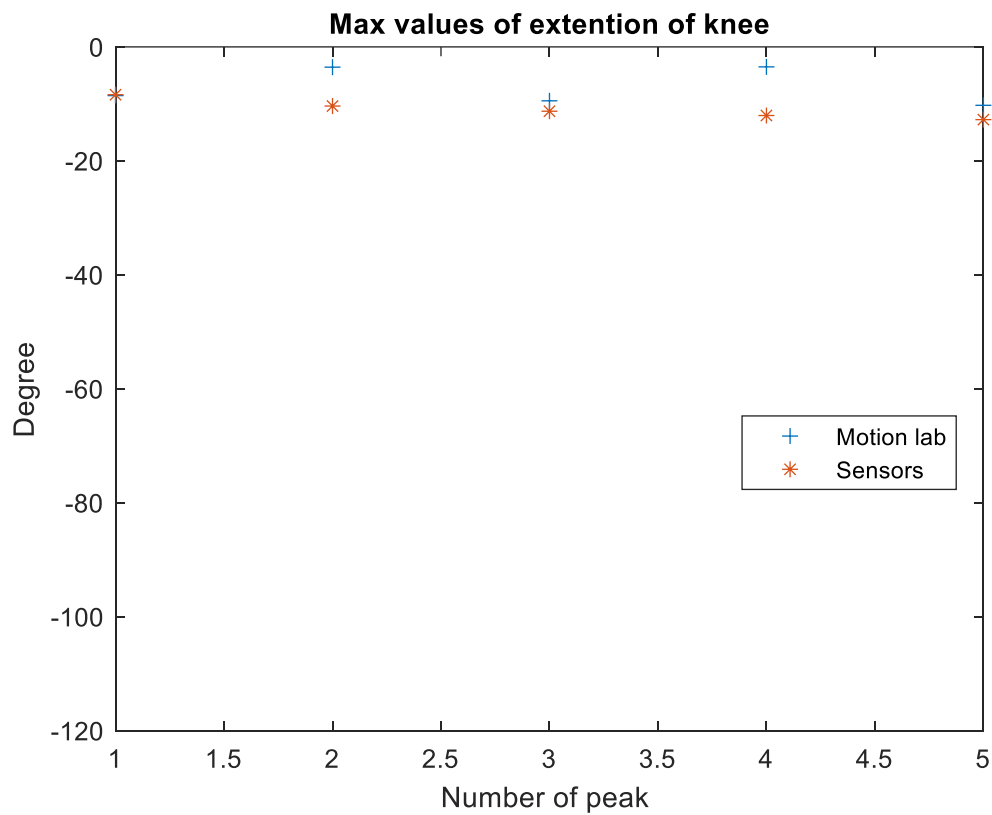
Figure 6.19. MoCap (blue) and black sensors (red) maximum values knee extension for each step in MT5

Table 6.5. Mean values of experimental data, calculated by both system and compared, during MT5

Mean value of max flection in MoCap measurements (degrees)	Mean value of max flection in black sensors measurements (degrees)	Mean value of max extension in MoCap measurements (degrees)	Mean value of max extension in black sensors measurements (degrees)	Mean difference between MoCap and black sensors in max flection measurements (degrees)	Mean difference between MoCap and black sensors in max extension measurements (degrees)
-89.9 ± 8.3	-84.6 ± 10.6	-6.3 ± 4.3	-11.0 ± 1.7	5.3 ± 3.1	4.7 ± 4.4

MT6- 1° Repetition
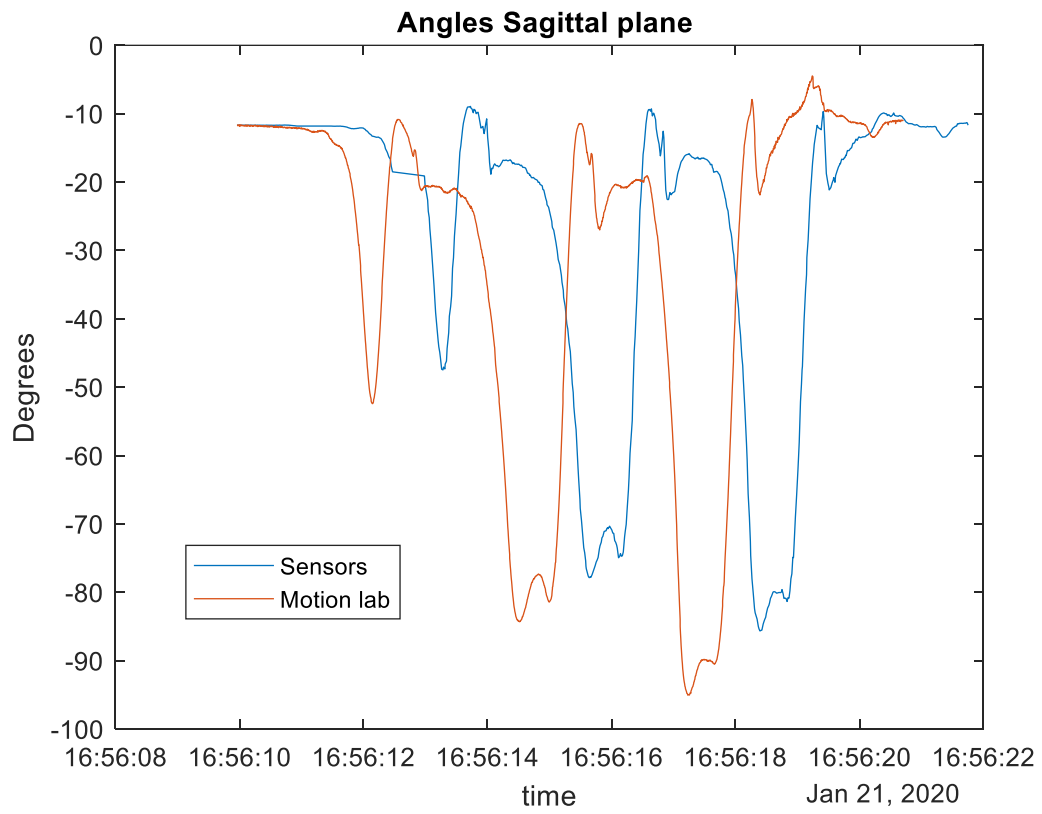
Figure 6.20. MoCap (red) and black sensors (blue) knee angle in MT6-1°Repetition
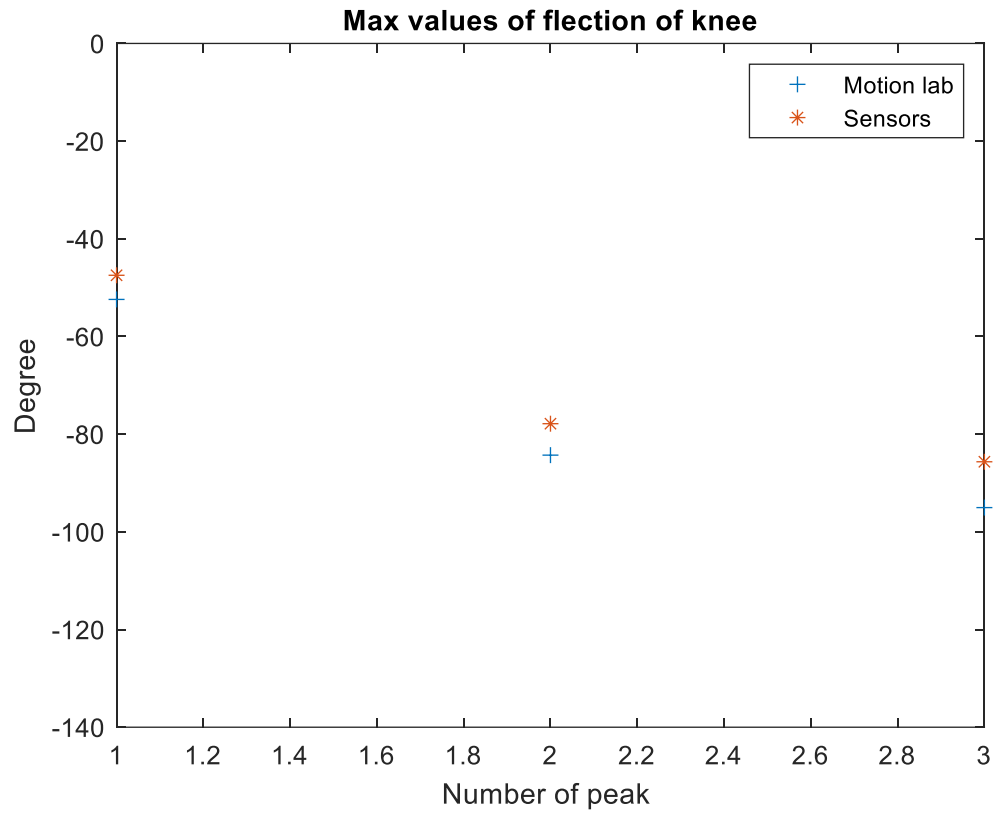
Figure 6.21. *MoCap (blue) and black sensors (red) maximum values knee flection for each step in MT6-1°Repetition*
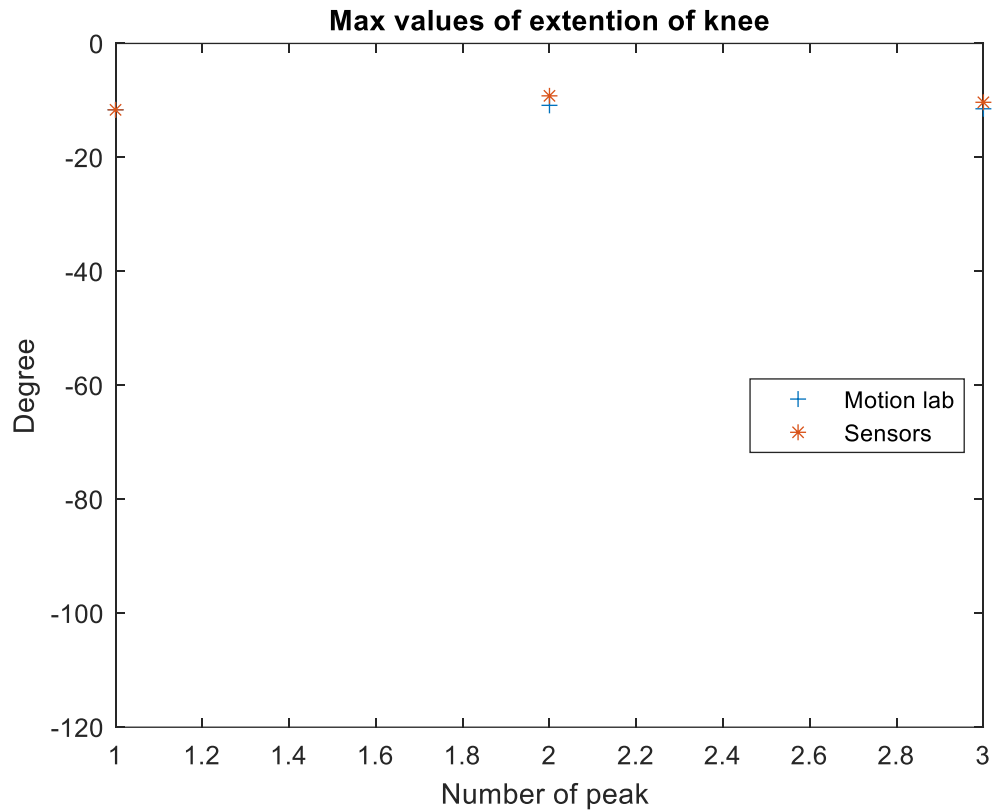
Figure 6.22. *MoCap (blue) and black sensors (red) maximum values knee extension for each step in MT6-1°Repetition*

Table 6.6*. Mean values of experimental data, calculated by both system and compared, during MT6-1° Repetition*

Mean value of max flection in MoCap measurements (degrees)	Mean value of max flection in black sensors measurements (degrees)	Mean value of max extension in MoCap measurements (degrees)	Mean value of max extension in black sensors measurements (degrees)	Mean difference between MoCap and black sensors in max flection measurements (degrees)	Mean difference between MoCap and black sensors in max extension measurements (degrees)
-77 ± 22.2	-70.3 ± 20.2	-11.3 ± 0.4	-9.9 ± 1.5	6.9 ± 2.3	1.4 ± 1.2

MT6- 2° Repetition
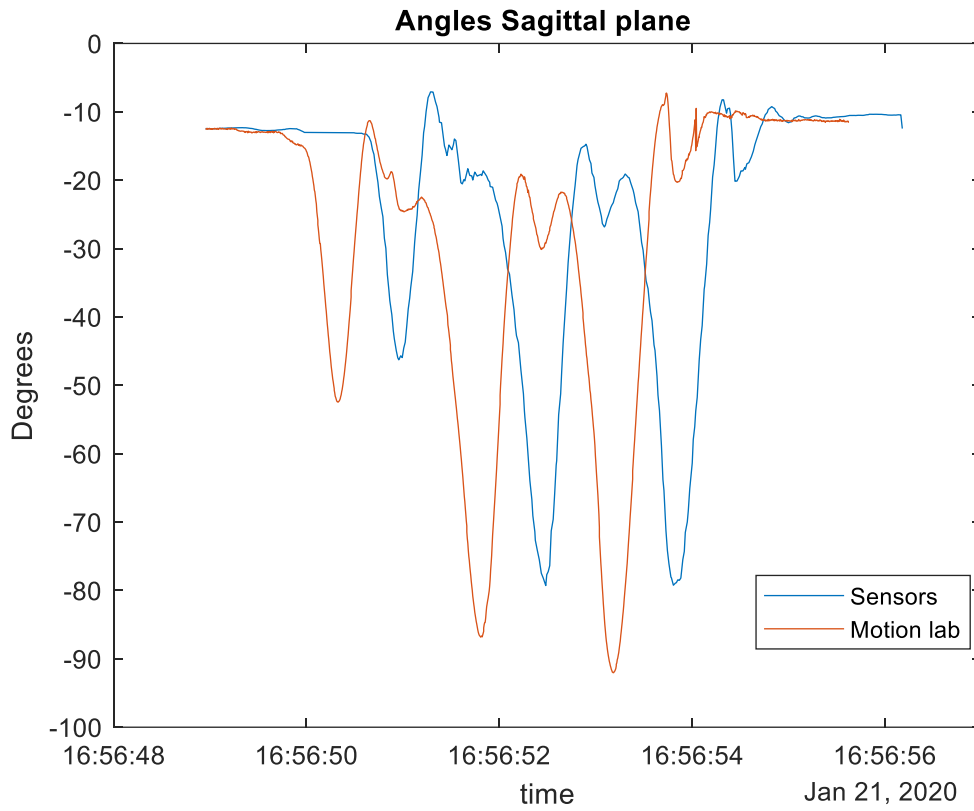
Figure 6.23. *MoCap (red) and black sensors (blue) knee angle in MT6-2°Repetition*
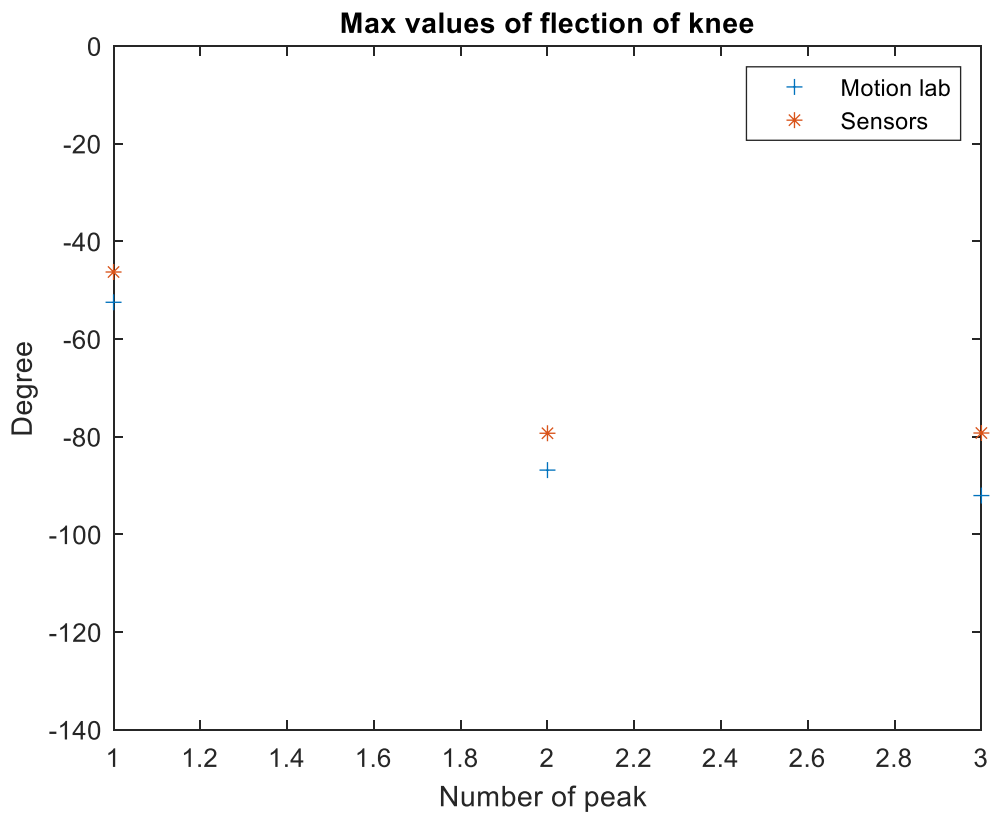
Figure 6.24. MoCap (blue) and black sensors (red) maximum values knee flection for each step in MT6-2°Repetition
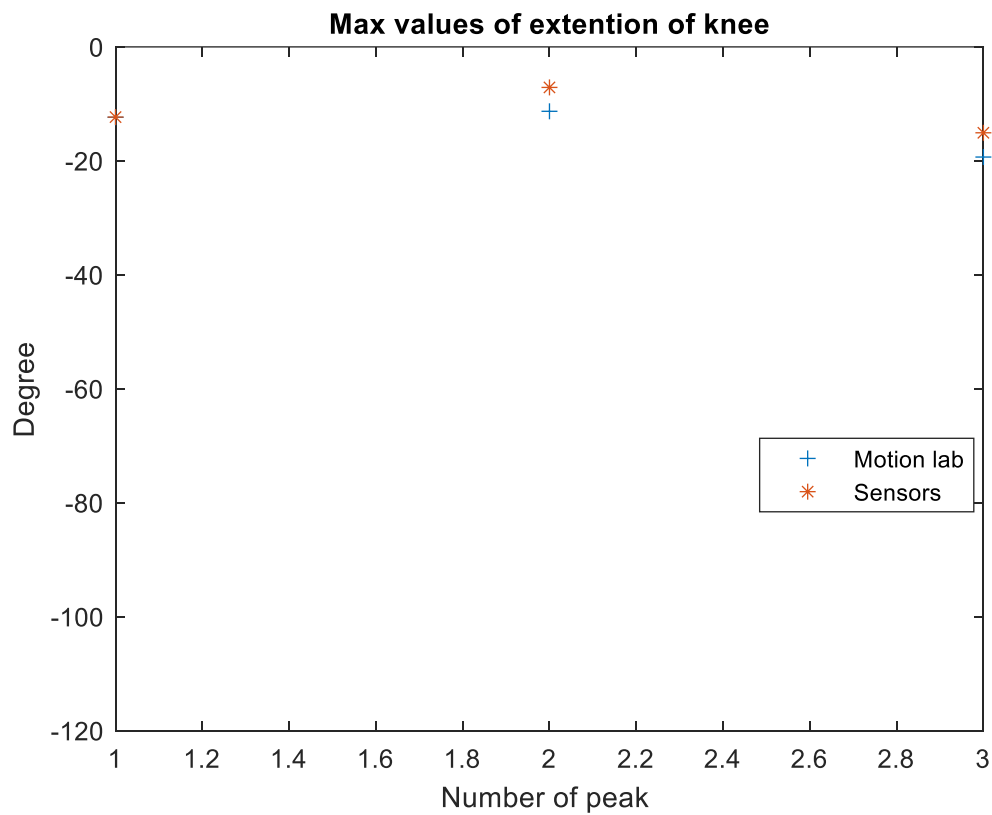
Figure 6.25. MoCap (blue) and black sensors (red) maximum values knee extension for each step in MT6-2°Repetition

Table 6.7. Mean values of experimental data, calculated by both system and compared, during MT6-2° Repetition

Mean value of max flection in MoCap measurements (degrees)	Mean value of max flection in black sensors measurements (degrees)	Mean value of max extension in MoCap measurements (degrees)	Mean value of max extension in black sensors measurements (degrees)	Mean difference between MoCap and black sensors in max flection measurements (degrees)	Mean difference between MoCap and black sensors in max extension measurements (degrees)
-77.1 ± 21.5	-68.3 ± 19.0	-14.3 ± 4.2	-11.4 ± 3.9	8.8 ± 3.5	2.9 ± 2.4

MT6- 3° Repetition
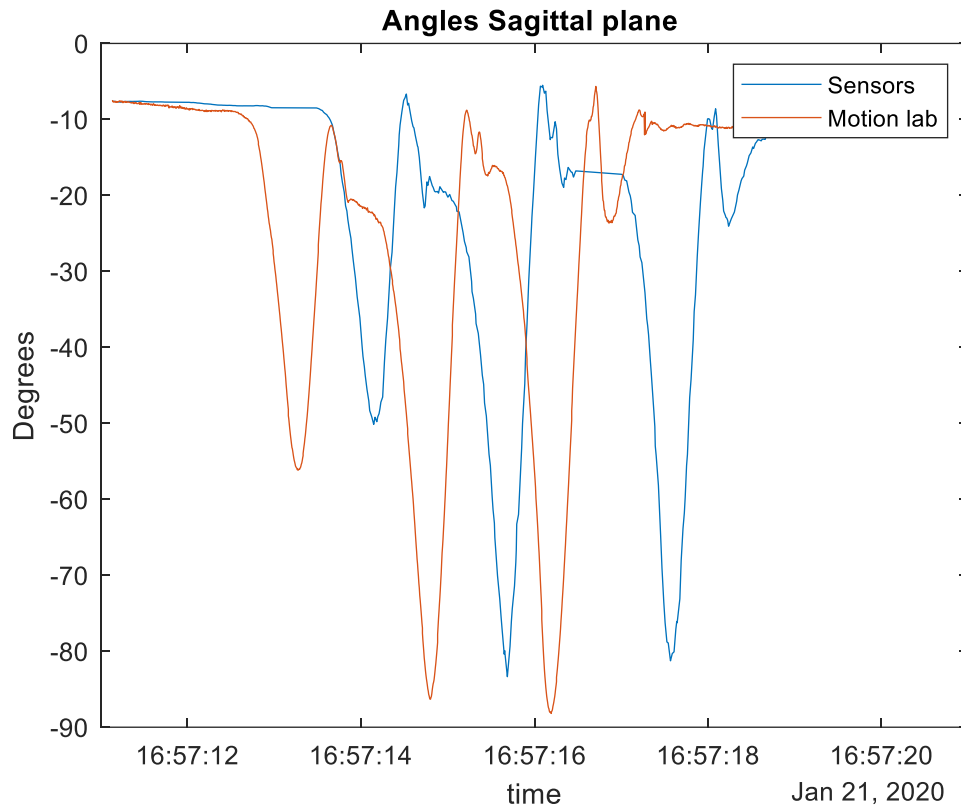
Figure 6.26. *MoCap (red) and black sensors (blue) knee angle in MT6-3°Repetition*
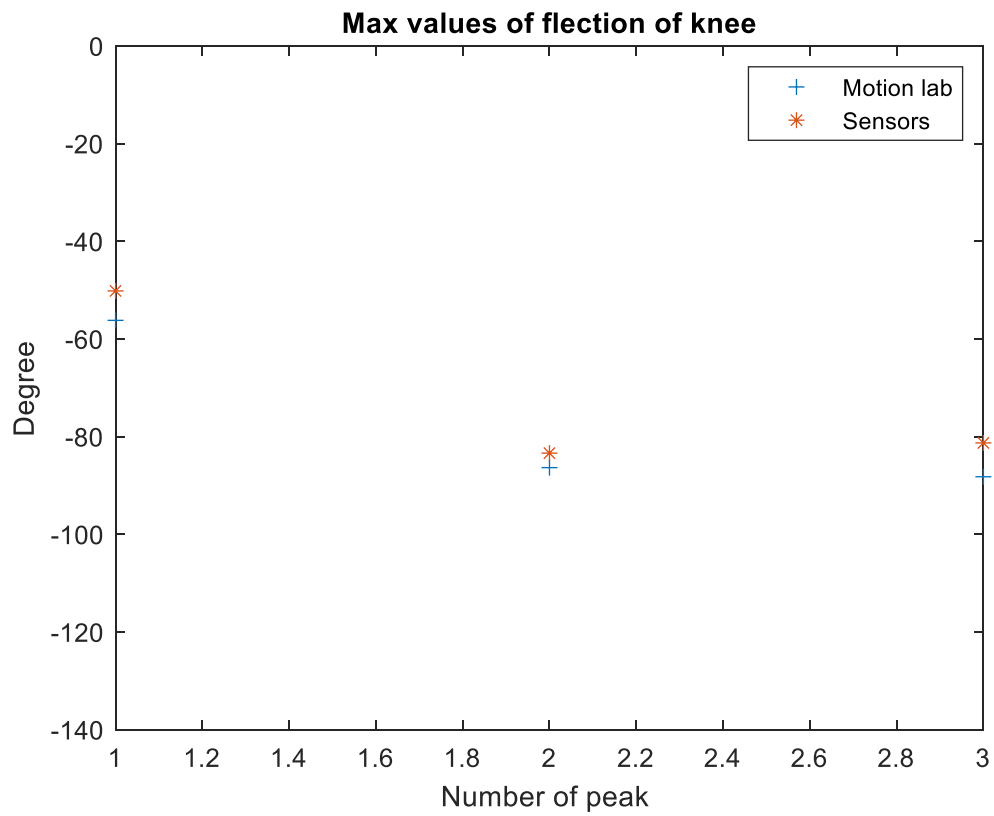
Figure 6.28. MoCap (blue) and black sensors (red) maximum values knee extension for each step in MT6-3°Repetition

Table 6.8. Mean values of experimental data, calculated by both system and compared, during MT6-3° Repetition

Mean value of max flection in MoCap measurements (degrees)	Mean value of max flection in black sensors measurements (degrees)	Mean value of max extension in MoCap measurements (degrees)	Mean value of max extension in black sensors measurements (degrees)	Mean difference between MoCap and black sensors in max flection measurements (degrees)	Mean difference between MoCap and black sensors in max extension measurements (degrees)
-76.9 ± 18.0	-71.6 ± 18.6	-9.0 ± 1.6	-6.6 ± 1.0	5.3 ± 2.1	2.5 ± 2.1
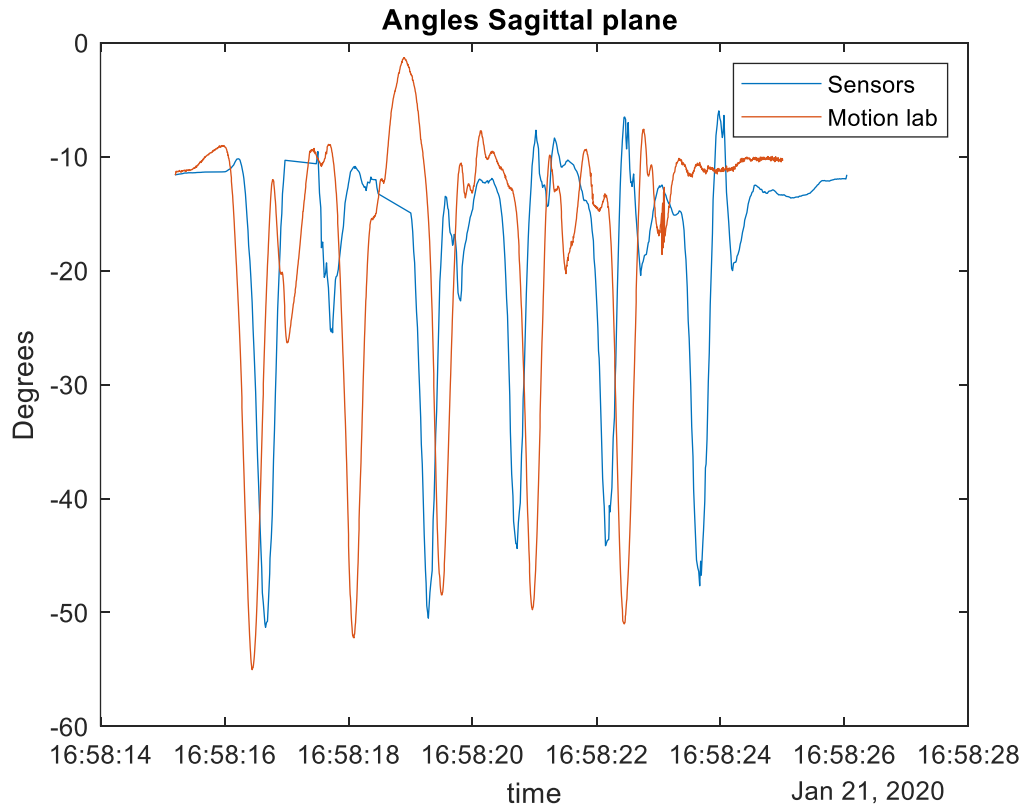
Figure 6.29. *MoCap (red) and black sensors (blue) knee angle in MT7-1°Repetition*
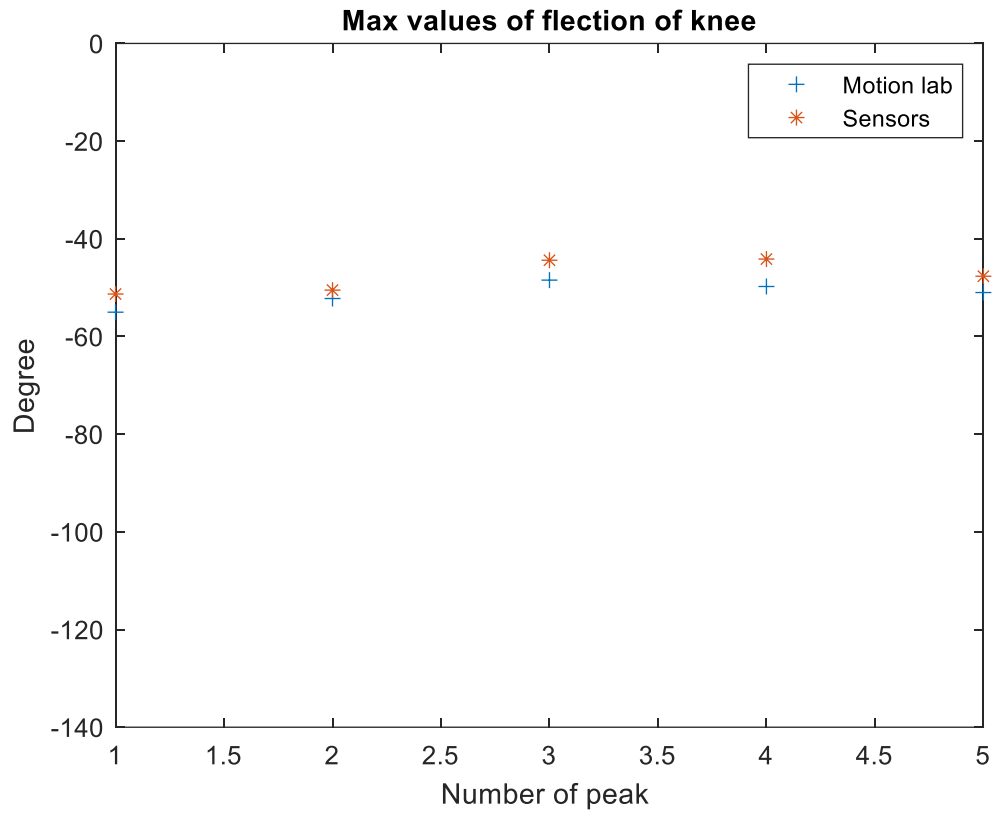
Figure 6.30. *MoCap (blue) and black sensors (red) maximum values knee flection for each step in MT7-1°Repetition*
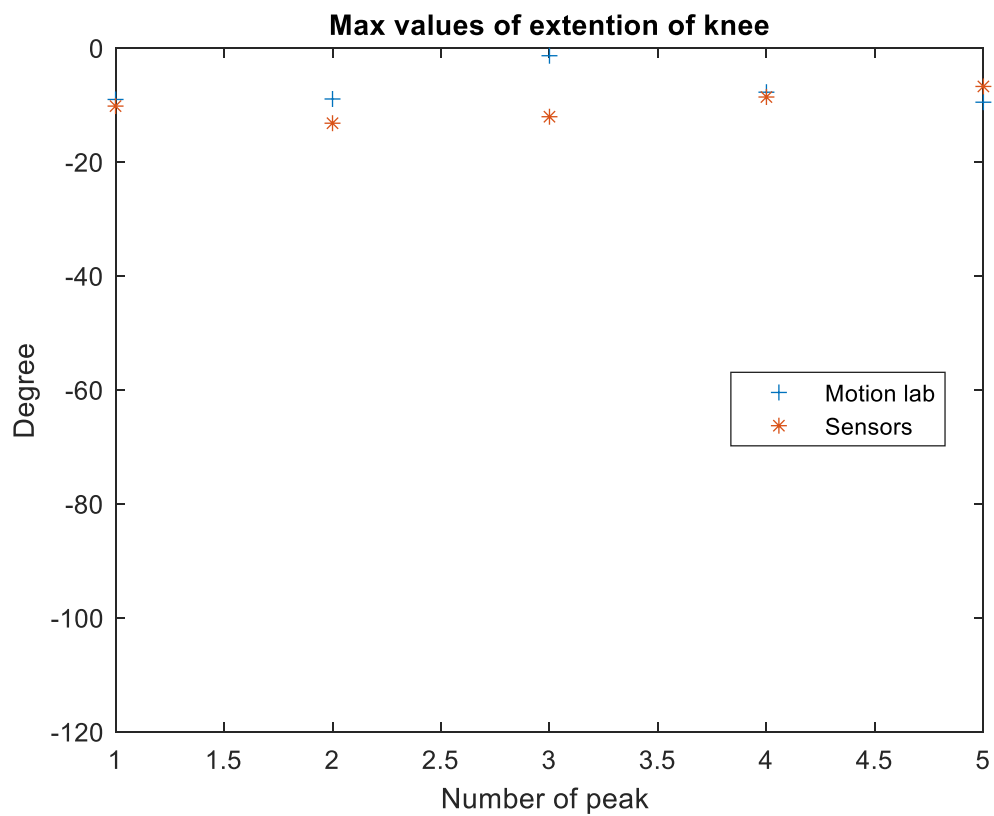
Figure 6.31. MoCap (blue) and black sensors (red) maximum values knee extension for each step in MT7-1°Repetition

Table 6.9. Mean values of experimental data, calculated by both system and compared, during MT7-1° Repetition

Mean value of max flection in MoCap measurements (degrees)	Mean value of max flection in black sensors measurements (degrees)	Mean value of max extension in MoCap measurements (degrees)	Mean value of max extension in black sensors measurements (degrees)	Mean difference between MoCap and black sensors in max flection measurements (degrees)	Mean difference between MoCap and black sensors in max extension measurements (degrees)
-51.3 ± 2.5	-47.6 ± 3.3	-7.3 ± 3.4	-9.2 ± 2.1	3.7 ± 1.4	3.0 ±4.3

MT7-2° Repetition
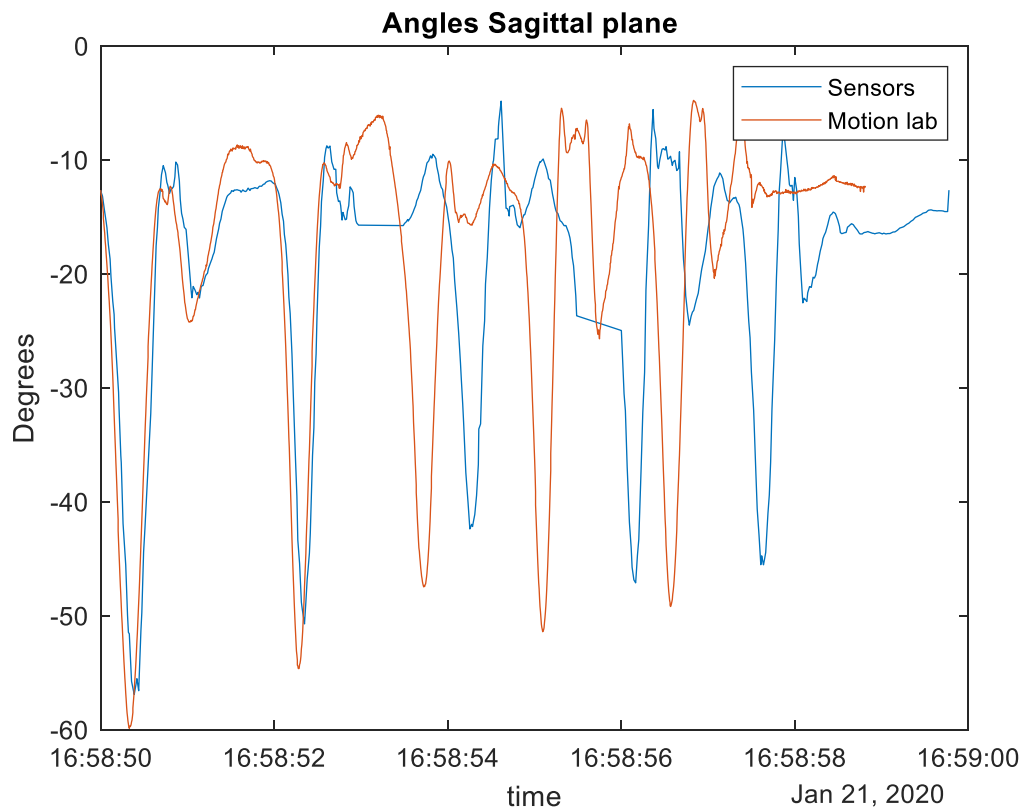
Figure 6.32. MoCap (red) and black sensors (blue) knee angle in MT7-2°Repetition
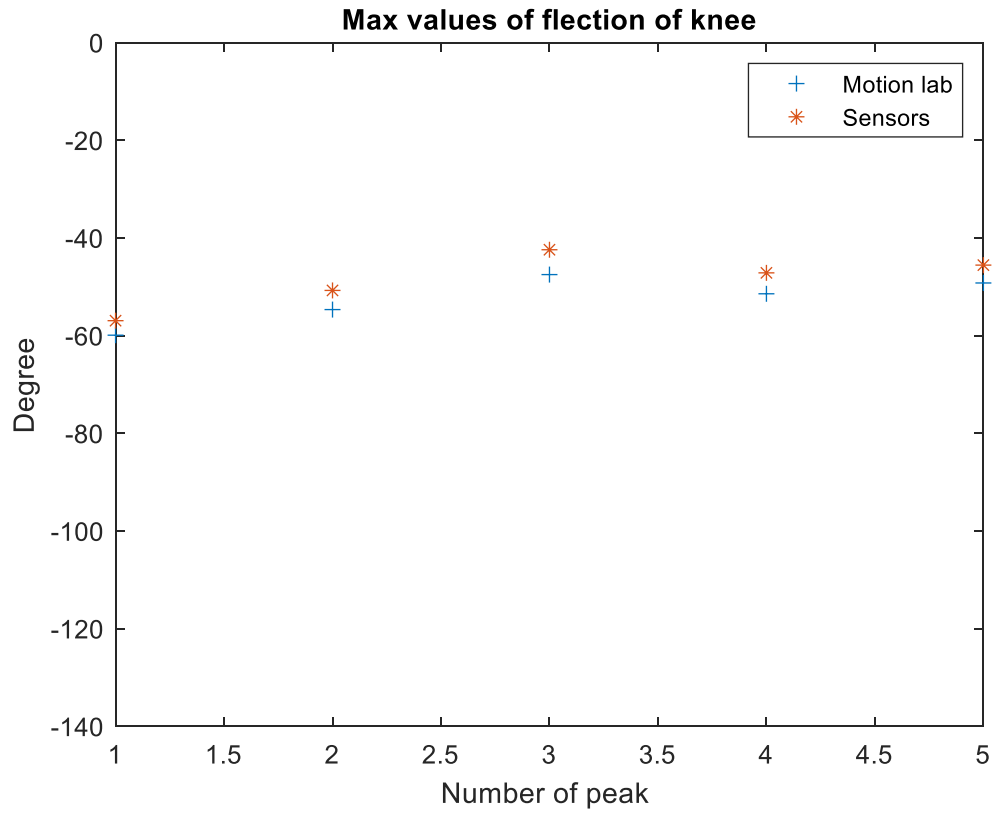
Figure 6.33. *MoCap (blue) and black sensors (red) maximum values knee flection for each step in MT7-2°Repetition*
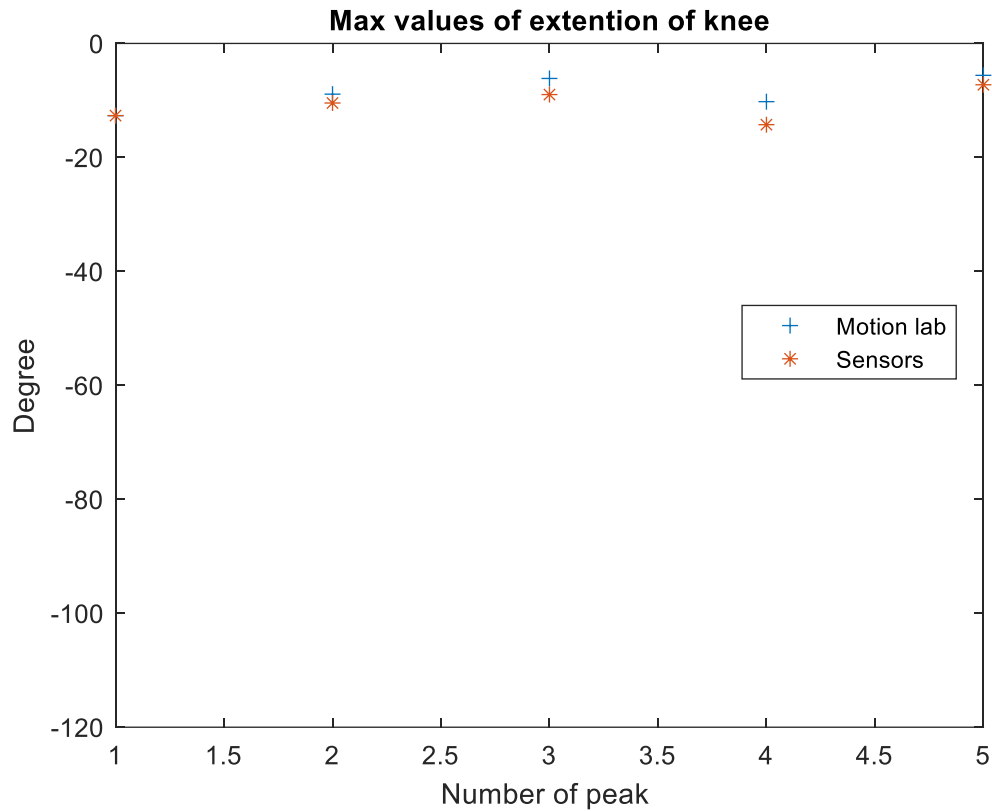
Figure 6.34. *MoCap (blue) and black sensors (red) maximum values knee extension for each step in MT7-2°Repetition*

Table 6.10. *Mean values of experimental data, calculated by both system and compared, during MT7-2° Repetition*

Mean value of max flection in MoCap measurements (degrees)	Mean value of max flection in black sensors measurements (degrees)	Mean value of max extension in MoCap measurements (degrees)	Mean value of max extension in black sensors measurements (degrees)	Mean difference between MoCap and black sensors in max flection measurements (degrees)	Mean difference between MoCap and black sensors in max extension measurements (degrees)
-52.5 ± 4.9	-48.5 ± 5.6	-8.6 ± 3.0	-8.4 ± 3.2	4.0 ±0.8	1.9 ± 2.2

BLAND-ALTMAN GRAPH CALCULATION TABLE

Table 6.11. *Table with mean of each row of the matrix explained in Results 3.3*

Range of Motion n°	Mean values from MoCap Table	Mean values from Sensor Table
1	-96.7500	-87.1674
2	-107.6268	-95.1901
3	-105.4140	-95.7643
4	-100.0655	-90.2543
5	-99.2341	-91.0253
6	-52.7816	-50.5936
7	-63.0548	-63.1307
8	-67.5400	-68.5365
9	-68.8570	-71.0501
10	-68.5661	-72.6745
11	-69.7655	-73.4637
12	-67.2335	-71.4151
13	-67.9903	-72.4688
14	-67.8017	-71.3648
15	-65.3856	-67.9962
16	-65.5794	-67.9224
17	-65.9549	-68.4109
18	-65.9607	-68.2863
19	-65.2620	-68.3511
20	-64.7399	-68.0004
21	-64.1216	-67.6740
22	-64.7444	-66.1852
23	-65.0629	-67.6481
24	-64.8663	-67.1238
25	-64.8005	-67.1616
26	-65.0793	-67.2652
27	-64.5945	-66.7152
28	-66.2151	-68.9452
29	-66.3522	-67.9736
30	-68.3634	-69.3455
31	-68.2592	-70.9081
32	-67.1795	-68.6779